HELMHOLTZ
Centre for Environmental Research

Florian Schunck

Effects of Esfenvalerate on Daphnia magna under Multiple Levels of Biological Complexity – The Influence of Time, Competition and Environmental Stressors

PHD DISSERTATION 1|2024
Helmholtz Centre for Environmental Research – UFZ
Department of Computational Biology and Chemistry

ISSN 2941-3885 (Online)

Effects of Esfenvalerate on *Daphnia magna* under Multiple Levels of Biological Complexity

The Influence of Time, Competition and Environmental Stressors

Von der Fakultät für Mathematik, Informatik und Naturwissenschaften der RWTH Aachen University zur Erlangung des akademischen Grades eines Doktors der Naturwissenschaften genehmigte Dissertation

vorgelegt von

M.Sc.

Florian Schunck

aus

Göttingen

Berichter:

Prof. Dr. Matthias Liess

Prof. Dr. Andreas Schäffer

Tag der mündlichen Prüfung: 06. November 2023

Acknowledgements

Meeting the challenges of this project would not have been possible without the support of countless people who have helped and supported me throughout this work. First and foremost, I would like to thank Prof. Dr. Matthias Liess from the Helmholtz Centre for Environmental Research—UFZ for his guidance and support throughout this project. I am especially grateful for the scientific arguments we had and for his persistence in helping me to focus on the important aspects of my research. I would also like to thank Dr. Eberhard Küster, whose thoughtful comments and literature recommendations have helped me improve my work and anticipate future challenges. In addition, I would like to thank Prof. Dr. Andreas Schäffer of RWTH Aachen University for his continued support and kind words that motivated me throughout my project.

My sincere thanks also go to my colleagues in the Department of Systems Ecotoxicology, without whom this project would not have been possible. In particular, I would like to thank Oliver Kaske and Franz Dussl for their insights and support in the laboratory and for rewarding conversations. Ingrid Ränker deserves my thanks for helping me to take my first steps with the small organisms that have been central to this work. I would also like to thank Klaus Seyfarth, whose experience with laboratory equipment was invaluable when things did not work as expected. Finally, I would like to thank the many undergraduate students who helped with this research. In particular, I would like to thank Lisa Hertges for her inspiring dedication to the minute

details of the experiments and for her support in the lab throughout the pandemic.

This project would not have been the same without my friends at the UFZ in Leipzig, who shared moments of joy and frustration with me, especially Friedrich, Tim, Saskia, Paul, Polina and Anh. I look forward to more lunch breaks. My deepest gratitude goes to my family and friends for always believing in me and encouraging me to go the last mile. Finally, my heartfelt thanks go to Vera for her thoughtful advice, enduring patience, and for always being by my side.

Abstract

Worldwide, ecosystems are increasingly stressed due to rapidly changing environmental conditions. Simultaneously, the nutritional needs of a growing world population require a highly productive agriculture, which will still rely on fertilizers and pesticides in the forseeable future. Pesticides, however, are also one of the largest contributors to the global loss of invertebrate diversity, biomass and the associated, agriculturally relevant, ecosystem functions. We are, metaphorically speaking, cutting the branch on which we all sit. In order to maintain this delicate balance, it is essential to protect the ecosystems close to arable lands. Invertebrates in surface waters are very susceptible to pesticide runoff from the field. This leads to unpredictable effects in complex aquatic communities—effects that are often much larger than thresholds determined in single species laboratory tests. Despite the increased interest in the conservation of stressed ecosystems, the mechanistic understanding of pesticide effects under higher levels of biological complexity is still limited.

This work is therefore set out to understand the processes that regulate the effects of low concentrations of pesticides under environmental complexity. To this end a sequence of investigations was conducted, increasing the complexity step by step from the individual level, to the population level until the species–species competition level. To allow for comparisons between the investigations, the standard model organism *Daphnia magna* (water flea) was exposed in all experiments to pulses of the insecticide *esfenvalerate*.

In Chapter 3, the effects of interacting stressors on individuals of *D. magna* are described. Esfenvalerate was combined with ultraviolet-B (UV-B) radiation in varying order of exposure and with different pauses between exposures in order to identify the influence of time on stressor interactions. It was shown that increased temporal distance between an esfenvalerate pulse and an environmental stress pulse, shifted the interaction between the stressors from antagonism to synergism on the individual level. It was also shown that low stressor doses elicited antagonistic responses while high doses led to synergistic responses.

The next level of complexity investigated was that of the population (Chapter 4). *D. magna* populations were non-invasively monitored during a complete development cycle. When populations at carrying capacity were exposed to ⅓ of the half maximal effective concentration (EC_{50}), 2 out of 4 replicates collapsed due to direct mortality effects of esfenvalerate. In contrast, concentrations at 1/30 and 1/10 of the EC_{50} significantly increased the population biomass for up to 7 weeks after the exposure. It was hypothesized that population increases are due to a hormetic response, where reduced *intra*specific competition is the trade-off that enabled this response.

In the final investigation (Chapter 5), populations of *D. magna* and *Culex pipiens* (mosquito larvae), competing for a limited amount of food, were exposed to repeated pulses of esfenvalerate at extremely low concentrations ($^1/_{1000}$–$^1/_{10}$ of the EC_{50}). This was done to test if the presence of a competitor changes the *inter*specific competition between co-existing species with a shared ecological niche. It was revealed that species–species correlations significantly increased after the exposure. This was associated with a decrease in *inter*specific competition. In contrast to the results shown in the previous investigation, low concentrations of esfenvalerate did not provoke a stimulatory response in the density and biomass of either population.

The level of ecological complexity had a substantial influence on the detected effects of esfenvalerate in this work. Ecological organization, stressor timing and pesticide dose had strong influences on the stress response. Those non-linearities can help to explain why it is so difficult to predict effects of pesticides in the field. The approach taken in this work suggests that environmental risk assessment (ERA) should consider *intra*specific and *inter*specific competition when assessing the effects of very low doses of pesticides on the biodiversity of ecologically similar species. By combining the results from Chapter 4 and Chapter 5, it was hypothesized that the stimulatory hormesis response, which is an increasingly discussed phenomenon, only emerges, when associated trade-offs are *not* penalized by environmental conditions.

Zusammenfassung

Aufgrund der sich rasch verändernden Umweltbedingungen stehen Ökosysteme weltweit zunehmend unter Druck. Gleichzeitig erfordert der steigende Nahrungsmittelbedarf einer wachsenden Weltbevölkerung eine hochproduktive Landwirtschaft, welche auch zukünftig auf Düngemittel und Pestizide angewiesen sein wird. Allerdings werden Pestizide auch mit dem weltweiten Rückgang der Biodiversität und Biomasse von wirbellosen Tieren in Verbindung gebracht. Die damit verbundene Reduktion von landwirtschaftlich relevanten Ökosystemfunktionen ist sehr besorgniserregend. Um diese Funktionen zu erhalten, müssen Ökosysteme in der Nähe von Ackerflächen besser geschützt werden. Wirbellose Tiere in Oberflächengewässern sind sehr anfällig gegenüber Pestiziden, die vor allem bei Starkregen von Feldern gespült werden. Dies führt zu unvorhersehbaren Auswirkungen in komplexen, aquatischen Gemeinschaften, welche oft um ein Vielfaches größer sind als Effekte, die in Labortests für einzelne Arten ermittelt wurden. Trotz des zunehmenden Interesses am Erhalt von Ökosystemen ist das mechanistische Verständnis der Wirkungen von Pestiziden bei biologischen Systemen höherer Komplexität noch immer begrenzt.

Ziel dieser Arbeit ist es daher, jene Prozesse zu verstehen, die die Auswirkungen niedriger Pestizidkonzentrationen unter komplexen Umweltbedingungen regulieren. Zu diesem Zweck wurde eine Reihe von Untersuchungen durchgeführt, bei denen die Komplexität schrittweise von der individuellen Ebene über die Populationsebene bis hin zur Ebene der kompetitiven Gemeinschaft erhöht wurde. Um Vergleiche

zwischen den Untersuchungen zu ermöglichen, wurde in allen Experimenten der Standardmodellorganismus *Daphnia magna* (Wasserfloh) verwendet und die Auswirkungen des Insektizids Esfenvalerat untersucht.

In Kapitel 3 wurden die Auswirkungen von interagierenden Stressoren auf Individuen der Art *D. magna* untersucht. Esfenvalerat wurde mit ultraviolett-B (UV-B) Strahlung in unterschiedlicher Reihenfolge und mit verschieden langen Pausen zwischen den Expositionen kombiniert, um den Einfluss der Zeit auf die Wechselwirkungen zwischen Stressoren zu ermitteln. Es zeigte sich, dass ein größerer zeitlicher Abstand zwischen den Expositionen die Interaktion zwischen UV-B Strahlung und Esfenvalerat auf individueller Ebene vom Antagonismus zum Synergismus verschob. Außerdem wurde beobachtet, dass niedrige Dosen von Stressoren antagonistische Reaktionen auslösten, während hohe Dosen zu synergistischen Reaktionen führten.

Die nächste Ebene der untersuchten Komplexität war die der Population (Kapitel 4). *D. magna* Populationen wurden nicht-invasiv über einen kompletten Entwicklungszyklus beobachtet. Wenn Populationen nach exponentiellem Wachstum an der Grenze ihrer Tragfähigkeit mit ⅓ des EC_{50} exponiert wurden, brachen 2 von 4 Wiederholungen aufgrund direkter Mortalitätseffekte von Esfenvalerat zusammen. Im Gegensatz dazu führten Konzentrationen von 1/30 und 1/10 des EC_{50} zu einem signifikanten Anstieg der Populationsbiomasse, der bis zu 7 Wochen nach der Exposition andauerte. Es wurde angenommen, dass die Zunahme der Populationen auf eine Hormesis-Reaktion zurückzuführen ist, wobei die reduzierte *intra*spezifische Konkurrenz der energetische *Trade-off* war, der diese Reaktion ermöglichte.

In der abschließenden Untersuchung (Kapitel 5) wurden konkurrierende Populationen von *D. magna* und *Culex pipiens* (Stechmückenlarven) wiederholten Esfenvaleratpulsen in extrem niedrigen Konzentrationen (1/1000–1/10 des EC_{50}) ausgesetzt. Damit wurde getestet, ob eine Pestizidexposition den *inter*spezifischen Wettbewerb zwischen koexi-

stierenden Arten mit einer gemeinsamen ökologischen Nische verändert. Es zeigte sich, dass die Korrelationen zwischen den Arten nach der Exposition mit extrem niedrigen Pestizidkonzentrationen deutlich zunahmen. Dies konnte mit einer Abnahme der *inter*spezifischen Konkurrenz in Verbindung gebracht werden. Im Gegensatz zu den Ergebnissen der vorangegangenen Untersuchung hatten niedrige Esfenvaleratkonzentration keine stimulierende Wirkung auf die Dichte und Biomasse der beiden Populationen.

In dieser Arbeit hatte der Grad der ökologischen Komplexität einen wesentlichen Einfluss auf die festgestellten Auswirkungen von Esfenvalerat. Die ökologische Organisation, der Zeitpunkt der Stressexposition und die Pestiziddosis hatten starken Einfluss auf die Stressreaktion. Diese Erkenntnisse können einen Beitrag leisten, die Auswirkungen von niedrigen Pestizidkonzentrationen im Feld zu erklären. Der in dieser Arbeit verfolgte Ansatz legt nahe, dass die Bewertung von Auswirkungen sehr niedriger Pestiziddosen auf die biologische Vielfalt ökologisch ähnlicher Arten sowohl die *inter*spezifische als auch die *intra*spezifische Konkurrenz berücksichtigen sollte. Durch die Zusammenführung der Ergebnisse aus Kapitel 4 und Kapitel 5 wurde die Hypothese aufgestellt, dass zunehmend diskutierte stimulierende Hormesis-Reaktionen nur dann auftreten können, wenn damit verbundene *Trade-offs* nicht durch entsprechende Umweltbedingungen kompensiert werden.

Contents

List of Figures

List of Tables

List of Symbols

$\mathbf{CO_2}$	carbon dioxide
C	carbon
$\mathbf{NH_4^+}$	phosphate
$\mathbf{NO_2^-}$	nitrite
$\mathbf{NO_3^-}$	nitrate
N	nitrogen
$\mathbf{PO_4^{3-}}$	phosphate
P	phosphorus

List of Abbreviations

ADaM	Aachener Daphnien Medium
CA	concentration addition
CAS	Chemical Abstracts Service
CI	credible interval
DMSO	dimethylsulfoxide
DNA	deoxyribonucleic acid
drc	dose–response curves
EC	effect concentration
$\mathbf{EC_{50}}$	concentration at which 50% of a population shows an effect (e.g. mortality)
EFSA	European Food Safety Authority
EPA	Environmental Protection Agency
ERA	environmental risk assessment
ESR	environmental stress response
GC-MS	gas chromatography–mass spectrometry
GC-MS/MS	gas chromatography–triple quadrupole mass spectrometry
HDI	highest density interval
IA	independent action
KDE	kernel density estimate

LOQ	limit of quantification
MAP	maximum a posteriori
MCMC	Markov Chain Monte Carlo
NaN	Not a Number
OECD	Organisation for Economic Co-operation and Development
pd	probability of direction
pdf	probability density function
PDI	posterior density interval
PyMC	a probabilistic (bayesian) programming library for Python
R	a programming language for statistical computing
RHS	right hand side
ROS	reactive oxygen species
SAC	stressor action curve
SAM	stress addition model
SVM	support vector machine
TKTD	toxicokinetic-toxicodynamic
UV-B	ultraviolet-B
VGSC	voltage gated sodium channels
WFD	Water Framework Directive

Chapter 1

Introduction

Species are going extinct at rates 100–1000 times larger than prehistoric background extinction rates (Pimm et al., 2014). As if studies like this were not disconcerting enough, a growing number of studies report the decline of abundance and biomass of insects (Hallmann et al., 2017; Rundlöf et al., 2015; Wagner, 2020; Stuligross and Williams, 2021), reflecting anecdotal reports of fewer smashed insects on windshields of cars or lower number of moths buzzing around street lamps. All this while novel substances are emitted into the environment at increasing rates, overwhelming the capacity of ecosystems to deal with constantly renewing challenges (UNEP, 2019; Persson et al., 2022).

The loss of biodiversity and ecosystem quality leads to impoverished ecosystem functions. This harms not only wildlife but undermines the foundations that human existence is built upon. Functioning ecosystems produce biomass, decompose organic matter, cycle and retain nutrients (Hooper et al., 2012; Cardinale et al., 2012) and provide services like pollination (Vanbergen and the Insect Pollinators Initiative, 2013). If the provision of these services ended, the global annual cost of the pollination service alone would be an estimated $215 billion.

Of all animal species, invertebrates are by far the most abundant (May, 1988), and it is recognized that invertebrates are the workhorses of

ecosystems, both on land and in the water. In a response to the question, *"Why should I care about bugs in the mud?"*, Suter and Cormier (2015) listed an extensive catalogue: Invertebrates are food for fish and birds, insects retain nutrients in their biomass and return them to the terrestrial landscape when they emerge. As shredders they break down leaf litter, ensuring the integrity of forest streams and thus maintain habitats. Filter feeders grow in spring and summer and keep the algae blooms in eutrophic lakes at bay. Finally, invertebrates serve several recreational and educational purposes—so, we should care.

1.1 Pesticides in the Aquatic Environment and Their Influence on the Invertebrates in Freshwater Bodies. Limitations of Aquatic Risk Assessment

Pesticides are an ubiquitous source of pollution in water bodies around the world. They have been linked to altered invertebrate community composition (Schäfer et al., 2007) and were repeatedly associated with the loss of invertebrate biodiversity (Beketov et al., 2013; Stehle and Schulz, 2015) and deterioration of ecosystem services (Malaj et al., 2014).

Many classes of pesticides are used today including herbicides, fungicides and insecticides. Insecticides like neonicotinoids can accumulate in the soil and leach to surface waters (Goulson, 2013) and affect waterborne emerging insects. The most sensitive taxa are *Trichoptera*, *Diptera* and *Ephimeoptera* (Morrissey et al., 2015). The case of neonicotinoids exemplifies very well that a risk assessment, which is until today predominantly based on single species tests (Figure 1.1), can severely underestimate the risks of pesticides. Because the standard test species, *D. magna*, is insensitive to neonicotinoid insecticides (Beketov and Liess, 2007; Wood and Goulson, 2017), the risks for other non-target organisms were largely underestimated leading to the well

known decline of bee populations (Rundlöf et al., 2015; Cressey, 2017; Stuligross and Williams, 2021).

Of course a growing world population will still rely on the use of pesticides for the coming years in order to sustain high productivity of agricultural systems and support the growing demand for food. However, considering the previously listed ecological side effects of pesticide use, it is vital to understand their effects in complex ecosystems, so that damage of pesticide use can be minimized and neonicotinoid-like scenarios can be prevented.

In order to monitor and protect the ecological functioning of its water bodies, the European Union launched the Water Framework Directive (WFD) (European Union, 1988; European Parliament, 2000) and implemented Directive 2009/128/EC for the sustainable use of pesticides (European Parliament, 2009). This legislation enabled the EU to restrict the use of harmful pesticides, such as neonicotinoids (Stokstad, 2018). However, other pesticides quickly filled this gap and today pyrethroids emerge as the main replacement in agricultural applications (Jactel et al., 2019). Therefore, it comes as no surprise that the ecological status of 60% of surface waters in the European Union are still in moderate, poor or bad ecological status. In densely populated areas such as Germany this figure is much higher (80%), indicating that still in 2018 surface waters in the vicinity of human activity are under massive stress (EEA, 2018).

While the ecological status of ecosystems is also affected by nutrients (Gieswein et al., 2017; Birk et al., 2020), it is assumed that the risks of pesticides are still underestimated (Stehle and Schulz, 2015). Reasons for this include the insufficient monitoring of pesticides, missing peak exposures after heavy rain events (Chow et al., 2020; Halbach et al., 2021). In a large scale study on small rivers in Germany, Liess et al. (2021) showed that pesticides are the main driver of loss of sensitive invertebrate species in lowland streams at concentrations 3 orders of magnitude below the half maximal effective concentration

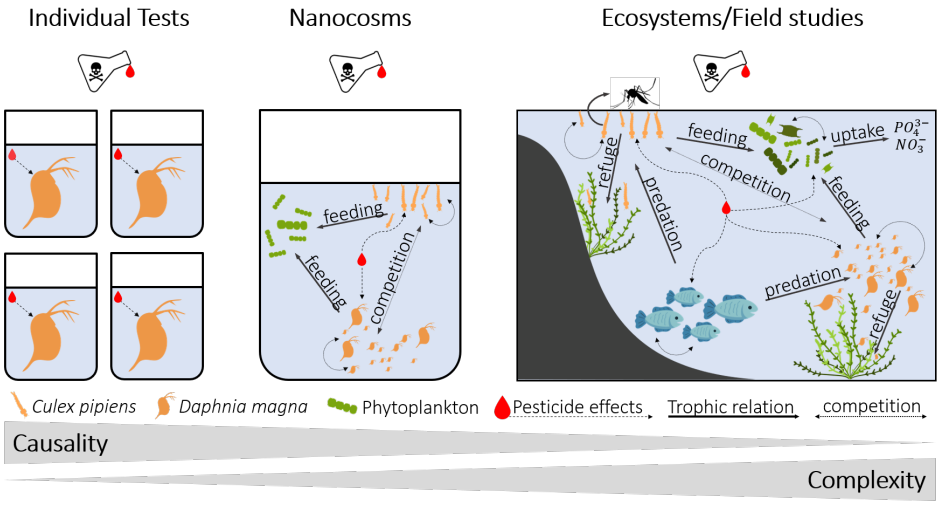

Figure 1.1: Pesticide effects on 3 levels of biological complexity. Individual tests, used in routine risk assessment, have a low complexity. The causality between pesticide exposure and effect is easily established, but this comes at the cost of low environmental realism, which limits the transfer of effects observed in the laboratory to conditions present in the field. The other extreme is encountered in field studies, where pesticide may elicit effects on multiple groups in trophic networks. Under such complex conditions it is difficult to understand the mechanisms by which pesticides act. Nanocosms that are employed in Chapters 4 and 5 are a middle ground and allow insights into effects mechanisms.

(EC_{50}) determined in single-species laboratory studies. Even scales of complexity lower, single organism dose-response relationships cannot be extrapolated to experimental mesocosms (Gessner and Tlili, 2016). Similar studies recently accumulate and support the assumption that risks of pesticides cannot be predicted from single species laboratory tests (Fleeger et al., 2003; Knillmann et al., 2012a,b; Alexander et al., 2016; Vaugeois et al., 2020; Allen et al., 2021). This relationship between decreasing predictability between pesticide exposure and effects under increasing complexity is illustrated in Figure 1.1.

1.2 Considering the Environmental Context to Assess the Effects of Ultra-Low Concentrations of Pesticides

The mismatch between concentrations at which effects are observed in the field and those determined in low-level laboratory studies indicates that unknown factors confound the effect of pesticides and other anthropogenic stressors (see Box 1, Figure 1.1). Interactions of pesticides with environmental stressors can increase the impact of toxicants in the field (Lemm and Feld, 2017; Laetz et al., 2009) and in the laboratory (Holmstrup et al., 2010; Shahid et al., 2019). On the contrary, other studies show that stressors may not interact at all (Dinh et al., 2016; Cheng et al., 2015; Kath et al., 2018). Finally, meta-analyses show that toxicants can interact synergistically, antagonistically, or additively with environmental stressors without identifying a central tendency (Jackson et al., 2016; Birk et al., 2020).

Box 1: Stress

Stress is defined as environmental change that affects functioning of an organism (Calow, 1989; Parker et al., 1999; Heugens et al., 2001). Environmental change can be physical (temperature, radiation), chemical (oxygen, pH, toxicants) or biological (density of competitors, predators). However, in the course of evolution, changing environmental conditions have been the norm rather than the exception, and it can be assumed that the organism is adapted to tolerate stressful conditions up to species specific energetic constraints (Sokolova et al., 2012; Sokolova, 2013). Depending on the frequency and intensity, exposure to multiple stressors can lower the threshold for adverse effects. This concept has been partially dealt with in the formulation of the concentration addition (CA) model where concentrations of toxicants with a similar mode of action can be summed to an effect concentration (Bliss, 1939; Altenburger et al., 2000). It has been extended with the stress addition model (SAM) by Liess et al. (2016) to model the effects of environmental stress and toxicants (multiple stress).

The issue is confounded even further by hormesis theory, which postulates beneficial effects from low doses of stressors (Schulz, 1888; Stebbing, 1998; Calabrese, 2010). Due to a rising research interest, a number of studies accumulated showing positive feedbacks of small doses of toxicants (Calabrese and Mattson, 2017; Wolz et al., 2021; Shang et al.,

2021). While these findings are usually constrained to effects on the individual or population level (Agathokleous et al., 2022), they certainly raise the question, whether such non-linear dose-response relationships (Calabrese and Baldwin, 2003; Costantini, 2019; Liess et al., 2019a) need to be considered in environmental risk assessment (ERA).

This bouquet of results paired with the repeated discovery of strong ecological effects under low exposure concentrations indicates that comprehensive understanding of the ecological effects of especially low doses of pesticides is still lacking (Liess et al., 2019b). There are several reasons that can explain this lack of accuracy in predicting the effect of toxicants in complex ecosystems. Habitat structure and physico-chemical parameters can obscure causal effects between chemical stress and biological responses in field studies (Rico et al., 2016). Moreover, pesticide contamination can trigger cascading effects in ecosystems (Figure 1.1), leading to indirect community effects depending on interactions between species in food webs (Fleeger et al., 2003). In order to overcome this difficulty, Orr et al. (2020) suggest to study the effects of stressors under temporal and biological complexity. Especially, understanding the role of biological organization in effects of stressors is emerging to become the top priority of researchers and risk assessors (van den Brink et al., 2018; Simmons et al., 2021) to foster safer use of chemicals in the environment.

Due to multiple levels of biological organization, the supposed non-linearity in dose–response relationships (hormesis), and the interaction with anthropogenic and environmental stressors, disentangling cause and effect of single or multiple stressors is very difficult. As illustrated by Figure 1.1, standard tests are too simple to predict effects and field studies too complex to understand the causes of effects of pesticides. In order to gain mechanistic understanding, it is therefore necessary to take a step back in the complexity of experiments and investigate stressors in the context of controlled but complex laboratory systems.

1.3 Aims and Hypotheses

Understand Low Dose Effects

The aim of this work is to investigate the effect mechanisms of ultra-low pesticide doses. Reasons are findings of ecological effects in the field far below the EC_{50} and conflicting reports of stimulatory effects of low doses (hormesis) on individuals and populations.

This work studies the factors and mechanisms, which are suspected to play a central role in the emergence of strong ecological effects under exposure to ultra-low concentrations of pesticides. In addition, this works aims to shed light on the reasons for the reported variability of interactions between multiple stressors. Given the limited scope of this work, those factors that are ubiquitous in nature have been selected to advance our understanding of pesticide effects in complex biological systems.

THE DIMENSION OF TIME is ubiquitous in the research of multiple stressors. Due to a large variety of possible patterns of stress events and the infinite number of resulting combinations when long term development of ecological systems is considered (Ryo et al., 2019), time becomes an inevitable variable when confounding factors for risk assessment are studied. In ecological environments, pulses of pesticides (Liess and Schulz, 1999; Wittmer et al., 2010; Halbach et al., 2021) and environmental stressors such as heat waves and ultraviolet-B (UV-B) radiation (Lhotka et al., 2018; Masson-Delmotte et al., 2021) may occur in arbitrary order and temporal distance. It is assumed that the likelihood for non-additive interaction between stressors increases if they occur in temporal proximity (Gunderson et al., 2016) and it was shown that past stress exposure can increase the effect of a second exposure, if the toxicokinetic and toxicodynamic properties of the principally exposed toxicant prolong the duration of its effect so that it can interact with a later exposed substance (Ashauer et al., 2007, 2017). It has so far not been researched if this phenomenon extends to interactions with environmental stressors,

Time Hypothesis (1)

Interactions between pesticides and environmental stress depend on the timing and order of exposures. (Chapter 3)

and, if it holds for exposures to different doses. This leads to Hypothesis 1, which will be discussed in Chapter 3.

Competition Hypothesis (2)

The effect of low-dose pesticides on aquatic populations is dependent on the degree of competition in the system. Related questions to be considered, are:

How do populations respond to exposure to low concentrations of pesticides when the competition within the population is large? (Chapter 4)

In what ways does strong competition between species modulate the effects of repeated exposure to low concentrations of pesticides? (Chapter 5)

THE DEGREE OF COMPETITION WITHIN AND BETWEEN SPECIES in the environment and laboratory experiments is of superior importance for the assessment of pesticide effects. Density dependent processes regulate the abundance of populations in many ecological systems (Malthus, 1798; Volterra, 1928; de Roos et al., 1992). In other words, populations grow, when their food source is abundant and decline when it is depleted, which in turn leads to renewed growth of the food source. Especially, when the food source for a population is scarce, the influence of competition between individuals within populations (*intra*specific competition), but also between populations of different species (*inter*specific competition) is expected to increase. Therefore, it is no surprise that populations react differently to acute pesticide exposure depending on their developmental stage (Stark and Banken, 1999; Hanazato and Hirokawa, 2004). Young, exponentially growing populations, can overcome the effects of acute exposure to pesticides faster then mature, stationary population (Pieters and Liess, 2006). What, however, are the population responses of exposure to ultra-low doses of pesticides when the competition for resources is high? This question is addressed in Chapter 4. In nature, competition for resources between different species is extremely common. This process leads to diversification of the less fit species into its own ecological *niche* (Gause, 1936; Hardin, 1960). Often, however, competitors co-exist that share resources to varying degrees (MacArthur, 1958; Pastore et al., 2021). Such co-existence is a cornerstone of resilient ecosys-

tems, since functions and food-chains can be maintained even if one population breaks down. Repeated exposure to pesticides can disrupt the balance between competitors at acute concentrations (Liess et al., 2013), but how do competing species react to the repeated exposure of ultra-low concentrations of pesticides? This question will be studied in Chapter 5. Hypothesis 2 will be assessed in Chapter 6 by jointly discussing the findings from Chapters 4 and 5 and comparing them to results from Chapter 3, where no competition was present.

ENVIRONMENTAL CONDITIONS can influence the effects of pesticides. Increased mortality of test organisms has been observed at low food concentrations (Heugens et al., 2001; Pieters et al., 2005; Beketov and Liess, 2005; Shahid et al., 2019). While this result is intuitive, it is even more surprising that risk assessment is routinely conducted unter standard conditions that assume saturated food conditions, which is a rare environmental scenario (Stevenson et al., 2017). Also other environmental parameters have been shown to interact with pesticides, but, as indicated in Section 1.2, findings do not conclusively indicate whether interactions with environmental stressors always result in synergistic or antagonistic interactions with pesticides. Throughout Chapters 3 to 5, the question of interactions between environmental conditions and pesticides will be addressed and common factors will be discussed in Chapter 6.

The next Chapter will outline the overarching experimental approach to tackle the listed questions and hypotheses. The selected pesticide, esfenvalerate, which has been used in all studies will be introduced in Section 2.1 along with the main test organism, *D. magna* (Section 2.2). The method of non-invasive population monitoring will be described in Section 2.3, and the bayesian approach to statistical inference will be briefly summarized in Section 2.4.

Chapter 2

Overall Experimental Approach

As a methodological approach, the complexity of the studied systems will be stepwise increased to build an understanding of the underlying mechanisms of the studied systems. At the same time, the main characteristics of the experiment will be kept constant in order to learn about the influence of varying factors across biological scales. *Daphnia magna* was used as a well studied model organism to study pesticide effects from the individual to the community level. The pesticide *esfenvalerate* was used as a chemical stressor of the class of pyrethroids. In order to approach realism the applied concentrations of esfenvalerate were reduced with increasing order of complexity, assuming that higher levels of complexity can reveal subtler effects as compared to low levels of complexity.

2.1 Properties of the Pyrethroid Insecticide Esfenvalerate

After concerning reports about the ecological effects of neonicotinoids (Rundlöf et al., 2015; Cressey, 2017), most neonicotinoids were banned in Europe and their usage is also being reevaluated in the USA. Farmers now turn to pyrethroids, which emerge as the most common alter-

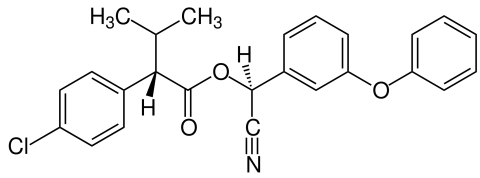

Figure 2.1: Structure formula of esfenvalerate. Chemical Abstracts Service (CAS)-number: 66230-04-4, molecular weight = 419.9 g mol^{-1}, logP = 6.2, solubility = 2 µg/L at 25°C

native in agricultural applications (Jactel et al., 2019). Esfenvalerate, as a type-II pyrethroid, affects the peripheral nervous system and its main mode of action is the blockage of voltage gated sodium channels (VGSC), which increases the opening times of these channels and disrupts the nerve signalling. Ultimately this process leads to incoordination, paralysis and convulsions (Soderlund, 2005; Werner and Moran, 2008; Palmquist et al., 2012). For filter feeders such as *D. magna*, these effects imply reduced feeding rates (Reynaldi et al., 2006) and if recovery does not take place, death occurs due to starvation after several days.

Consequently, pyrethroids produce a whole range of ecologically relevant effects on invertebrates such as increased mortality rates in insects at 1/100 half maximal effective concentration (EC_{50}) for the caddisfly *Limnephilus lunatus* (Liess, 2002) and at 1/1000 EC_{50} for the mayfly *Cloeon diperum* (Beketov and Liess, 2005). Further, low doses of pyrethroids affect feeding at 1/10 EC_{50} for *D. magna* (Christensen et al., 2005), reduce swimming behavior of *Hyalella azteca* (Hasenbein et al., 2018) and energy allocation to offspring between 1/1000–1/10 EC_{50} for *Daphnia schoedleri* (Martínez-Jerónimo et al., 2013). In addition, also stimulatory effects for various organism types are observed between 1/10–1/100 EC_{50} (Gottardi et al., 2017; Margus et al., 2019; Shang et al., 2021; Wolz et al., 2021). In the aquatic environment, pyrethroids generally occur as short pulses in the water phase, due to their fast dissipation from the water column. In surface waters, maximum concentrations of only 1–2 orders of magnitude below the acute EC_{50} (*D.*

magna) were detected (Rösch et al., 2019a,b) while median concentrations range around 3–4 orders of magnitude below the acute EC_{50}. In ditches close to agricultural fields (close to the source of input), the measured concentrations of pyrethroids may be much higher, even above the EC_{50} (Bennett et al., 2005). The *D. magna* EC_{50} of esfenvalerate lies approximately at 300 $ng\ L^{-1}$ (Table A.1). This means that test concentrations between 0.01–1000 $ng\ L^{-1}$ can be considered environmentally relevant.

Table 2.1: EC_{50} for *D. magna* immobility after 48 h. NR = not reported, AI = Active Ingredient. F = Formulation. Data retrieved from Environmental Protection Agency (EPA) database (`https://cfpub.epa.gov/ecotox/search.cfm`). Mean $EC_{50} = 0.31 \pm 0.33$ µg/L

Exposure Type	Organism Age (h)	Concentration (AI µg/L)	Source
Static (AI)	NR	0.89	Chevalier et al. (2015)
Static (AI)	< 24	0.05	Bjergager et al. (2012)
NR (AI)	< 24	0.16	Bjergager et al. (2012)
Static (F)	< 24	0.18	Ma et al. (2009)
Static (AI)	< 24	0.27	Fairchild et al. (1992)

2.2 *Daphnia magna* as a Model Organisms

Systematically the species *Daphnia magna* belongs to the genus of water fleas (*Daphnia*). It is placed in order of *Cladocera*, which resides in the phylum of invertebrate organisms (*Arthropoda*). In an excellent review, Ebert (2022) outlines several unique properties of this versatile model organism, such as its transparent body and short and predominantly asexual reproduction cycle (Figure 2.2).

Due to such properties, D. magna is the preferred toxicological test species for aquatic toxicology screening. In fact Organisation for Economic Co-operation and Development (OECD) protocols exist for acute (OECD, 2004) and chronic (OECD, 2012) toxicity testing that

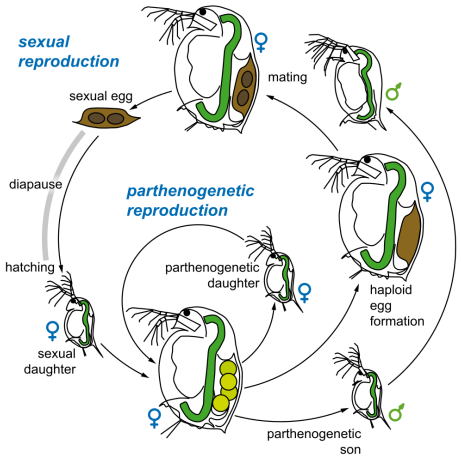

Figure 2.2: The life cycle of *D. magna*. Under laboratory conditions, *D. magna* predominantly follow the (haploid) parthenogenic reproduction cycle. The sexual reproduction cycle can be triggered by adverse environmental conditions. Diploid (sexual) eggs, can survive many years until favorable conditions occur again, launching another cycle of haploid reproduction. Figure conceptualized by D. Vizoso and D. Ebert, Drawing by D. Vizoso (`https://upload.wikimedia.org/wikipedia/commons/3/37/DaphniaMagna_LifeCycle_DVizoso.svg`)

were specifically developed for *D. magna*. As a filter feeder it is considered a keystone species in standing water bodies and ponds across a wide area of geographical distribution, contributing to its relevance as a test organism (Ebert, 2022). For risk assessment in the aquatic environment, the European Food Safety Authority (EFSA) and EPA rely on D. magna for it's lowest level (Tier 1) screening to assess eligibility of novel compounds for approval of use and determination of safe levels of application (European Food Safety Authority, 2013).

Responses of *Daphniae* are studied over a wide range of toxicants and environmental stressors, for example pesticides and their mixtures (Maggio and Jenkins, 2021; Chevalier et al., 2015; Martínez-Jerónimo et al., 2013; Navis et al., 2013; Bjergager et al., 2012; Relyea and Diecks, 2008; Werner and Moran, 2008; Andersen et al., 2006), predator presence (Graeve et al., 2021), metals and their mixtures (Hansul et al., 2021; da Silva et al., 2020; Soetaert et al., 2007) nanoparticles

(Lesser et al., 2022), nutrients (Serra et al., 2019), ultraviolet-B (UV-B)-radiation (Song et al., 2020; Wonkwon et al., 2019; Beketov et al., 2011; Hansson and Hylander, 2009), and temperature (Betini et al., 2019; Wojtal-Frankiewicz, 2012; van Doorslaer et al., 2009).

2.3 Non-Invasive Population Monitoring through Imaging and Motion Detection

Populations of single and competing species should be monitored to understand the alterations of population dynamics provoked by the exposure to acute and low doses of pesticides. How these populations are monitored also influences how successful and how sensitive such studies can be. Typically, experimental systems are filtered and organisms are returned to the systems after a census (Vlaeminck et al., 2020; Palamara et al., 2022). While this method is obviously the most accurate, it has 2 major caveats. It is time and labor consuming making this method unattractive for routine assessment of risks of toxicants, and the removal of organisms itself is a disturbance of the system (Sims et al., 1993; Rousseaux et al., 2010). Therefore, it can be doubted whether this method is suitable to assess subtle effects of extremely low dosed pesticides.

For this reason, in population studies conducted in this work, non-invasive monitoring via imaging and detection algorithms was applied. Because the applied methods differ in the studies in Chapter 4 and Chapter 5, here, only the general approach will be outlined.

The basis for this approach is build on the detection of motion in a series of consecutive images that are taken from a single system with a static camera (Pieters and Liess, 2006; Foit et al., 2012). Computationally, images are just arrays of integers. Each index of the array contains an integer in the interval [0, 255]. The principle of motion detection lies in the background subtraction. Consider two exactly identical images. Subtracting one from the other would result in a

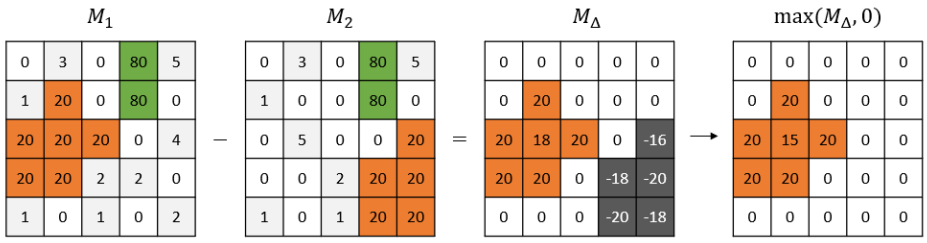

Figure 2.3: Basic algorithm of motion detection for the example of a grayscale image of size 25 pixels. Values indicate the brightness of a pixel. Orange pixels indicate a moving object which changes its position from M_1 to M_2, and dark-gray pixels represent its negative (the position it has moved to). White and gray pixels represent white noise on the background and green pixels represent a fixed object which is of greater brightness than the moving object. By element-wise computation of the difference M_Δ and $\max(0, M_\Delta)$

difference of zero in all indices of the matrix. Now consider two images M_1 and M_2 with a static background, where parts of the image are moving (Figure 2.3). The difference of such a pair of images will contain all moving objects twice (M_Δ). For this reason the resulting matrix should be trimmed to positive numbers to only include the initial location of the moving objects.

Due to white noise in the imaging process, pre- and post-processing steps can improve the sensitivity of the algorithm. To reduce noise, and consequently false-positive detections, images can be convoluted during pre-processing. This process takes the average of an $n \times n$ kernel. A very typical post-processing step is thresholding to separate movement from noise. In the example given above (Figure 2.3), a good threshold would lie between 0 and 15, in order to capture the complete signal. Static objects that are brighter than the objects of interest (green pixels, Figure 2.3) can complicate the detection and the associated problems will be discussed in Section 5.4.

2.4 Using Bayesian Methods to Quantify Uncertainty in Ecology

In this work, bayesian methods will be used throughout all chapters. In order to familiarize the reader with the method, some introductory concepts are provided and the theory is explained with a bayesian model that is used in Chapter 5.

$$Pr(\theta \mid Y) = \frac{Pr(\theta)\ Pr(Y \mid \theta)}{Pr(Y)} \tag{2.1}$$

$$Posterior \approx Prior \times Likelihood \tag{2.2}$$

Equation 2.1 is also known as Bayes Theorem and it is used to calculate conditional probabilities. It reads as: The probability of a set of parameters θ, conditional on the observed data Y is equal to the joint probability of the probability of the parameters and the probability of the likelihood of the data given the set of parameters, divided by the probability of the observations Y. Because the calculation of the denominator $Pr(Y)$ of the equation is complicated, it is usually ignored due to its independence of the parameters (no θ is involved) and considered as a proportionality constant, which ensures that the resulting probability function integrates to 1. Thus, equation 2.2 contains the remaining components of the equation that actually bear relevant concepts for the understanding of uncertainty in statistics—*posterior*, *prior* and *likelihood*.

For simple examples it is possible to calculate an analytical solution of equation 2.1. However, due to the rise of computational power, it is nowadays much easier to simply calculate results of the right hand side (RHS) of equation 2.1 very often for random samples of the parameter θ, and to record parameters with a high probability proportionally more often than parameters with a low probability. This is essentially a description of Markov Chain Monte Carlo (MCMC) (Robert and Casella, 2011), which removes the constraint to assume normality of

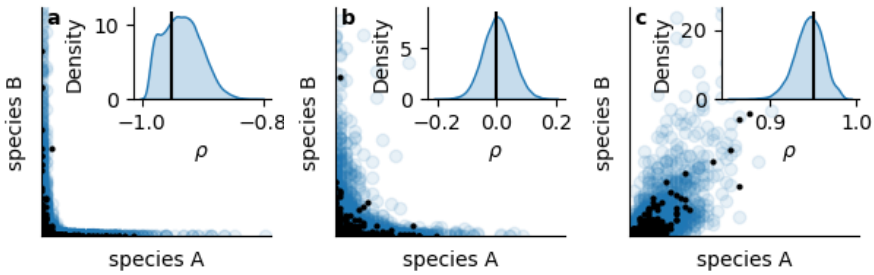

Figure 2.4: Estimation of covariance structure and its associated uncertainty of simulated population abundance ($N = 1000$). The black vertical line indicates the true correlation between species A and B and black dots are simulated samples. The blue markers indicate the observational uncertainty of in the phase-space of species abundances (i.e. where, conditional on the data, the model would expect to observe abundance pairs.). The blue curve shows the estimated posterior of the correlation between A and B recovered from the and its associated uncertainty. It indicates that the true correlation can be recovered very well with the model specified in equations 2.3–2.8). **a**) highly negative correlation ($\rho = 0.95$), impossible co-existence. **b**) no correlation ($\rho = 0.0$), species do not interact or are not influenced by the same environmental drivers. **c**) strongly positive correlation ($\rho = 0.95$), species share a common resource or have a highly dependent synchronized mutual dependence.

the underlying parameter distributions. As an example, consider the relationship between the covariance of two species and their degree of coexistence, which will be needed in Chapter 5 to assess the competition between species across replicated test systems. Suppose two species (A and B) cannot coexist in the same environment. In any snapshot of an environment, if species A is abundant, the density of species B must be very low and vice versa. This state is reflected by Figure 2.4a. Note that the bayesian posterior density estimate of the correlation between species A and B was estimated to lie between -0.8 and -1.0 with a maximum near -0.95, which is the true correlation coefficient that was used to simulate the data. In comparison, calculating the Pearson or Spearman correlation coefficient, will estimate a correlation of -0.1 or -0.5, respectively, which is a gross underestimation of the true effect. The following bayesian model explains how to derive such solutions.

$$N_s \sim Poisson(\lambda_s) \tag{2.3}$$
$$\lambda_s = e^{log(\lambda_s)} \tag{2.4}$$
$$log(\lambda_s) \sim MultivariateNormal(mu = \mu_s, covariance = cov) \tag{2.5}$$
$$cov \sim LKJ(\eta = 1, \sigma_s) \tag{2.6}$$
$$\mu_s \sim Cauchy(0, 1) \tag{2.7}$$
$$\sigma_s \sim HalfCauchy(1) \tag{2.8}$$

Box 2: Bayesian Statistics

A bayesian *posterior* estimates the parameters of a statistical model along with their associated **uncertainty**. Modern probabilistic frameworks like **PyMC** can be used to directly estimate interpretable parameters of ecologically relevant questions, by formalizing them in statistical models (e.g. equations 2.3–2.8).

The degree of co-existence between two species directly corresponds to the correlation between their *log* occurrence-rates, which follow a multivariate Normal distribution.

The above system of equations can be related to the RHS of the posterior (equation 2.2). The *likelihood* in this example is represented by equation 2.3. It states that the probability of observing N individuals of species s is Poisson distributed with the rate parameter λ. So, how to get the correlated rate parameters λ for both species? The answer is sampling. For each of the model parameters a random sample θ_i^* is drawn and compared against the specified prior distributions (equations 2.5–2.8); and the resulting data distribution (equation 2.3, the likelihood) is compared against the observed data. Sometimes, parameters need to be transformed to follow requirements of the used distributions; in the case of equation 2.4, the rate parameters λ_s of Poisson distribution can only be positive, which is why the $log(\lambda_s)$ parameter was exponentiated. Finally all computed probabilities are multiplied so that the posterior probability of any random parameter sample is the product of the likelihood and the probability of the parameter sample under their specified priors. With an increasing amount of samples, parameters that are likely to represent the data are sampled proportionally more often than parameters that are less likely to represent the data well. The resulting distri-

bution (histogram) of samples approximates the posterior parameter distribution (equation 2.2).

Translated into plain language this means, the parameters of a bayesian model will represent the best possible compromise between the data and the *a priori* assumptions of its parameters. In this work, weakly informative priors were used, which rule out extreme parameter combinations but allow the posterior estimate be governed by the data. For a comprehensive overview of the theory of bayesian statistics the reader is referred to McElreath (2015) and Salvatier et al. (2016) for the original publication of the probabilistic modeling framework, *PyMC*, for Python which is used in this work.

Chapter 3

Time Between Stressors Turns Antagonism into Synergism[1]

3.1 Introduction

Multiple stress effects are of emerging concern as interactions between drivers of ecosystem change may result in synergistic effects on populations (Liess et al., 2016), resulting in unexpected unpredictable effects for ecosystems (Vinebrooke et al., 2004; Chapin and Díaz, 2020; Simmons et al., 2021). The problem is further exacerbated by the existence of a variety of temporal sequences of different stressors (Ryo et al., 2019). Among these, stress pulses are particularly common in nature. For example, storm events channel pesticides from fields into aquatic environments in the form of pulses (Liess and Schulz, 1999; Liess et al., 1999; Wittmer et al., 2010; Halbach et al., 2021; Liess et al., 2021). Also, ultraviolet-B (UV-B) radiation is an intrinsically pulsed stressor due to its dial nature and dependence on cloud cover. Heat waves may further increase the risk of occurrence and intensity

[1]Published in a slightly modified form as: Schunck F, Liess M. 2022. Time between Sequential Exposures to Multiple Stress Turns Antagonism into Synergism. Environ. Sci. Technol. 56(20):14660–14667.

(Schoetter et al., 2015; Lhotka et al., 2018; Masson-Delmotte et al., 2021; Neale et al., 2021; Singh et al., 2021) of those pulsed stressors, which can occur in any arbitrary order or temporal alignment in nature.

In such dynamic exposure scenarios, it is key to understand the effect of time gaps between stress pulses and the effects of stressor order. For instance, short time gaps are hypothesized to increase stressor interactions (Gunderson et al., 2016) both synergistically (Bible et al., 2017) or antagonistically (Brooks and Crowe, 2019). Also, it has been shown that the sequential order affects the outcome of exposure to multiple stress (Fukami, 2001; Ashauer et al., 2007, 2017; Meng et al., 2020). However, due to the enormous complexity of necessary experiments (Rozman and Doull, 2000), the knowledge about the effects of timing and order on the quality and quantity of interactions between multiple pulsed stressors is limited. Still, most aquatic studies on multiple stress focus on simultaneous exposure (Backhaus and Faust, 2012; Altenburger et al., 2013; Heys et al., 2016; Altenburger et al., 2019). On longer time scales, the trans-generational effects (Beketov and Liess, 2006; Stuligross and Williams, 2021), culmination (Liess et al., 2013), and recovery (Liess and Schulz, 1999; Kattwinkel et al., 2012), are studied. Research on intermediate time gaps between stress exposures, however, is sparse (2 weeks (Ashauer et al., 2007), 3 days (Ashauer et al., 2017), 1 week (Brooks and Crowe, 2019), 2–4 weeks (Liess et al., 2013; Bible et al., 2017)). So far, the effects of temporal dynamics in stress exposure have been investigated based on a maximum of three exposure levels at high doses in the range of the half maximal effective concentration (EC_{50}) per substance (Ashauer et al., 2007, 2017; Bible et al., 2017; Brooks and Crowe, 2019; Meng et al., 2020). This is insufficient because high-dimensional investigations with more than two factors (Leavitt, 2020) and gradient-based designs with many factor levels (Kreyling et al., 2018) are needed to reveal interactions of stressors and nonlinear (non-additive) effects. In sum, we identify a

relevant knowledge gap in the effect of the timing and order on the outcome of interactions between multiple stressors.

Interactions between multiple stressors are predominantly studied at doses far above realistic environmental concentrations (Cedergreen, 2014). In this context, it is hypothesized that synergism between toxicants occurs only at doses comparably close to the EC_{50} (Bjergager et al., 2017). Antagonistic interactions, on the other hand, have been observed at low doses (Johnson et al., 2013; Bjergager et al., 2017). It was shown that low stress doses can induce stimulatory effects (Schulz, 1888; Stebbing, 1998; Calabrese and Baldwin, 2003; Christopher Cutler et al., 2009; Calabrese, 2010; Cutler, 2013) and antagonistic effects at ultra-low concentrations, leading to the occurrence of bi-phasic and tri-phasic (non-monotone) dose–response relationships, respectively (Liess et al., 2019a). Despite this, few studies show that pesticide mixtures at environmental realistic concentrations can cause synergistic interactions (Laetz et al., 2009; Shahid et al., 2019). This controversial evidence underlines the importance of improving the understanding of stressor interactions at doses on several orders of magnitude below the EC_{50} (Shahid et al., 2019).

The aim of the present study is therefore to investigate the interaction effects between an environmental stressor and a toxicant, exposed at doses ranging from lethal effects to doses below observed effect levels, under different time gaps between exposures and exposure orders. For this, we pulse-exposed populations of *D. magna* to UV-B radiation and the pyrethroid insecticide esfenvalerate under four different exposure scenarios. Additionally, we analyzed the data with an abstract, mechanistic-empirical model to quantify the relationship between the timing and order of stress exposure and stressor interaction.

3.2 Material and Methods

3.2.1 Experiment Design

In total, 720 neonates of D. magna (age < 24h), cultured in the Department of System Ecotoxicology, Helmholtz Centre for Environmental Research—UFZ, Leipzig, Germany, were used as experimental organisms. The organisms were subdivided into separately kept groups of three individuals. The resulting groups were pulse-exposed to esfenvalerate for 24 h, followed by one UV-B radiation pulse of varying duration or in reverse order (Figure 3.1).

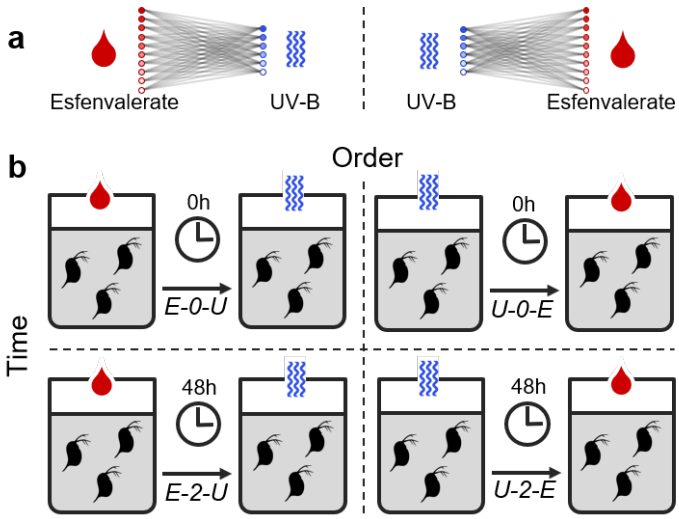

Figure 3.1: Fully-crossed multiple stress experiment design with four factors. **(a)** Employed stressors: esfenvalerate concentration (9 + 1 levels: 0.01–2.56 µg/L + control) and UV-B radiation exposure duration (5 + 1 levels: 4–14 h + control). **(b)** Temporal factors of the experiment: order of exposure (2 levels: esfenvalerate then UV-B, UV-B, then esfenvalerate) and periods between exposures (2 levels: 0, 2 days). The corresponding temporal dynamics treatments are denoted E-0-U, U-0-E, E-2-U, and U-2-E.

Exposure to the second stress began immediately after ending the first stressor or with a time gap of 2 days. Simultaneous exposure was left out deliberately to avoid physicochemical interactions between the stressors. To analyze the full spectrum of potential interactions be-

tween esfenvalerate and UV-B radiation under varying exposure scenarios, a full factorial treatment design with 240 treatments was set up (Figure 3.1) featuring 9 esfenvalerate concentrations plus controls (0.0, 0.01–2.56 µg/L), 5 UV-B exposure durations plus controls (0, 4–14 h) at 0.2 mW/cm2, two exposure scenarios (UV-B first, esfenvalerate first), and two intervals between exposure (0, 2 days). Note that this setup includes controls for all exposure scenarios (no stress, UV-B-only, esfenvalerate-only). In total, the experiment lasted for 11 days.

3.2.2 Experimental Conditions

During the first week, populations were kept in beakers of 20 mL containing Aachener Daphnien Medium (ADaM) (Klüttgen et al., 1994) which was exchanged three times per week. After 1 week, the organisms were transferred to 80 mL beakers. Due to the short duration of the experiment as well as sufficient water volume and food, negligible effects of *intra*specific interaction were expected. Total food rations were adapted to maintain a constant algae concentration of 3.75 and 7.5 µg C mL–1 in 20 and 80 mL in week 1 and 2, respectively. This averages to the proposed amount of 0.15 mg C per individual per day (OECD, 2012) to ensure no food limitation over the entire duration of the experiment. Individual monitoring of survival as well as feeding with freshly prepared suspensions of *Desmodesmus subspicata* (Shahid et al., 2019) were conducted on a daily basis. During the whole duration of the experiment, constant temperature conditions were maintained at 20.0 ± 1 °C under a photoperiod of 16:8 h day/night cycle.

3.2.3 Exposure to Stress

Treatments receiving UV-B radiation were placed on a randomized grid in a UV test chamber (*UV test chamber BS-04*, Opsytec Dr. Grobel GmbH, Ettlingen, Germany) to avoid positional effects due to varying irradiation intensities inside the chamber. In all exposure

scenarios, UV-B radiation treatments were aligned according to their duration of exposure to ensure a constant time gap between all exposures. If UV-B radiation was exposed first, treatments were started with a delay according to their duration so that all treatments would end at the same exact time. Afterwards, organisms were pulse-exposed for 24 h to esfenvalerate immediately (U-0-E) or with a 2-day delay (U-2-E). For organisms that were first exposed to a 24 h pulse of esfenvalerate, all UV-B treatments were commenced simultaneously immediately after decontamination (E-0-U) or with a 2-day delay (U-2-E). In this scenario, UV-B exposure treatment ended in a staggered manner in accordance with the duration of exposure.

Exposure to esfenvalerate was performed in the absence of food to avoid potential sorption of esfenvalerate to algae cells. After esfenvalerate exposure, the organisms were rinsed with an uncontaminated medium to completely remove traces of the insecticide and subsequently placed in a fresh, uncontaminated medium. Esfenvalerate (CAS 66230-04-4) stock solutions were prepared by serial dilutions in dimethylsulfoxide (DMSO) at the beginning of the experiment and stored at 5 °C. All tested solutions, prepared in exactly the same way as during exposure, were analyzed once on the first day of the experiment to assert the quality of stock solutions. Test vessels were then spiked individually with corresponding stock solutions on each exposure to Esfenvalerate (day 0, 1, 3). DMSO never exceeded a maximum concentration of 0.1% (v/ v), which is an order of magnitude below observed lethal effects on D. magna after 24 h exposure to DMSO (Huang et al., 2018). Chemical analysis of the test solutions was performed by Wessling GmbH, Landsberg OT, Oppin, Germany, using *Thermo Fisher Scientific TSQ 8000 Evo* gas chromatography–triple quadrupole mass spectrometry (GC-MS/MS). Measured concentrations are shown in Table A.1 and are well in line with the nominal concentrations, except for the nominal concentration of 0.32 µg/L, which, however, follows a clear dose–response relationship (Figure A.5k–n).

Therefore, the results in the following sections are analyzed and displayed using the nominal concentrations.

3.2.4 Data Analyses

The aim of the analysis was to compare the degree of interactions ranging from antagonistic via additive to synergistic responses across temporal treatments. (1) For this, dose–response curves were estimated with a log-logistic model with the bayesian inference framework Python Markov Chain Monte Carlo (MCMC) library (PyMC) (Salvatier et al., 2016). Note that effects of both stressors are reported in effect concentration (EC), although UV-B exposure is technically a duration. (2) Next, dose–response curves were normalized to the EC_{50} value of the corresponding control treatment by linear scaling. Linear transformations did not affect statistical inference and were used to facilitate the comparison of stressors operating on different scales (µg/L vs min). (3) For evaluation of significant EC_{50}-deviations from the control treatments, Not a Number (NaN)-estimates, resulting from intercept samples > 0.5, were discarded. Then, bayesian probability of direction (pd) values were computed, which are closely related to p-values (Makowski et al., 2019). This was done for differences between treatment-EC_{50} and control-EC_{50}. (4) Following this, the uncertainty of EC_{50} values was calculated with 95% posterior density intervals (PDI), which represent the region of highest plausibility of the true EC_{50}. (5) Two-sided t-tests were computed with all observations that continuously deviated from the control in the same direction to test if low doses led to a significant increase in the EC_{50} response. (6) Further, EC_{50} predictions of the stochastic independent action (IA) model (Bliss, 1939) were calculated from the esfenvalerate-only and UV-B-only treatments of the respective exposure scenario. This accounted for the different ages of organisms at the start of exposure. We chose IA as the predictive null model because IA was assumed for the joint effects arising from independent molecular effect cascades of esfenvalerate and UV-B radiation. Esfenvalerate acts by

blockage of voltage gated sodium channels (VGSC) (Soderlund, 2005), while UV-B induces deoxyribonucleic acid (DNA) breakage, protein oxidation, lipid peroxidation, and altered energy metabolism mainly through a reactive oxygen species (ROS) and photoproduct formation (Song et al., 2020). Although there may be a slight overlap in target sites through oxidized membrane proteins impeding the functioning of VGSCs, we consider the main routes to be independent. For comparison, we additionally included the stress addition model (SAM) (Liess et al., 2016) in the analysis. (7) Predictions were compared to experimental EC_{50} values by calculating pd-values for deviations of treatment-EC_{50} from predicted values. (8) Finally, dose–response curves were fitted through experimental EC_{50} values with cubic splines ($df = 3$). Those were compared to IA predictions by integration of model prediction and dose–response curves and calculation of their differences. Before integration, doses (x-axis) were harmonized by scaling to the EC_{50} value of the respective dose of the stressor that was exposed first (Figure 3.1a). This was done to achieve comparability across the different temporal treatments.

The resulting dose–response curves (drc) and their comparison to conventional maximum likelihood fits obtained with the R language (R) package *drc* (Ritz et al., 2015) can be reviewed in Figures A.4 and A.5. Additionally, the posterior distributions of EC_{50} values for all treatments are provided in Figure A.6 to show the uncertainty of the data. For the bayesian fitting procedure, mildly regularizing priors were used for slopes and inflection points to avoid separation, i.e., to avoid overfitting of logistic regression models with small sample sizes (Gelman et al., 2008; Gordóvil-Merino et al., 2012). Detailed information about the chosen priors is provided in the (method A.1). Any further data processing and statistical analysis were performed with the software R (R Core Team, 2018).

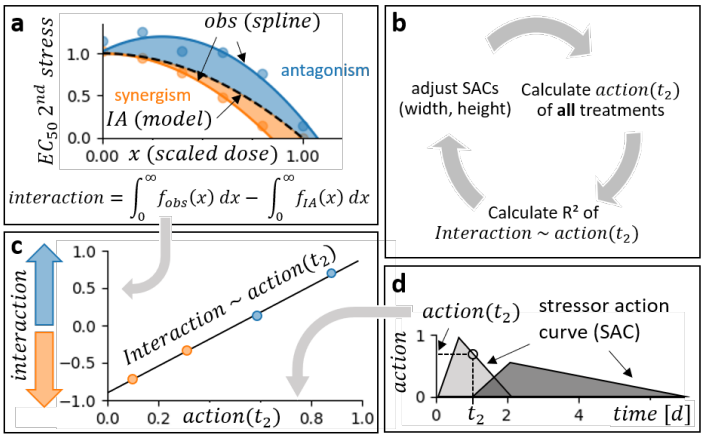

Figure 3.2: Description of action–effect analysis: **(a)** interaction is estimated as the integrated difference between cubic splines of observed scaled EC_{50} values and IA-EC_{50} predictions; stressor doses on the x-axis were scaled to an average EC_{50} value of the respective stressor. **(b)** Model fitting procedure. **(c)** Regression model yielding the adjusted R^2 value, which serves as the loss function for optimization process. **(d)** Stressor action curves (SACs) of a first stressor (light gray) and a second stressor (dark gray) with an exemplary computation of action of the first stressor at the beginning of the second stressor, denoted action (t_2).

3.2.5 Description of Action–Effect Analysis

The goal of this analysis was to assess whether the total interaction between both stressors depends on the duration between exposures and stressor order. For this, we designed an abstract-mechanistic model inspired by the concept of *Einwirkung* (action) and *Auswirkung* (effect) introduced by Loewe in 1953. This concept understands *Einwirkung* as the principal action in the early phase after a stress event that does not directly induce changes in the organism's performance. Following this, the *Auswirkung* of these changes influences the performance of the organism in the late stage of the stress response. As a more tangible example, consider a racing sprinter who is pushed (stress exposure), loses balance (action), and finally falls (effect). Interactions between multiple stressors can take place at any time point in the stress response, but their outcome may depend on whether this occurs in the action or effect phase.

With an abstract-mechanistic model, we can formalize our assumptions and test if the direction and magnitude of stressor interactions can indeed be predicted by the delay between exposures and order of stressors, based on those assumptions. Explicitly, we assume that (1) the abstract quantity action follows a stressor-specific temporal dynamic and that (2) the magnitude of action at the beginning of exposure to a second stress modulates the overall stress response. In the following, we refer to the stress-specific temporal dynamics of the early-stage response as action, otherwise known as the SAC.

We tested if SACs can be fitted such that the action of the first stressor at the beginning of exposure of the second stressor (Figure 3.2d) can predict the interaction between both stressors for all tested temporal treatments (Figure 3.2c). X-axis scaling described in point (8) of the data analysis section and in Figure 3.2a was necessary to harmonize the magnitude of interactions for different types of dosing scales (min vs µg/L). Due to this scaling, the shape of the characteristic SACs is no longer concentration-dependent but only responds to the magnitude and direction of the total interaction (Figure 3.2a). It is not informed a priori and converges to those shapes that best reflect the interaction between esfenvalerate and UV-B radiation under all treatments, given their specific exposure order and timing. Triangular shapes, parameterized by base length (action duration) and peak position (time point of maximum action after the beginning of exposure to stress), were chosen over Gaussian or Gamma distributed shapes because such a form introduces no assumptions, apart from (i) following linear increase, then linear decrease (ii) satisfying the unit area of the triangle with a base at an action equal to zero (when the area of a triangle is one, slopes are only determined by the position of its peak and base length). The final curve fitting process (Figure 3.2b) was carried out with the R package *optim*, using the adjusted R^2 of the regression shown in Figure 3.2c as a loss function and thereby optimizing the curve parameters for esfenvalerate and UV-B radiation.

3.3 Results and Discussion

3.3.1 Interaction Shifted from Antagonism to Synergism when the Second Stressor was Applied with a 2-Day Delay

When UV-B radiation and esfenvalerate were exposed directly in succession, the interactions between the stressors were dominantly antagonistic (Figure 3.3a,b). This was expressed by significant antagonistic deviations from the independent action prediction in the esfenvalerate EC_{50} after 240 min UV-B exposure (increase factor of EC_{50}: 2.7, $p < 0.001$) and significant antagonistic deviations in the UV-B-EC_{50} after exposure to 0.01–0.08 µg/L esfenvalerate (increase factor of EC_{50}: 1.5–1.9, $p < 0.05$). No synergistic deviations were observed in these treatments. In contrast, with a 2-day delay between exposures, synergistic interactions at high concentrations were observed (Figure 3.3c,d). Here, significant synergistic deviations were observed after exposure to 0.16 µg/ L esfenvalerate (increase factor UV-B-EC_{50}: 0.44, $p = 0.02$) and after exposure to 720 and 840 min of UV-B exposure (increase factor esfenvalerate-EC_{50}: 0.05 and 0.002, respectively, $p < 0.001$). One significant antagonistic interaction was recorded after 0.02 µg/L esfenvalerate exposure (increase factor UV-B-EC_{50}: 1.6, $p = 0.02$).

We tested whether the total interaction, calculated as the integrated difference between observed IA and predicted effects (Figure 3.3, arrows), can be predicted by a linear regression model, where the regression predictor is determined by the timing and order of exposure through SACs (see the model description for a detailed explication, Figure 3.2). The resulting SACs are shown in Figure 3.4a–d and indicate that a perfect model fit was possible (slope = 3.1, y-intercept = -0.75, adj.-$R^2 = 1.0$, Figure 3.4e). Therefore, under the assumptions of the model, action can correctly predict antagonisms and synergisms of all temporal treatments, suggesting that a causal link exists

between exposure time and order and stressor interaction. Note, however, that the analysis does not discriminate between the effects of different stressor doses, since all interactions are summed into the integral. Consequently, this method does not consider the possibility of nonlinear interactions between the stressors (Duncan and Kefford, 2021), which still may exist beside the dominant effect revealed in this study.

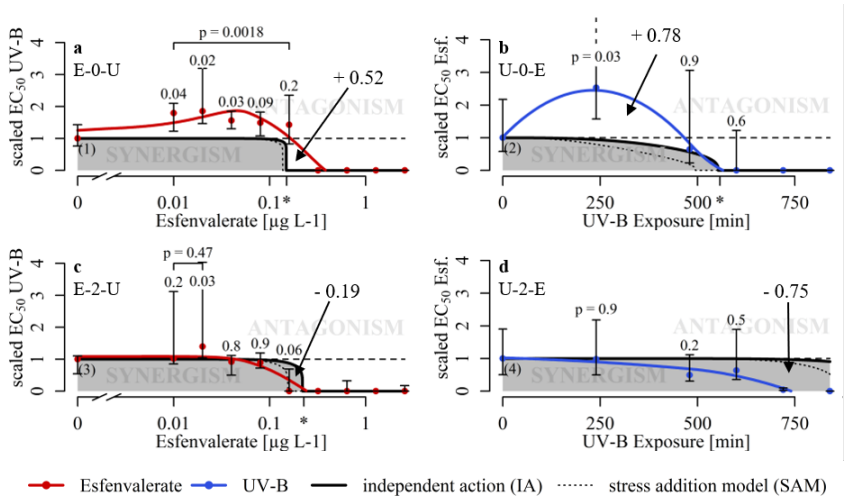

Figure 3.3: Effect of first stressor (red: esfenvalerate, blue: UV-B) on the EC_{50} of the second stressor applied in sequence with a 0-day delay **(a, b)**; and with a 2-day delay **(c, d)**. Each colored dot (a, c: $n = 18$, b, d: $n = 30$) corresponds to the maximum a posteriori (MAP) EC_{50} value of a dose–response curve with 95% posterior density interval (PDI). The colored lines are cubic splines ($df = 3$) fitted to the EC_{50} values and symbolize idealized response relationships between the first and second stressors. Dots above the solid line (IA prediction) indicate antagonism, and dots below the line indicate synergism. Total interaction, quantified as the integrated difference between effect and prediction, is indicated by the black arrows. The values on top of confidence intervals are approximated p-values from bayesian posterior density intervals. The p-value above the squared bracket is the probability that the group of EC_{50} values is not different from the control-EC_{50} value. The asterisk (*) indicates the control-EC_{50} of the first stressor. Fitted control-EC_{50} of the second stressor (scaling values): (1) 330 (95%-PDI [240, 460]), (2) 0.6 (95%-PDI [0.40, 1.2]), (3) 640 (95%-PDI [380, 690]), and (4) 0.58 (95%-PDI [0.33, 1.0]). Complete EC_{50}-histograms, including estimated p-values of the posterior distribution are displayed in Figure A.6.

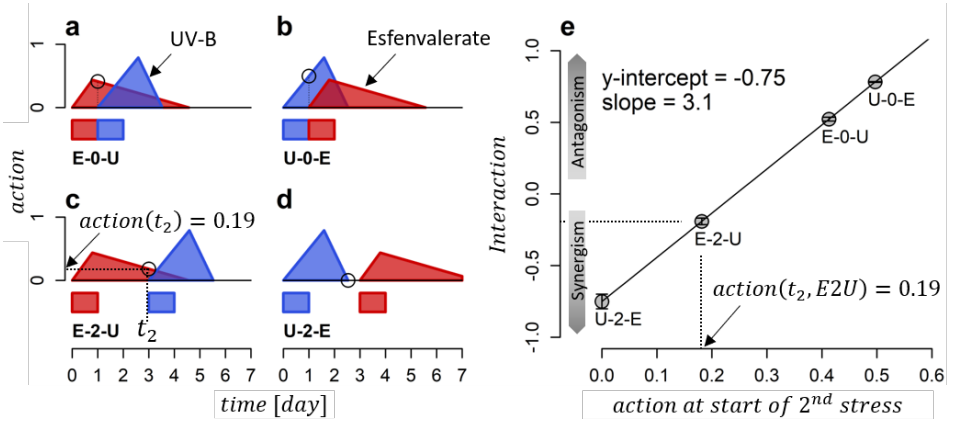

Figure 3.4: Results of action–effect analysis. Relationship between delay between exposures and order of stress exposure and interactions between the stressors through fitting of stressor action curves (SACs). Panels **(a–d)** show triangular SACs of esfenvalerate (red) and UV-B radiation (blue) over time. The shapes of the colored curves are equal for each panel, varying only by shifts along the time axis, according to order and delay of exposure of the employed treatments. The central value of this analysis is the magnitude of the abstract quantity action of the first stressor at the beginning of exposure to the second stressor, which represents unmanifested effects in the organism. It is denoted action (t_2) and indicated by an empty circle (∘). The shape of the curves is optimized so that action (t_2) can predict the interaction between both stressors. Panel (**e**) shows the resulting regression. The adjusted R^2 of the regression model is close to one, in accordance with the expectation due to optimization of the curve shapes, with R^2 as the loss value.

We interpret SACs as the intensity of the initial, unmanifested effects in an organism during the early stage of a stress response (Loewe, 1953). If stressors are applied without delay, action of the first stressor appears to be able to reduce unmanifested effects of the second stressor and explain the observation of antagonism. When transient effects of the first stressor have disappeared (after 2-day time gap between exposures) and physiological effects have manifested, resulting effects can be synergistic when the reduced organism fitness induces larger effects as compared to control treatments. This could explain why synergism is most strongly observed in the absence of SAC overlap (Figure 3.4d). With increasing SAC overlap, synergistic effects

are progressively reduced by antagonistic effects caused by action. Although the action–effect analysis does not provide a mechanistic model for the observed effects, it does provide a consistent explanation of the relationship between temporal stressor setup and observed effects across all treatments.

An increase of combined effects on various end points with increasing delay (2–4 weeks) between pulses of chlorpyriphos and copper was reported by Brooks and Crowe (2019). Their findings match the results obtained in this study for a different exposure time scale and other scales of ecological complexity (cellular viability, community respiration, and clearance rate). In contrast, our findings differ from those of Bible et al. (2017) who reported disappearance of synergism with an increasing delay between exposures. However, in their work, a long recovery (2–4 weeks) was the likely cause for the disappearance of synergistic effects. Also, in the work of Ashauer et al. (2017) the chosen recovery times may have been too large to produce antagonistic effects, especially because the toxicants used were chosen because of their fast toxicokinetic recovery time. A comparison of SAM and IA models showed that SAM outperformed IA when synergism was present. However, both models did not predict the antagonism of the stressor effect.

Fitted SACs also tentatively reveal temporal attributes of the analyzed stressors. These attributes reflect aggregated values for all tested doses but may also differ in relation to the applied dose. Action of esfenvalerate persisted for approximately 4.5 days, with a maximum after one day. The UV-B radiation SAC was fitted with a duration of 2.5 days and maximum action after just 1.5 days (Figure 3.4a–d). Whereas esfenvalerate induces adverse effects via nerve damage that interrupts feeding and causes mortality after several days (Palmquist et al., 2012), UV-B radiation mainly induces DNA damage due to ROS and photoproduct formation, causing mortality by excessive apoptosis (Song et al., 2020). Such effects were observed 12 h after UV-B exposure in freshwater prawns (Schramm et al., 2017), indicating similar

durations of action as reported in this study. Despite the accuracy of the proposed action–effect model, we are aware of its limitations. The estimated SACs (Figure 3.4a–d) can be seen only as first approximations to the true forms and the quantification of action used in predicting interaction and may depend on more factors than the magnitude of the action of the first stressor at the beginning of exposure to the second. However, due to the simplicity of the model and the resemblance of fitted SACs to physical modes of action, we believe it to be of great value for interpreting stressor interactions in dynamic exposure scenarios, and we are confident that existing frameworks such as toxicokinetic-toxicodynamic (TKTD) (Jager et al., 2011) can benefit from the conceptual progress made in this study. Especially, because, to our knowledge, the prediction of antagonism between stressors is outside of the scope of current TKTD models. Whether our findings also extend to other stressors and different timings must be analyzed in future work. Also, a characterization of the involved biochemical processes and a molecular description of action identified in our study are missing pieces in this study and would be a very desirable goal in future research.

3.3.2 Low Doses of the First Stressor Increased Resistance to the Second Stressor

The application of low stress doses, independent of the stress type, significantly increased the EC_{50} response of second stressor applied without delay (EC_{50} shift = +0.85, $p = 0.01$). Thus, an exposure to UV-B radiation of 240 min led to a significant positive shift of the esfenvalerate-EC_{50MAP} values (EC_{50} shift = +1.5, $p = 0.03$) (Figure 3.3b). EC_{50MAP} values of UV-B radiation, calculated at the five lowest esfenvalerate concentrations, were combined significantly higher from the EC_{50} value of the control (EC_{50} shift = +0.6, $p = 0.002$) (Figure 3.3a). When the organisms were exposed to the second stressor with a 2-day delay (Figure 3.3c,d), the majority of antagonistic effects of the primary stressor disappeared (EC_{50} shift = +0.04, $p = 0.7$);

however, the concentrations 0.01 and 0.02 µg/L of esfenvalerate still elicited an EC_{50} increase, which was significant under 0.02 µg/L. In contrast, significant synergistic interactions were only provoked by high doses of the first stressor (Figure 3.3c,d). This evidence suggests that increased resistance to a second stressor is induced only by low doses of the first stressor, but this process is more effective if the stressors are applied without delay. Observations of antagonism at low doses and synergism toward doses near the EC_{50} response were also made by Loureiro et al. (2010) and Bjergager et al. (2017). It is possible that sub-lethal doses of the first stressor triggered a general homeostasis-maintaining response mechanism only at low doses, resulting in a bi-phasic response (Calabrese and Baldwin, 2003; Costantini et al., 2010; Shahid et al., 2019). Such a mechanism could counteract the effects of the second stressor and invoke an EC_{50} increase above the control, as observed in this study. Also, a reduction of system stress (Shahid et al., 2019) that is outlasted by direct effects of the stressors could explain the present results. Both explanations are supported by the finding that each of the stressors, esfenvalerate and UV-B radiation, elicited an EC_{50} increase above control levels of the second stressor at low doses and the disappearance of antagonistic effects at higher doses. An identification of the mechanisms responsible for the antagonistic response to low doses of the first stressor would benefit future investigations into the combined effects of multiple stressors.

Sequential exposure to esfenvalerate and UV-B radiation may be characterized by competing processes between interactions in both the early- and late-stage of the stress response dependent on the timing of stress exposure. We believe that the developed action–effect analysis can be seen as a promising contribution toward quantifying the influence of timing and order on interactions between multiple stressors. Our research further points out that low doses may serve a more critical role than previously assumed. Low doses had a significant antagonistic effect on the second stressor when applied without delay.

This result indicates that risk assessment of interactions between multiple stressors should be based on broad dose–response relationships so that the combined effects are not overlooked or underestimated. Finally, with this study, we underline the importance of including more realistic exposure scenarios in environmental risk assessment.

Chapter 4

Ultra-low Esfenvalerate Concentrations Increase Biomass and May Reduce Competitiveness of *Daphnia magna* Populations[2]

4.1 Introduction

Current environmental risk assessment (ERA) aims to safeguard species and populations in the environment by combining exposure and effect assessment. The concentrations at which adverse effects of pesticides occur in toxicity tests are lowered by assessment factors so that populations in the field should also be protected. Field-studies, however, show that the ecological status of most streams with agricultural catchments is still affected by pesticides below regulatory acceptable concentrations (Liess et al., 2021). Similarly, the effects of low-dose neonicotinoids have been underestimated by the same risk assessment

[2]Published in a slightly modified form as: Schunck F, Liess M. 2023. Ultra-low Esfenvalerate concentrations increase biomass and may reduce competitiveness of *Daphnia magna* populations. Sci Total Environ. 163916.

that is based on lethal effects and short-term observations (Rundlöf et al., 2015; Cressey, 2017). Therefore, to identify truly protective thresholds for pesticide applications the population effect mechanisms of low pesticide concentrations need to be assessed.

With the ban of most neonicotinoids in Europe and pending decisions in the US in 2024, pyrethroid insecticides emerge as the most common alternative in agricultural applications (Jactel et al., 2019). In the aquatic environment, pyrethroids generally occur as short pulses. This is due to their fast dissipation from the water column; in stream water, only 3% of pyrethroids are bioavailable (dissolved in water and bound to dissolved organic matter), while 97% are bound to suspended solids (Lu et al., 2019). Nevertheless, maximum concentrations only 1–2 orders of magnitude below the acute half maximal effective concentration (EC_{50}) (*D. magna*) have been detected in surface waters (Rösch et al., 2019b).

At such concentrations, stimulatory effects of pyrethroids have been reported (Margus et al., 2019; Shang et al., 2021; Wolz et al., 2021) and discussed in the context of hormesis theory (Townsend and Luckey, 1960; Stebbing, 1982; Calabrese and Baldwin, 2003; Liess et al., 2019a; Agathokleous et al., 2022). In contrast to linear no threshold or threshold models, hormesis assumes that dose–response relationships are bi-phasic. This identifies that low levels of toxicants can have stimulatory effects, while high concentrations have adverse effects. It is hypothesized that positive, hormetic effects have associated negative trade-offs, predicting that net population growth cannot be positive (Forbes, 2000), due to limitations of available resources (Calow and Sibly, 1990), or due to interactions with physical or biological ecosystem components (Agathokleous et al., 2021). These trade-offs, however, remain poorly understood (Agathokleous et al., 2021), as do the effects of hormesis within populations.

Thus, the aim of this study is to investigate the consequences of low-dose pyrethroid exposure on the multi-generational development of

aquatic populations. To this end, we exposed *D. magna* populations close to their carrying capacity to the pyrethroid insecticide, esfenvalerate. We tested concentrations of 1/3, 1/10 and 1/30 of the EC_{50}, which are expected to induce sublethal and hormetic responses, and contrasted them with concentrations that induce lethal population responses. Effects on population biomass and abundance were monitored with a non-invasive imaging technique 3 times per week for a total of 89 days.

4.2 Material and Methods

4.2.1 Experiment Design

The nanocosm experiment consisted of 40 *D. magna* populations, each initialized from 15 neonates (age <24 h). After 4 weeks of development, the populations were assigned to 8 exposure groups (control, 0.01, 0.032, 0.1, 0.32, 1.0, 3.16, 10.0 µg/L esfenvalerate). This assignment of nanocosms to one of the exposure groups was based on the pre-exposure population density to achieve a balanced treatment design. The populations were subsequently exposed to a single pulse of the pyrethroid insecticide esfenvalerate at the respective concentration. Following this, the experiment was continuously monitored for another 9 weeks. Throughout the entire duration of the experiment, populations were monitored 3 times per week using an image analyzing system. In general, the experimental design followed the works of (Liess et al., 2006) and (Foit et al., 2012).

4.2.2 Test Systems

Each experimental unit consisted of a 5.5 L glass beaker (Harzkristall, Derenburg, Germany), filled with 500 g of washed aquarium sand of 1–2 mm diameter. The sediment layer served as a habitat for microorganisms to facilitate self-purification of the systems. Aachener Daphnien Medium (ADaM) (Klüttgen et al., 1994) was used as the

test medium for the experiment. Throughout the duration of the experiment, the medium was not changed and kept at a constant volume of 4.5 L by replenishing the beakers with double distilled water on a weekly basis. Water loss due to evaporation was minimized by covering the systems with glass plates. A 2 cm cut at the edge of the glass plates provided access to the nanocosms. Sufficient oxygen saturation was ensured by aeration of the test systems with glass tubes, which were connected to *Osaga Air Compressor LK-35* air pumps (Fish farm Schierhölter, Glandorf, Germany) by silicon tubing. Aeration was turned on 3 times per day for 15 minutes each. The populations were fed three times per week with a diet of ground stinging nettle (*Folia urticae*), ground dog food (Organic dog biscuits, Yarrah Organic Petfood BV, Harderwijk, The Netherlands) and batch cultured green algae (*Desmodesmus subspicata*). The exact preparation of the feeding suspensions is detailed in method B.1. Throughout the experiment, the organisms received a total of 3.6 mg C per feeding. For the first 10 days only, this amount was doubled in order to promote the growth of microbial communities in the system.

4.2.3 Environmental Conditions

The experimental units were exposed to a 16:8 h, day/night cycle and were positioned with the water surface approximately 20 cm below 70 W cool-white fluorescent tubes. Throughout the whole duration of the experiment, the room temperature was maintained at 20 ± 1 °C. Due to the heat input from the lighting, the temperature of the systems was increased by approximately 1 °C, resulting in system temperatures of 21 ± 1 °C. The acidity of the systems reached a stable pH of 7.9 ± 0.1 within the first week. Conductivity was kept constant at approximately 1080 ± 17 µS/cm by water replenishment. In previously conducted experiments of the same type, chemical parameters did not differ substantially between treatments and were in bounds where no effects on aquatic organisms are expected (Liess et al., 2006). This

was asserted once, 4 weeks after exposure: NO_3^-, 0.3 ± 0.1 mg/L; NO_2^-, 0.02 ± 0.003 mg/L; $PO_4^{3-} < 0.15$ mg/L.

4.2.4 Exposure to Chemicals and Chemical Analysis

To study the effects of pyrethroids on *D. magna*, esfenvalerate (CAS 66230-04-4, HPC Standards GmbH, Cunnersdorf, Germany) was selected as a representative of the group of type-II pyrethroid insecticides. Esfenvalerate is approved for agricultural use in the EU until 2023, and additional type-II pyrethroids continue to be allowed until the end of the decade (`https://ec.europa.eu/food/plant/pesticides/eu-pesticides-database/active-substances/?event=search.as`). The hydrophobic insecticide esfenvalerate had to be dissolved to ensure bioavailability in aquatic environments; we used dimethylsulfoxide (DMSO) at concentrations of 0.01% and 0.02% v/v for this purpose. To maximize the number of replicates per treatment, no solvent controls were run in this study. However, we assessed the influence of DMSO on reproduction and survival of *D. magna*, by running chronic exposure tests on a range of DMSO concentrations according to (OECD, 2012). These tests were conducted under low feeding conditions (0.016 mg C/individual/day) and high feeding conditions (0.16 mg C/individual/day) to estimate the effects on organisms under food limitation, comparable to the conditions in the nanocosms. DMSO concentrations below 1% v/v, 2 orders of magnitude higher than the DMSO concentration used in this study, had no effect on the survival and the cumulative offspring of *D. magna* up to 21 days post exposure (Figures B.2 and B.3), regardless of whether the organisms were cultured under high or low feeding conditions. The solvent concentrations used in this study (Table B.1) were 2 orders of magnitude below this effect threshold. In addition, no effects on the movement of *D. magna* were observed below 0.1% v/v in a different study (Huang et al., 2018).

The stock solutions were prepared by serial dilutions in DMSO at the day of exposure and measured once for each test concentration in 1 L

volumes of ADaM, spiked parallel to the experimental units. Individual nanocosms were spiked with corresponding stock solutions, except for control treatments, which were not treated with DMSO. Chemical analysis of the test solutions was performed by Wessling GmbH, Landsberg OT, Oppin, Germany, using a *Thermo Fisher Scientific TSQ 8000 Evo* gas chromatography–triple quadrupole mass spectrometry (GC-MS/MS). Measured concentrations as well as used DMSO concentrations are shown in Table B.1 for each treatment and are well in line with the nominal concentrations. Therefore, we report the results in relation to the nominal concentrations of esfenvalerate.

4.2.5 Monitoring, Image Analysis and Calculations

D. magna populations were monitored 3 times per week for a total period of 13 weeks using a non-invasive image detection method described in (Liess et al., 2006) and improved by (Foit et al., 2012). The method uses *D. magna* phototaxis and background subtraction to detect abundance and estimate size. Images were captured using a *PowerShot G12* (Canon, Tokyo, Japan) mounted on a rectangular box attached to the cylindrical vessel, in order to prevent reflections on the glass surface. Prior to imaging, the observed system was briefly shaded so that only the front of the aquarium was exposed to light. Because *D. magna* are attracted to light, this resulted in a concentration of *D. magna* closest to the camera-exposed front of the systems. Immediately after the shading was removed, a series of three photographs were taken at a resolution of 2816×2112 pixels. The remaining camera settings are listed in Table B.4. Due to the static camera, three images with a fixed background and moving *D. magna* were obtained for each system and monitoring date. In a final step the images were converted to grayscale images and their difference was calculated. Consequently, the resulting images contained only moving objects. In the case of single-species systems, these objects must be exclusively *D. magna*. The pixels were then counted to estimate the size and biomass of the organisms. From the 3 resulting difference-

images, the image with the highest number of *D. magna* was selected. The exact procedure is detailed in (Foit et al., 2012).

The resulting abundance is the total number of organisms detected in the systems. Since the volume of 4.5 L was kept constant in the systems the reported abundance is comparable across all experimental replicates. The length L in mm of the organisms was calculated using the formula $L = \sqrt{n_{\text{pixel}}/35.5}$, where 35.5 is an empirical factor that was calibrated to a fixed camera distance (60 cm) and a resolution of 2048 × 1536 (Figure B.1), to which the images, also taken at a 4:3 ratio, were downscaled before calculation. The factor also accounts for the fact that organisms of *D. magna* have an ellipsoid shape rather than a square shape. From this, the dry-weight biomass W (µg) of a single organism was estimated using the empirical relationship $W = 1.5 \times 10^{-8} \times L^{2.84}$, derived for D. magna (Dumont et al., 1975). Since the length of the organisms is calculated and reported in mm, it was converted to µm before being used in the equation. The total biomass of the system was calculated as the sum $\sum W$ and converted to mg.

Population pre-exposure growth rates were calculated by $(\sum W_{t=0} - \sum W_{t=-5})\ \Delta t$, while post-exposure biomass growth rates were calculated by $(\sum W_{t=+5} - \sum W_{t=0})\ \Delta t$, where Δt indicates the time interval, $\sum W$ indicates the total system biomass in mg, and $t = 0$ corresponds to the time point of exposure to esfenvalerate. Division by $\Delta t = 5$ days gave biomass growth rates in mg/day. The 5–day interval was chosen for the calculation of population growth rates, because it represented a long-enough time frame to show early effects and was available symmetrically on either side of the time of exposure.

4.2.6 Statistics

During the 4-week pre-exposure period, 9 systems did not develop successfully. Systems were considered unsuccessful if the average population abundance stagnated during the pre-exposure period and was

below the initial abundance of 15 neonates. In contrast, populations in valid systems grew exponentially with an average of 98 neonates during the exponential growth period; the lowest pre-exposure average of successful systems was 50 neonates. Consequently, unsuccessful systems were removed from further investigation. Because the treatment groups were previously balanced for population density, this change harmoniously reduced the number of replicates per treatment from 5 to 4, except for the highest (10 µg/L) treatment, for which 3 valid replicates remained.

We used a bayesian model of a random walk to estimate the treatment trend μ_k that dominates the population time series Y_i of all observations i belonging to treatment k, which follows a random normal distribution around the trend at each time point t with a treatment specific variation of σ_k. The trend is estimated by a Gaussian random walk grw, where the size of each step-innovation follows a half-normal distribution with a standard deviation of 1. It is offset by a treatment-specific intercept, which follows a half-normal distribution with a standard deviation of 2. Before model computation, the response variable was centered and scaled, and back-transformed after computation to calculate effect sizes.

$$Y_{i:i\in k,t} \sim Normal(\mu_{k,t},\ \sigma_k) \tag{4.1}$$

$$grw_{k,t+1} \sim Normal(grw_{k,t},\ innovation_k) \tag{4.2}$$

$$innovation_k \sim HalfNormal(sd = 1) \tag{4.3}$$

$$intercept_k \sim HalfNormal(sd = 2) \tag{4.4}$$

$$\sigma_k \sim HalfNormal(sd = 1) \tag{4.5}$$

We concluded that the trend of a treatment was significantly different from the control treatment if the lower bound of the 95% posterior density interval (PDI) of the difference distribution was greater than zero. This method is an application of bayesian null hypothesis testing (Kruschke, 2013). The Python Markov Chain Monte Carlo

(MCMC) library (PyMC) (Salvatier et al., 2016) was used to compute the bayesian models. Further data analysis was done with *Python* and statistical tests were computed with the package *statsmodels* (Seabold and Perktold, 2010). The *xarray* package (Hoyer and Hamman, 2017) was essential for handling high-dimensional data sets.

4.3 Results

The results shown in Figure 4.1 are time series of *D. magna* population over the entire three-month period of experimentation. The 95% PDI indicates the trend uncertainty due to variation in experimental replicates. Trends were highly similar during the exponential growth phase, prior to exposure to esfenvalerate, after which time series of all treatments diverged significantly in terms of abundance and biomass from control populations.

The development of the control populations followed a density dependent trajectory typical of *D. magna* populations. Before exposure, replicate populations grew exponentially. As expected, the smallest size class ($\leq$ 1.68 mm), approximating the neonate population (Figure 4.1a,e,i,m,q), grew fastest and reached a maximum growth rate 2 weeks after the start of the experiment. After 3 weeks, the neonate abundance peaked in the control treatments, indicating that carrying capacity had been reached. From this point on, the development of this size class was characterized by a steady decline. Only towards the end of the experiment did a second neonate growth cycle become apparent. Juvenile organisms, approximated by the intermediate size class (1.68–2.28 mm), continued to grow until 2 weeks after exposure, when the abundance stabilized for the remainder of the experiment (Figure 4.1b,f,j,n,r). The largest size class ($\geq$ 2.28 mm), which approximates mature organisms, grew briefly in the exponential growth phase, then decreased until 8 weeks after the start of the experiment and showed strong growth thereafter (Figure 4.1c,g,k,o,s). The initial growth and decrease of the largest size class can be associated

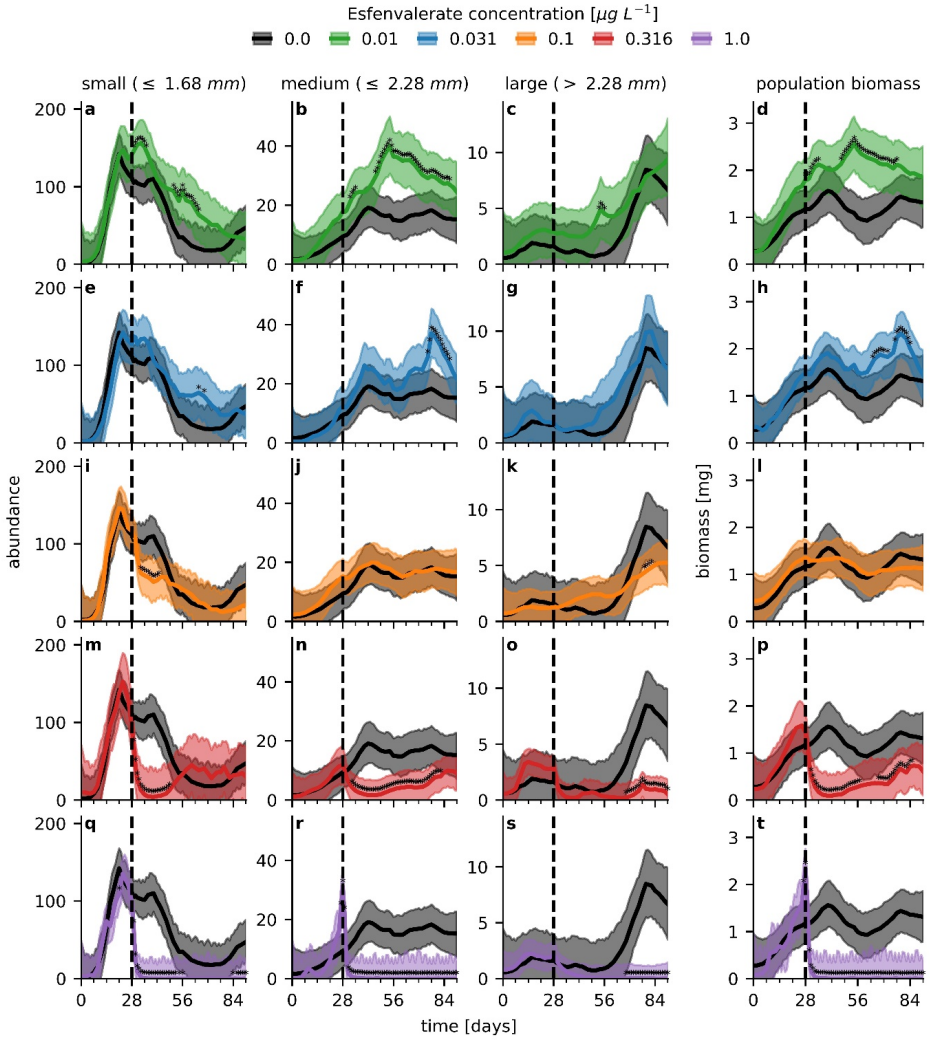

Figure 4.1: Time series of mean abundance and biomass of *D. magna* populations ($N = 4$). Each row corresponds to a tested esfenvalerate concentration, with increasing levels from top to bottom. Solid lines indicate the bayesian estimates of the mean trend in abundance (columns 1–3) and biomass (column 4) of experimental replicates over time. Shaded areas indicate the uncertainty in the trend with 95% PDI intervals. Asterisks (*) indicate significant deviations from the control trend (black). The dashed line indicates the time point at which the experimental systems were exposed to esfenvalerate. The minor ticks on the x-axis represent 1-week intervals.

with the initial population, which was the first to reach maturity and slowly decreased in numbers due to aging and starvation. The second growth cycle of *D. magna* adults emerged only when the populations of adults and neonates were sufficiently low. This pattern is typical of *D. magna* populations that, in the absence of predation or other stressors, are dominated by few adult individuals.

Approximately 1 week after the smallest individuals reached their initial maximum, the systems were exposed to pesticides; this was 2 weeks before the medium-sized individuals and approximately 7 weeks before the large-individuals reached their maxima. Related to the population biomass, exposure occurred close to the control carrying capacity (Figure 4.1).

4.3.1 Effects of Low Doses

During first week after the exposure, especially the smallest size class of the populations exposed to 0.01 µg/L esfenvalerate (1/30 EC_{50}) showed a significant increase in abundance compared to pre-exposure values (+7%), while exposure to 0.031 µg/L only led to an insignificant increase in the abundance of small organisms (+5%). At the same time, the abundance of the smallest size class in control treatments decreased by 10%. The increased population growth of the lowest esfenvalerate treatment was also reflected in the significantly increased population biomass during this period. In contrast, the medium and largest size classes were generally not significantly increased by the two lowest concentrations during the first week after the exposure. In weeks 2–3 after exposure, the population dynamics of the low esfenvalerate treatments showed similar trends to the control treatments with respect to the abundance of all size classes and also for the biomass (Figure 4.1a–h). Beginning in week 3 after exposure, systems dosed with 0.01 µg/L esfenvalerate again increased significantly from control treatments in both abundance and biomass in all size classes, lasting until the end of week 7 after exposure:

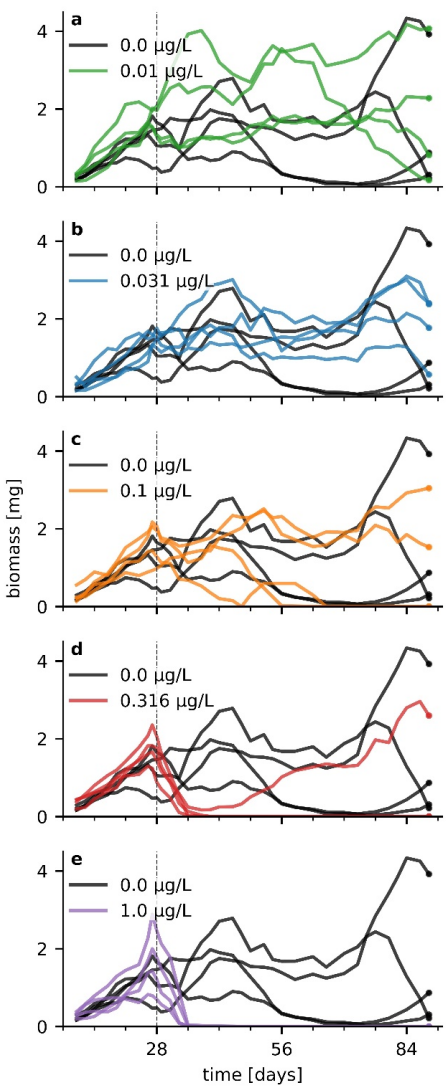

Figure 4.2: Population biomass (mg dry-weight) trajectories of experimental replicates of the control treatment (black) and esfenvalerate treatments (colored lines). Lines represent the aggregated population development overall size classes. The trajectories were smoothed with a moving average (10-day backward window) to focus on the trend of each time series.

Small organisms peaked in week 3–7 (+160% of control values), medium-sized organisms peaked in weeks 3–5 (+130%) and large organisms peaked in weeks 3–4 (+370%). Total biomass was approximately twice that of the control during weeks 3–7 after esfenvalerate application. Exposure to 0.031 µg/L esfenvalerate resulted in similar but milder and later deviations from the control trajectories: small organisms peaked in weeks 5–6 after exposure (+200% of control values), medium-sized organisms peaked in weeks 6–8 (+80%), and large organisms were not significantly more abundant in this treatment than in the control. Population biomass was significantly increased in weeks 5–8 after exposure (+60%). Figure 4.2 shows the individual biomass trajectories of the different treatments compared to the control trajectories. The figure shows that 2 out of 4 control populations went through an episode of low population density in weeks 3–7 post exposure. These were also the systems with the highest pre-exposure biomass.

4.3.2 Effects of Moderate and High Doses

Towards the end of the experiment, the onset of a new cycle of population growth was observed in these systems. Episodes of low population density prior to the onset of a new population growth cycle were not observed in any of the systems exposed to low concentrations of esfenvalerate (Figure 4.2a,b). Concentrations of 0.1 µg/L (⅓ EC_{50}) induced mortality in *D. magna*. During the first week after exposure, these concentrations induced a significant reduction in small sized organisms: 0.1 µg/L esfenvalerate resulted in a significant reduction of 60%, 0.31 µg/L resulted in a 90% reduction and 1 µg/L and above eliminated all small organisms. Such a concentration-response relationship was also observed in the larger size classes. Concentrations of 1 µg/L esfenvalerate and above also completely eliminated the larger size classes of the populations entirely with no chance of recovery.

Moderate doses of 0.1 µg/L (1 order of magnitude below the esfenvalerate EC_{50} on *D. magna*) appear to have little effect on population trends in the medium and large size classes (Figure 4.1j,k). However, closer examination of the individual trajectories (Figure 4.2c) shows that, contrary to the control populations, 50% of the *Daphnia* populations exposed to 0.1 µg/L esfenvalerate collapsed completely, while others recovered to levels of control populations. Such a complete population collapse did not occur in the controls. Exposure to 0.316 µg/L esfenvalerate resulted in stronger responses compared to 0.1 µg/L treatments—only one population recovered from the pesticide effects (Figure 4.2d). This is also reflected in the significant decrease in abundance and biomass trends from the control treatment in all size classes. Figure 4.1m–p shows that the size classes of this treatment recovered sequentially and that effects persisted until the end of the experiment. Experimental replicates exposed to 1 µg/L esfenvalerate and above (data not shown) collapse completely within 1 week after exposure to esfenvalerate (Figure 4.1q–t).

4.3.3 Short-Term Esfenvalerate Toxicity and Population Density Effects

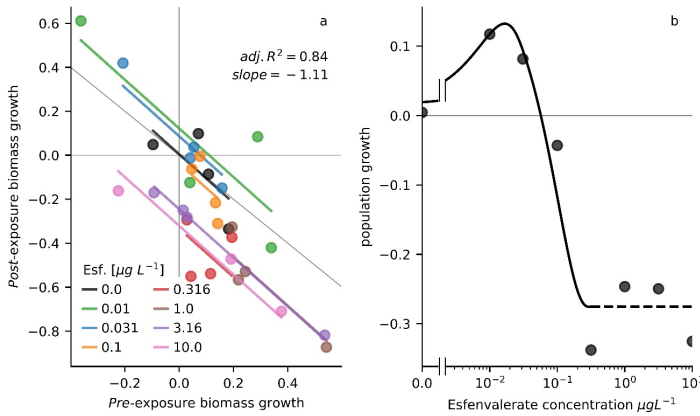

Figure 4.3: Post-exposure biomass growth rate in relation to the pre-exposure biomass growth rate and esfenvalerate effects. **(a)** Relationship between 5-day *pre*-exposure and 5-day *post*-exposure growth rates of population biomass. The colored lines represent the regression line, offset by the respective effects of esfenvalerate exposure. The diagonal thin line indicates the inverse 1:1 relationship; observations on this line indicate that the post-exposure biomass growth was the opposite of the pre-exposure growth. Shifted regression lines on the y-axis indicate that the post-exposure growth rate changed with the same negative correlation. Observations in the lower-right quadrant are indicative of populations that were at carrying capacity during exposure. **(b)** Esfenvalerate effect on 5-day *post*-exposure growth rates, assembled in a dose-response curve. The black markers are the resulting y-intercepts of the linear regression model (see Table B.2). The line through the points is based on a cubic spline calculation. The dashed-extension of the spline indicates that the maximum effect was reached and a reasonable fit of the cubic spline was no longer possible at these concentrations.

Figure 4.3 shows that the population biomass growth after the exposure to esfenvalerate is strongly dependent on the biomass growth before the exposure (slope $= -1.1$, $p < 0.001$). The more biomass grew before exposure, the more it decreased after exposure, and vice versa. The accumulation of observations in the lower-right quadrant (75% positive pre-exposure growth and negative post-exposure growth) and the few observations in the upper-right quadrant (9% continued positive growth) of Figure 4.3a suggest that the population

was approaching carrying capacity, regulated by density-dependent processes. In the treatments exposed to 0.01 µg/L and 0.0316 µg/L esfenvalerate, a slightly offset relationship was observed. Post-exposure growth rates were offset by +0.12 mg/day and +0.08 mg/day, respectively (Figure 4.3a,b). In contrast, control populations did not deviate from the effect of pre-exposure growth rates (+0.005 mg/day post-exposure growth rate), and concentrations of 0.316 µg/L esfenvalerate and above resulted in significantly decreased post-exposure growth rates (avg. $= -0.29$ mg/day, $p < 0.05$). In fact, the comparison with a model without concentration effects (Table B.3) shows that the concentration explains an additional 24% of the variation in post-exposure growth rates. The resulting hormetic response (Figure 4.3) was also present in the long-term increase in abundance and biomass, with the 2 lowest concentrations increasing and the higher concentrations decreasing (Figure 4.3).

4.4 Discussion

4.4.1 Density Dependent Oscillations of *D. magna* Populations

We observed a substantial and significantly increased population abundance and biomass in *D. magna* populations exposed to concentrations of 0.01 and 0.031 µg/L esfenvalerate for up to 7 weeks after pulse-exposure (Figure 4.1a–h). To understand the processes governing the observed systems, the population dynamics of the control populations must be considered. The control populations went through an exponential growth phase, which in the case of neonates reached a maximum after 3 weeks (dominance phase). In the following weeks, the number of neonates decreased and the population was dominated by adult organisms. This resulted in a low but variable population biomass (suppression phase). Such demography is very common in *D. magna* population dynamics (McCauley and Murdoch, 1987; Faerøvig et al., 2002; Rutter et al., 2017). Oscillating population dynamics

are a well-known phenomenon (Halbach, 1970; May, 1974), and have been repeatedly observed in *D. magna* populations even in the absence of an external forcing (Murdoch and McCauley, 1985; Grover et al., 2000; Preuss et al., 2009). The behavior of *D. magna* to reproduce in batches can lead to high growth rates and corresponding overshoots with delayed corresponding strong downward fluctuations (McCauley and Murdoch, 1987), with a large potential for demographic stochasticity. Due to the limited size of the experimental units (4.5 L), the variation in the observed control replicates is therefore most likely due to demographic stochasticity and has been frequently observed in laboratory *Daphnia* populations (Palamara et al., 2022; Vlaeminck et al., 2022).

In this study, none of the populations exposed to low concentrations of esfenvalerate (0.01, 0.03 µg/L esfenvalerate) went through a low-density phase (Figure 4.2a,b). Instead, abundance and biomass of *D. magna* were significantly increased compared to the control (Figure 4.1a–h). Hence, we consider the observed stimulatory effects as positive deviations from the typical suppression phase in *D. magna* after reaching peak population density. Possible hypotheses to explain this observation are presented below.

4.4.2 Reductions in Individual Competitiveness May Explain Hormetic Stimulation in Single Species Laboratory Populations

Hormesis theory proposes that low doses of toxicants can induce stimulatory effects in individuals and populations. This was first reported by (Schulz, 1888) who identified increased CO_2 production in yeast populations exposed to various toxicants. Similar, beneficial effects of toxicants well below acute mortality have been observed in a number of other studies (Stebbing, 1998; Christopher Cutler et al., 2009; Calabrese, 2010; Cutler, 2013; Carvalho et al., 2020; Wang et al., 2021). For pyrethroids, positive effects of sublethal concentrations have also

been observed in *Daphnia* (Liess et al., 2019a) and mayfly survival (Beketov and Liess, 2005), trans-generational increases in aphid reproductive rates (Shang et al., 2021), trans-generational beetle hatching success (Wolz et al., 2021), and beetle body mass increases (Margus et al., 2019). In *D. magna*, increased reproduction rates of population were observed under sublethal concentrations of esfenvalerate (Bjergager et al., 2012). A hormesis-induced increase in reproduction (e.g. Costantini, 2019) following exposure to 0.01 and 0.03 µg/L esfenvalerate is a possible explanation for the observed results (Figure 4.1a–h, Figure 4.3b). Hormesis-induced stimulation, however, demands that free resources were available for the increased population growth. Figure 4.3a shows very clearly that the growth rates before and after the exposure were inversely proportional, indicating that reaching carrying capacity of the populations coincided with the exposure to esfenvalerate. In addition, the clear peak in the smallest size class prior to the exposure event indicates that the carrying capacity was reached. Thus, simple stimulation is not sufficient to explain the sustained increase in abundance and biomass for several weeks after exposure. Hormesis theory also suggests that positive responses to low doses of stress can result from conditioning (Costantini, 2019), but since organisms are only exposed to esfenvalerate only once in their lifetime, this explanation is ruled out. Considering the high *intra*specific competition under carrying capacity, it is very likely that not only a hormetic-induced increase in reproduction, but also trade-offs affecting resource availability contributed to the observed results.

Environmental change may induce stimulation of some functions and repression of others in the transcriptional programs of the environmental stress response (Gasch et al., 2000; Hackley and Schmid, 2019). Therefore, stimulatory effects should come at the expense of energetic trade-offs, resulting in net neutral population growth rates (Calow and Sibly, 1990; Forbes, 2000). We show that, contrary to this assumption, the resulting net population growth was positive, suggesting that hormetic trade-offs may not be detectable in conventional population

responses such as density and biomass. To explain the significant and long-lasting positive deviation from control treatments within populations at carrying capacity, some other resource-consuming process must have been reduced. We hypothesize that at the population level, *intra*specific competition is reduced by pesticide exposure at low, sublethal concentrations. The concept of an intrinsic longsys that can be reduced by external stress has been previously described at the individual level (Liess et al., 2019a), and has been successfully applied to model the stimulatory effects of low toxicant concentrations (Liess et al., 2020). A reduction in *intra*specific competition, along with an associated reduction in resource requirements, may have allowed the short-term increase in population growth (Figure 4.3b) to take hold and result in an increased population biomass throughout most of the life span of *D. magna*. Only 8 weeks after exposure—at the end of the life span of *D. magna*—did population density and biomass return to control levels. Therefore, we conclude that the reduction in individual competitiveness is the likely trade-off of hormesis in population growth rates of *D. magna* exposed to sublethal concentrations of pyrethroids. It is a limitation of this study that no indicators of reduced *intra*specific competition were measured. Reduced metabolism, activity, or swimming speed while maintaining filtration rates could mechanistically explain the observed results and should be tested in future work. It should also be noted that the results cannot necessarily be extrapolated to environmental ecosystems, where predator-prey dynamics greatly complicate the system. Nevertheless, the study provides mechanistic information on the effects of ultra-low doses on the population dynamics of *D. magna*.

4.4.3 Considerations for Esfenvalerate Effects in the Environment

In this work's experimental setup—which mimicked a natural system with sediments and suspended organic matter—a single pulse of ⅓ of the esfenvalerate EC_{50}, resulted in a collapse of 50% of the popula-

tion; and, as argued above, even much lower concentrations affected the population dynamics of *D. magna*. Our study therefore shows that single pulses of pyrethroids are a relevant threat to aquatic organisms even far below acute concentrations. This contradicts the assumption of (Yang et al., 2006) and (Lu et al., 2019), who argued that the toxicity of pyrethroids is overestimated when using the total chemical concentration, due to high sorption to sediments and consequently low bioavailability. Despite the quick dissipation of esfenvalerate, initial pulses occur and result in long-term detrimental effects in populations, as demonstrated in this experiment. While we acknowledge the low bioavailability of pyrethroids after chemical equilibrium is reached, effects at the individual level do occur after ultra-low pulses (Liess, 2002; Beketov and Liess, 2005), and our study shows that pyrethroid pulses even have long-term effects at the population level. Given the demonstrated occurrence of such pyrethroid pulses (Rösch et al., 2019a) and the likely increase in pyrethroid use in the future (Jactel et al., 2019), we argue that the effects of transient pyrethroid pulses should be considered in aquatic risk assessment.

Finally, it could be argued that low concentrations of pyrethroid insecticides are acceptable as they lead to increased stability of the exposed systems. However, we do not consider this to be a valid argument, as the presumed long-term reduction in competitive strength under conditions of *inter*specific competition with another species could have a negative effect on population development. To clarify, suppose that sublethal effects of a pesticide induce a population increase in biomass and abundance, conditional on a reduction in individual competitiveness. Then, in an ecological community, a less sensitive competitor could exploit this competitive advantage and outcompete the more sensitive species. Such a mechanism is supported by the theory that changes in the competitive difference between species can lead to the exclusion of one species (Pastore et al., 2021) and has already been observed for the case of acute concentrations (Liess et al., 2021).

We conclude that concentrations below 1/10 of the acute EC_{50} significantly increased the population abundance and biomass for several weeks following exposure to the pyrethroid insecticide esfenvalerate. This provides evidence that responses to low-dose toxicants may reduce long-term *intra*specific competition by reducing the competitive strength of individuals. We therefore propose the use of long-term non-invasive population monitoring to detect subtle but relevant effects on the performance of individuals within populations. Furthermore, we propose to conduct multi-species experiments to assess population performance under the influence of *inter*specific competition and ultra-low pesticide exposure.

Chapter 5

Persistent Disruption of *Inter*specific Competition after Ultra-low Esfenvalerate Exposure[3]

5.1 Introduction

Effect assessment is centered around the screening for toxic effects with single species, single substance tests (European Food Safety Authority, 2013). However, a growing number of studies indicate that whenever complex biological systems are exposed to a stressor, results diverge from expectations (Fleeger et al., 2003; Knillmann et al., 2012a,b; Liess et al., 2013; Arce-Funck et al., 2016; Alexander et al., 2016; Allen et al., 2021; Vaugeois et al., 2020). Due to this gap between single species lab experiments and mesocosm experiments, the inclusion of species interactions is one of the most important aspects of strengthening risk assessment (Gessner and Tlili, 2016). Indeed, the question "how [...] interactions among different stress factors operating at different levels of biological organization [can] be accounted for in environmental risk

[3]Published in a slightly modified form as: Schunck F, Liess M. 2024. Ultra-low esfenvalerate exposure may disrupt interspecific competition. *Sci Total Environ.*

assessment", was ranked first place by experts on the topic of how to advance sustainable development of environmental quality (van den Brink et al., 2018). Unfortunately, little progress has been made, as studies considering biological stressors such as species interactions are still underrepresented in literature (He et al., 2023).

The population state is an important co-variate for toxic effects of chemicals. *Intra*specific competition can delay recovery of the population structure (Pieters and Liess, 2006; Liess et al., 2006; Liess and Foit, 2010). The competitive exclusion principle states that complete competitors (i.e. those that compete for exactly the same ecological niche) cannot coexist (Gause, 1936; Hardin, 1960), in natural ecosystems species diversify into their own niche, however, usually some overlap between shared resources remains, allowing for co-existence of competitors (MacArthur, 1958; Hawlena et al., 2022). When such communities are exposed to toxicants, species–species interactions can therefore be expected. This is because usually one species will have a competitive advantage if exposed to a toxicant due to differences in the species' sensitivity. *Inter*specific competition can delay recovery of species after disturbances (Knillmann et al., 2012b) and increase toxic effects of pesticides (Knillmann et al., 2012a). Under repeated lethal exposure to toxicants, the more sensitive species is gradually excluded, even when food density is abundant (Liess et al., 2013). In a synthetic freshwater community, the exposure to acute concentrations of an insecticide lead to reduced abundance in both competitors when they had a comparable sensitivity towards the toxicant and led to compensatory dynamics if sensitivities were different (Mano and Tanaka, 2016).

How do pesticides alter interactions between competing species? Do they cease or do they change when concentrations are far below levels that elicit acute effects? In the field, pesticide exposure 3 orders of magnitude below the half maximal effective concentration (EC_{50}) results in severe degradation of community composition with the loss of sensitive species (Liess et al., 2021). Recently, it was shown that expo-

sure to esfenvalerate at 1–2 orders of magnitude below the acute EC_{50} may lead to a long-term increase in abundance of *D. magna* populations at their carrying capacity (Schunck and Liess, 2023), reinforcing the question how subacute concentrations act on the ecological level of the community.

This experiment aims to reveal the effect of ultra-low dosed esfenvalerate concentration on the population development of two competing species (*D. magna* and *C. pipiens*) in a food limited system that facilitates high competition between the species. For this we set up 80 laboratory nanocosms and repeatedly exposed them with esfenvalerate concentrations as low as 3 orders of magnitude below the acute EC_{50}. The system state was monitored over a period of 4 months through non-invasive weekly monitoring of species abundance and measurement of physico-chemical parameters to assess the influence of environmental parameters on population development. The correlation between competing species was estimated with bayes methods in order to identify effects of esfenvalerate on the interaction between *D. magna* and *C. pipiens*.

5.2 Material and Methods

5.2.1 Experiment Design

To study the effects of low doses of esfenvalerate on competing populations under limited availability of food and varying environmental conditions, 80 artificial 2–species systems were assembled in November 2020, under controlled temperature (20 $\pm$ 1 °C) and light conditions (16:8 day/night cycle). *D. magna* and *C. pipiens* were selected as competitors, both of which are common invertebrates that dwell in standing freshwater and brackish water bodies (Ebert, 2022). While *D. magna* spends its entire life cycle in the water, the species *C. pipiens* emerges after an approximately 20 day underwater larval stage as an adult mosquito and can reproduce without feeding on animal

blood. Both species feed on suspended particles in the water column (Merritt et al., 1992; Ebert, 2022) or moved close to the sediment to graze on organic particles of periphyton.

Each experimental unit consisted of a 5.5 L glass beaker (Harzkristall, Derenburg, Germany), filled with 1.5 kg of washed aquarium sand of 1–2 mm diameter. The sediment layer served as a habitat for microorganisms to facilitate self-purification of the systems as well as substrate for periphyton growth. Aachener Daphnien Medium (ADaM) (Klüttgen et al., 1994) was used as the test medium for the experiment. Throughout the duration of the experiment, the medium was not exchanged and kept at a constant volume of 3.5 L by replenishing the beakers with doubly distilled water on a weekly basis. The systems were covered with a polypropylene net to prevent escape of the adult mosquitos. Two eyelets were embedded in the netting to grant access to the systems for measurement, sampling and supply of glucose solution. Additionally, a reaction vessel was fitted in the netting and immersed in the water column and filled with distilled water itself. This provided access for temperature monitoring without cross-contaminating the measurement device.

For 5 months, the systems were continuously colonized, while the systems were developing periphyton growth on the sediments, which served as a food source for the organisms. The systems were deliberately left to diverge from the initial homogeneous state to reflect random variation in environmental habitats. In contrast to previously conducted nanocosm experiments (Liess et al., 2006; Foit et al., 2012), no additional food was supplied to the systems after the end of the colonization period. Instead, nutrition came from periphyton growth on the sediments and suspended algae and bacteria in the water column. This set-up was chosen to mimic density dependent processes in natural systems (Halbach, 1970) and enforce competition between the two test species. Only adult mosquitoes were provided with a saturated glucose solution to enable reproduction.

5.2.2 Water Quality During the Pre-exposure Period

After 5 months of colonization, population monitoring of *C. pipiens* (once per week) and *D. magna* (twice per week) began. Those systems, with low emergence rates of adult *C. pipiens* were still populated with larvae and eggs to simulate spawning events for another two months. Physicochemical parameters were very homogeneous in the pre-exposure period (temperature 20.2 ± 0.3 °C, conductivity 987 ± 84 µS/cm, oxygen 10.1 ± 0.5 mg/L, pH 7.3 ± 0.4). Nutrient levels were similar to previously conducted studies (PO_4^{3-}: 0.2 ± 0.1 mg/L, NO_3^-: 0.7 ± 0.4 mg/L, NO_2^-: 0.02 ± 0.01 mg/L, NH_4^+: 0.03 ± 0.04 mg/L). The median suspended biomass of 0.2 mg/L was in the range of oligotrophic lakes, suggesting that most systems were strongly limited in biomass available for feeding however measurements had a considerable range (90%-quantile: 0.01–2.97 mg/L). The environmental parameters that characterized the systems are summarized in Table C.1 for the pre-exposure period and in Table 5.1 for the post-exposure period.

5.2.3 Exposure

After the 2-month pre-exposure period, the systems were exposed two times to the pyrethroid insecticide esfenvalerate with a recovery period of 1 month between exposures. The treatments consisted of 5 esfenvalerate exposure levels (solvent control, 0.1, 1, 10, 100 ng/L) with a treatment size of 16 replicates each. For the preparation of stock solutions, 5 mg esfenvalerate (CAS 66230-04-4, HPC Standards GmbH, Cunnersdorf, Germany) were dissolved in dimethylsulfoxide (DMSO) and diluted to a concentration of 1000 µg/L, which also served as exposure solution for the highest exposure treatment. From this stock, exposure solutions were diluted to 100µg/L, 10µg/L and 1 µg/L. An additional solution containing DMSO was prepared to serve as the exposure solution for the solvent control. The stocks were prepared on the day preceding the exposure and refrigerated overnight. On the day of exposure, 350 µL of the treatment specific exposure solutions were

Table 5.1: Average of environmental parameters per group during post-exposure. Values are reported as the average across time and experimental replicates with their associated standard deviation.

Variable	0.0 ng/L	0.1 ng/L	1.0 ng/L	10 ng/L	100 ng/L
Temperature (°C)	20.2 ± 0.3	20.1 ± 0.3	20.0 ± 0.3	20.0 ± 0.3	20.2 ± 0.3
Conductivity (µS/cm)	969 ± 49	977 ± 53	991 ± 53	997 ± 96	991 ± 78
Oxygen saturation (mg/L)	9.4 ± 0.3	9.4 ± 0.4	9.3 ± 0.3	9.4 ± 0.3	9.3 ± 0.3
pH (-)	7.1 ± 0.1	7.1 ± 0.1	7.1 ± 0.1	7.1 ± 0.1	7.2 ± 0.2
PO4 (mg/L)	0.45 ± 0.33	0.51 ± 0.39	0.77 ± 1.99	0.6 ± 0.89	0.65 ± 0.82
NO3 (mg/L)	1.42 ± 0.69	1.47 ± 0.62	1.31 ± 0.62	1.44 ± 0.77	1.5 ± 0.83
NO2 (mg/L)	0.03 ± 0.03	0.03 ± 0.04	0.04 ± 0.05	0.03 ± 0.05	0.05 ± 0.05
NH4 (mg/L)	0.0 ± 0.01	0.01 ± 0.01	0.01 ± 0.02	0.01 ± 0.04	0.03 ± 0.15
Suspended biomass (mg/L)	0.45 ± 1.0	0.41 ± 0.51	0.31 ± 0.3	0.67 ± 1.27	1.56 ± 5.8

added to the corresponding systems containing 3.5 L ADaM medium, amounting to a solvent concentration of 0.01% v/v.

The accuracy of the exposure concentrations was determined by measuring the concentration of the stock solutions spiked to 1 L samples of freshly prepared ADaM. In addition, 50 mL water samples from 4 selected replicates of the highest exposure treatment (100 ng/L) were taken exactly 1 h after exposure and 48 h after exposure. Chemical analysis of the tested samples was performed by SGS Analytics Germany GmbH, using a gas chromatography–mass spectrometry (GC-MS). Measured concentrations of stock solutions and samples of experimental replicates are shown in Table S3 and Table S4. The measured concentrations in experimental replicates in the 100 ng/L esfenvalerate treatment were very homogeneously at 38.8 ± 11 ng/L, 1 h after exposure and were always below the limit of quantification (LOQ) of 20 ng/L after 48h. Rapid dissipation of esfenvalerate from the water column due to sorption and photodegradation can explain the repaid decay in the first 48h hours after exposure. For the remainder of this work the nominal esfenvalerate concentrations are reported.

5.2.4 Biological Assessment of Exposure Concentrations

In addition to chemical analysis of the exposure solutions, the effect of esfenvalerate on standard test organisms was assessed. This was done under standard conditions and in the nanocosm medium. These standardized experiments were conducted in parallel to the exposure of the main experiment. For each test system, 2 × 25 ml beakers were filled with 20 ml samples of the test systems 1 hour after exposure. 5 neonates (< 24 h) of *D. magna* were placed in one beaker and 5 larvae (< 96 h) of *C. pipiens* in the other; then survival was observed for 48 h. During this duration organisms were not fed to mimic conditions in the test systems. In addition, the same setup was prepared for each exposure concentration, plus a test concentration of 1000 ng/L, in standard ADaM medium. Populations were monitored for survival for 2 days without feeding, according to the acute standard test for *D.*

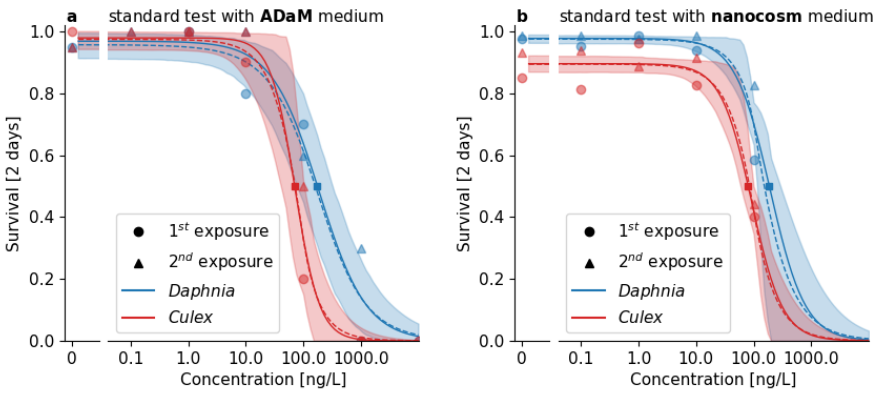

Figure 5.1: Similar sensitivity of *D. magna* (age < 24 h) and *C. pipiens* (age < 96 h) after 48 h of exposure to esfenvalerate. The average esfenvalerate EC_{50} for *D. magna* from Environmental Protection Agency (EPA) database is 0.31 ± 0.33 µg/L (Table 2.1). Survival data were obtained from standard tests conducted in parallel to the 1st and 2nd exposure of the nanocosm test systems with the same exposure solutions **(a)** under standard conditions (*Culex* EC_{50} = 71 ng/L, *Daphnia* EC_{50} = 176 ng/L), and **(b)** in samples of experimental units (nanocosms) taken 1h after exposure to esfenvalerate (*Culex* EC_{50} = 80 ng/L, *Daphnia* EC_{50} = 187 ng/L). The squares indicate the EC_{50} and shaded areas show the bayesian credible intervals (CIs) of the estimate. The solid line is the maximum likelihood estimate of a 3-parameter log-logistic function and the dashed line is the bayesian fit.

magna (OECD, 2004). Figure 5.1a shows that under standard conditions *C. pipiens* were slightly more sensitive (*Culex* EC_{50} = 71 ng/L, *Daphnia* EC_{50} = 176 ng/L). When tested in the nanocosm medium, *Culex* had 10% higher control mortality also under non-lethal esfenvalerate concentrations (Figure 5.1b), while no control mortality was detected in *D. magna*.

5.2.5 Monitoring of Species Abundance

Population development of *D. magna* was monitored by taking 3 images of each system with a *Panasonic DC-FZ1000-II* (Panasonic Corporation, Kadoma, Japan), twice per week and was analyzed with an

improved image analysis technic compared to the approach developed by Foit et al. (2012).

Initially, motion is detected by background subtraction; this method is based on differences between two consecutive images. Background subtraction removes all static parts of the image, so that only moving objects of both images remain. Taking the elementwise maximum of this difference results in only the moving objects of the first image. Depending on the amount of movement in the system, between 100–100000 proposal candidates are generated. Large numbers of proposals can occur when the background is even slightly moving, or the lighting conditions change during capture. In a second step, the bounding boxes around the coordinates of the detection are analyzed for characteristic properties and stored in a file. These data points comprise the basis for the classification. 50 randomly selected images were annotated based on the candidate proposals. After annotation, a support vector machine (SVM) classifier was trained with the annotated tags from the 50 images. The resulting accuracy of the unseen test set was 98%.

Of all labelled *D. magna*, 97% were correctly classified as such, however an arbitrary proposal of a moving object generated a 2% chance of a false positive detection, resulting in a slight tendency for overdetection (Figure 5.2a). This effect can result in problems if a large number of proposals is generated (e.g. when the camera is slightly moved during image capture). Therefore, in a 3rd step of the analysis, the image with lowest overall difference in pixels was chosen in each series and manual removal of few images, where no successful difference image could be calculated. This classification method was then used to detect population abundance in 7680 images taken throughout the experiment. Validation with the true organism count obtained at the end of the experiment shows that approximately 50% of the organisms are detected (Figure 5.2b), however, this divergence is consistent throughout the assessed systems, which allows to assess the relative effects in the system.

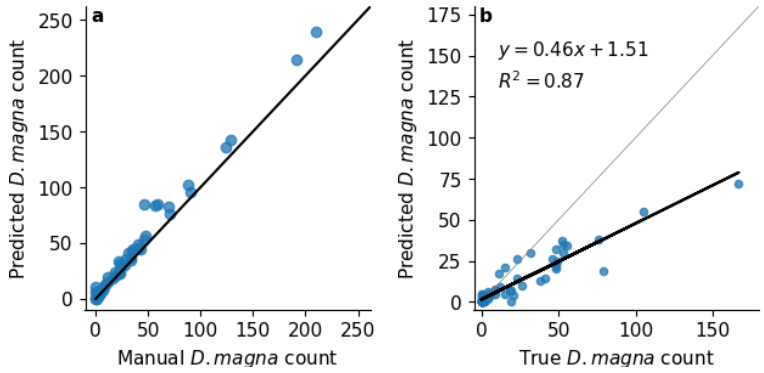

Figure 5.2: Validation of the detection method. The manual count indicates the number of organisms identified by visually counting *D. magna* in an image. In contrast, the true count is the actual number of organisms in the vessels determined when the experiment was ended. The predicted count is the number of organisms estimated by the classification algorithm. **(a)** Classifier evaluation of the capacity to detect organism from images. **(b)** Validation of the method by comparison of estimated organism count from image segmentation and classification with the true count from the last day of experimentation.

The abundance of larvae of *C. pipiens* was manually counted once per week. Since larvae of *C. pipiens* generally remain static in their positions below the water surface, it was possible to determine accurate population counts. Also, in contrast to automatic detection methods it was easily possible to distinguish between exo-skeletons of emerged larvae and their submerged siblings. In order to detect any organisms hiding in the sediments, the systems were gently moved to provoke escape reactions of *Culex* larvae. The abundance of *Culex* larvae directly after hatching is not included in the population count. Only organisms larger then approximately 2 mm (newly hatched) were included in the analyses.

5.2.6 Sampling and Measurement of Environmental Parameters

Weekly, a 5.5 mL sample was taken to measure physicochemical parameters and cell density. Every second week, an additional 20 mL

sample was taken to measure the nutrient status of the systems. Greatest care was taken to avoid cross contamination of the systems. For this, syringes were connected with silicon tubing to each nanocosm and reused for the entire duration of the experiment. After sampling, the samples were stored cool until analysis or measured directly and discarded thereafter. Sampling was conducted in parallel to the monitoring of the systems. Since this process took several hours, variations in the reported parameters due to daily temperature fluctuations are present in the dataset. Medium reductions due to sampling and evaporation were replenished with bi-distilled water. Major nutrient concentrations (NO_2^-, NO_3^-, NH_4^+, PO_4^{3-}) were measured every second week with a photometer (*PF-12plus*, Macherey-Nagel, Düren, Germany). To increase the accuracy, values were calculated from recalibrated spectral absorbance measurements and estimated concentrations (Figure C.1). Physicochemical parameters were measured with a multi-parameter device (*Portavo 908 Multi*, Knick Elektronische Messgeräte GmbH & Co. KG, Berlin, Germany). The density of suspended cells was measured with a *CASY-TTC cell counter* (Schärfe Systems, Reutlingen, Germany, now OMNI Life Science, Bremen, Germany). The raw count data was passed through a filter, discarding measurements where total counts were < 2, to separate white noise from signal. Data were then smoothed and the total volume in µL/L was calculated and estimated as suspended biomass density in mg/L, assuming a wet weight density of 1 mg/µl (e.g. Zhu et al., 2021). The pre-exposure measurement values are reported in Table C.1.

The measured levels of N and P were in the range of eutrophic lakes (compare e.g. Šorf et al., 2015; Beklioğlu et al., 2017). However, continuously high levels of dissolved oxygen and low densities of suspended cells indicate that the observed nutrient concentrations had no effect on the studied systems. Direct effects of these nutrients are also unlikely since, they were not near high enough to elicit direct effects on *D. magna* (Serra et al., 2019).

5.2.7 Statistics

For the entire analysis 17 systems were excluded from subsequent analysis. The detailed reasons for removal are listed in method C.1. For all analyses considering the temporal dynamic of the systems, the time series were smoothed by computing centered running averages with a time window of 11 days (Figure 5.3). This was done to reduce the influence of very short termed fluctuations in the signal, which makes the analysis more robust to measurement errors, but may rarely underestimate true treatment effects such as the saw tooth pattern visible in Figure 5.3a.

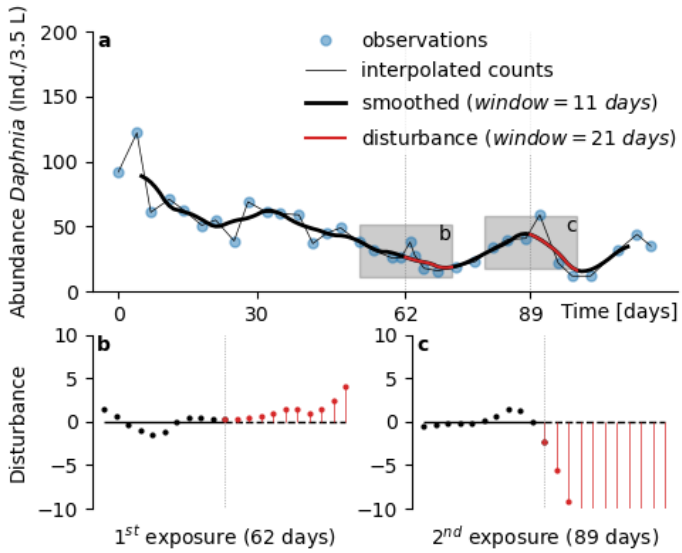

Figure 5.3: Time series smoothing and exemplary disturbance analysis of one experimental unit. **(a)** shows a running average (solid black line) that has been computed through the time series (blue dots). The lower panels show deviations from the linear pre-exposure trend that has been extrapolated (dashed line). **(b)** first exposure on the 3rd of June (day 62) **(c)** 2nd exposure on the 30th of June (day 89).

Disturbance Analysis to Identify Short Term Effects of Esfenvalerate

Due to the complexity of the analyzed systems, high variance between experimental replicates complicated the identification of general pat-

terns in the time series. The following analysis was developed to robustly identify immediate effects of the tested esfenvalerate concentrations in replicated time series with high variance between replicates. In smoothed time series, 21–day long segments, centered around the exposure events, were isolated (Figure 5.3, gray boxes). Then linear trends were computed through the 10–day pre-exposure sections (Figure 5.3b,c, solid horizontal lines) and were extrapolated to the following 11 days (Figure 5.3b,c, dashed horizontal lines). Disturbances were then estimated by calculating differences between extrapolated pre-exposure trends and the true development of smoothed time series (Figure 5.3b,c, red vertical lines). The described analysis allows the estimation of low disturbances when the population development is characterized by smooth, non-volatile cycles, which we interpret as normal behavior. On the contrary, high variance in the signal will lead to strong disturbance signals and be indicative of treatment effects.

Correlation Analysis to Identify Changes in *Inter*specific Competition

In the study of interaction between species, measuring the correlations between species can give insight into their relationship (Moran, 1953; Ranta et al., 1995; McCarthy, 2011). Strongly positive correlations between abundance will in theory emerge, when both species equally respond to low or high levels of resource availability. In essence, when they are coexisting with significant overlap of shared resources. On the other hand, if the exclusion of either one species occurs, strong negative correlations between species will be observed. Natural systems, repeatedly observed over time, will show correlations between these extremes. However, trends in either one of the directions are indicative of changes in the relationship between species and will be interpreted as such in this study.

Estimating the correlation between count data is a non-trivial task. The approximation with the Pearson correlation coefficient will underestimate negative correlations due to the constraint of count data to

be non-negative. In addition, multivariate Poisson distributions have been previously restricted to positive correlations (Ghosh et al., 2021). Modern bayesian inference frameworks (Salvatier et al., 2016) allow for flexible transformations of variables, which enabled us to approach the problem by modelling the count data (N_s) as Poisson distributed variables (Equation 5.1), modeling their log-rates ($log(\lambda)$) as correlated normal distributed variables (Equation 5.3), and transforming the log-rates positive constrained rate parameters by exponentiation (Equation 5.2).

$$N_s \sim Poisson(\lambda_s) \tag{5.1}$$
$$\lambda_s = e^{log(\lambda_s)} \tag{5.2}$$
$$log(\lambda_s) \sim MultivariateNormal(mu = \mu_s, covariance = cov) \tag{5.3}$$
$$cov \sim LKJ(\eta = 1, \sigma_s) \tag{5.4}$$
$$\mu_s \sim Cauchy(0, 1) \tag{5.5}$$
$$\sigma_s \sim HalfCauchy(1) \tag{5.6}$$

Weakly informative Cauchy distributions with heavy tails (Gelman et al., 2008; McElreath, 2015) were used as priors for μ_s and σ_s, which describes the log species occurrence rates (Equation 5.5) and their intrinsic deviation (Equation 5.6). An LKJ prior with uniform probability density over the correlation between the species ($\eta = 1$) was used as an uninformed prior for the covariance structure of the multivariate Normal (Equation 5.4). A calculation example for 3 imaginary test systems: Assume the numbers of organisms (*Culex*, *Daphnia*) in the respective systems were (5, 10), (10, 20) and (20, 40). A correlation coefficient close to 1 would be estimated, although with large highest density intervals (HDIs) representing the uncertainty, since only 3 samples are given. In an opposing example, where (1, 20), (50, 2), (0,0) are observed, a correlation coefficient near -1 would be estimated, representing the observation, at most one species was dominant. An estimation example for a simulated dataset is given in Figure C.2,

which shows that the correlation coefficient can be estimated very well, even with only 12 samples, which is representative for this study. The 95% posterior density interval (PDI) was computed to calculate the CIs, which are considered to be the bayesian analog to confidence intervals. However, in contrast to confidence intervals, a 95% CIs include the true parameter value with a 95% probability by definition. *Inter*specific correlation coefficients, including bayesian uncertainty estimates were recovered from the covariance matrix (Equation 5.4), which fitted estimated for whole pre- and post-exposure datasets (results: Fig. Figure 5.6) and for each day in the smoothed time series (see Figure 5.3) to obtain trends in the *inter*specific correlation (results: Figures 5.4 and 5.7).

5.3 Results

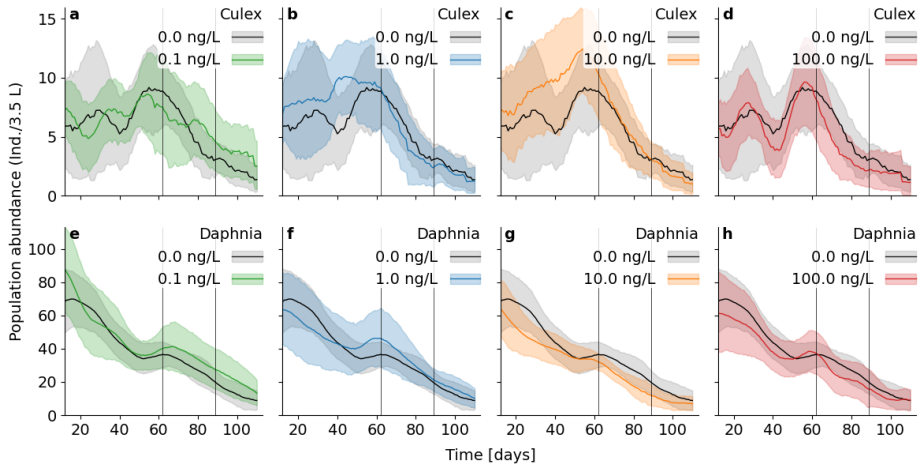

Figure 5.4: Species abundance (λ) per treatment over the time of the experiment in days computed with a bayesian model of correlated, Poisson distributed variables. The vertical lines indicate the times of exposure to esfenvalerate. Shaded areas are 95% CIs and indicate the uncertainty of the estimates. **(a–d)** Expected abundance *C. pipiens*. **(e–h)** Expected abundance *D. magna*.

Figure 5.4 shows the development of population densities of the competing species before and after exposure to esfenvalerate as a treatment

average. Larvae populations of *C. pipiens* were stable or increasing in the pre-exposure period with highly variable population densities across replicates, indicated by large CIs (Figure 5.4a–d). This is attributed to continued stocking of low density *Culex* populations with additional eggs and larvae in the pre-exposure period. Only when stocking was ceased in the post exposure period, negative trends were visible in the population density of *C. pipiens*. In contrast, *D. magna* populations, which were not artificially stocked in the pre-exposure period, follow a steady decline over the entire period of the experiment (Figure 5.4e–h). In general, the declining population density reflect that the systems were characterized by resource scarcity. This corresponds to the low density of suspended organic matter (median 0.21 mg/L, 90%-quantile: 0.01–2.97 mg/L). As expected, due to the necessity of artificial stocking in the pre-exposure phase and slightly but significantly higher baseline mortality in nanocosm medium (Figure 5.1b), *C. pipiens* were significantly less abundant then *D. magna* over the entire duration of the experiment.

After exposure to esfenvalerate, average trends of populations exposed to esfenvalerate did not significantly deviate from the controls. And, despite differences in relative population densities before exposure, the fractions of low-density populations towards the end of the experiment ($\leq$ 10% of the pre-exposure maximum) did not differ between *C. pipiens* and *D. magna*. Also, the physico-chemical parameters were remarkably similar across all treatments in the post exposure period (Table 5.1). Compared to the pre-exposure period (Table C.1), oxygen saturation slightly decreased by 7%, while the medium pH, conductivity and temperature did not change. PO_4^{3-} and NO_3^- concentrations approximately doubled in the post-exposure period, while NO_2^- and NH_4^+ did not change. Only suspended biomass differed among treatments, however, the differences are smaller than the standard deviations (Table 5.1).

5.3.1 Community Response to Esfenvalerate Exposure

Figure 5.5a shows that a concentration of 100 ng/L elicits a significant negative disturbance (-6.0, $p = 0.02$) on populations of *D. magna*. This is also visible in the volatile trajectories of Figure 5.4h (100 ng/L). While disturbances after exposure to 100 ng/L were negative after both exposures, an exposure to concentration $\leq$ 10 ng/L resulted in negative disturbances after the 1st exposure and positive disturbances after the 2nd exposure. On *C. pipiens*, exposure to esfenvalerate induced no significant short-term disturbances (Figure 5.5b). Under standard conditions the species had similar sensitivities to esfenvalerate (EC_{50} *Culex* = 80 ng/L, EC_{50} *Daphnia* = 180 ng/L, Figure 5.1). However, these sensitivities were not reproduced on the community level, where *D. magna* is the only species significantly disturbed by exposure to 100 ng/L esfenvalerate. This could be explained by different durations of the observed post exposure period in standard tests (2 days) and the nanocosm test systems (11 days).

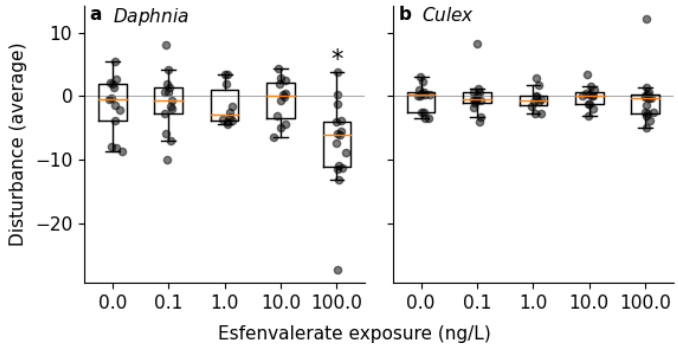

Figure 5.5: Average 11-day disturbance of competing populations calculated from the deviation of extrapolated pre-exposure trend (10 days) to observed post exposure development in a 21-day time window (see methods: disturbance analysis). **(a)** *Daphnia* disturbance after exposures to esfenvalerate. **(b)** *Culex* disturbance after exposure to esfenvalerate. A significant deviation from the control treatment is indicated by an asterisk.

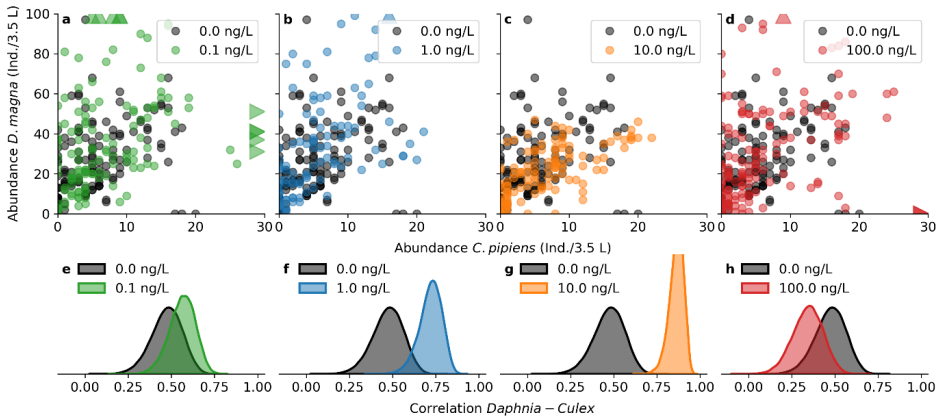

Figure 5.6: (a–d) Population densities of observed *Culex* and *Daphnia* during the entire post exposure period of all experimental replicates. High correlations indicate that fluctuations in population density were synchronized, while low correlations indicate that fluctuations in population density were not synchronized. The colored treatments are always compared to the same control dataset (gray). The displayed data-range was truncated to increase visibility of the dataset. Not shown data are indicated by triangles at the upper or right-hand side of the panels. (**e–h**) bayesian posterior density estimates of the *Daphnia–Culex* correlation coefficient, fitted on the data in panels a–d with the model described in equations 5.1–5.6.

5.3.2 Changes in Species Correlation after Exposure to Esfenvalerate

It was a key question of this study, whether exposure to pesticide influences the *inter*specific competition at low concentrations. To assess this question, the correlation between both species over time was evaluated by applying bayesian estimation of the covariance between two Poisson distributed variables.

Figure 5.6a–d shows the pairs of population density of *C. pipiens* and *D. magna* at each observation in the post-exposure period. States with simultaneously high population densities of both *D. magna* and *C. pipiens* were rarely observed. Figure 5.6c shows the population densities of highly correlated species across multiple systems. The development of *C. pipiens* and *D. magna* populations in these replicates was syn-

chronized, meaning that rarely one species was abundant while the other species was not. Figure 5.6e–h shows the estimated correlation coefficient between both species in the community. Small concentrations of esfenvalerate increased the correlation between competitors compared to the control treatment (Figure 5.6e–g). This deviation is significantly positive over the entire post-exposure period in systems that were exposed to 10 ng/L (Figure 5.6g). In contrast, exposure to 100 ng/L induced a slightly negative correlation shift between *Culex* and *Daphnia*. Considering the effect of 100 ng/L on the disturbance of *Daphnia* population (Figure 5.5a), the reduction of correlation is a sign of extinction, also visible in Figure 5.6d, which shows that one or the other species became dominant, while the other was excluded.

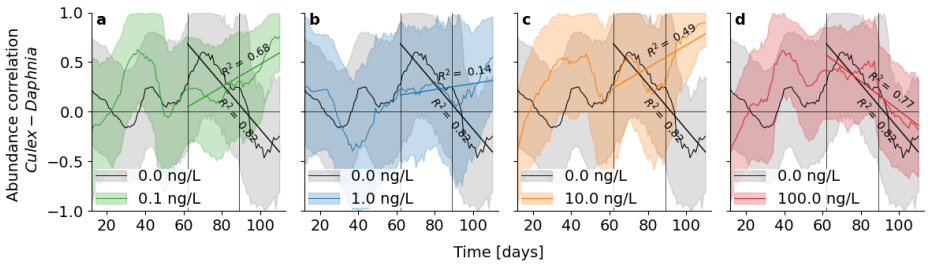

Figure 5.7: Estimation of the developing correlation between abundance of *C. pipiens* and *D. magna* in smoothed time series, showing the competitive exclusion in the control treatments and 100 ng treatments, and showing synchronized behavior in the low concentrations. For each day of the time series, the correlation coefficient was estimated that best predicted the abundance pairs of *C. pipiens* and *D. magna* in all systems of one treatment. The shaded area shows the 95%-CI and indicates the uncertainty of an estimate. The vertical lines indicate the times of exposure to esfenvalerate. Linear regression models were fitted to the correlations in the post-exposure period.

To show the temporal development of *inter*specific competition, the correlations between competitors were computed for each day in the monitoring period by fitting the model (equations 5.1–5.6) on interpolated and smoothed daily observations. Linear regressions were computed to show the treatment trends in competition in the post-exposure periods. We observed that the significantly negative trend in

the control treatment emerged shortly after the exposure ($p < 0.001$), i.e. shortly after addition of manual stocking of *C. pipiens* larvae to the systems was stopped. Figure 5.7a–c shows that after exposure to 0.1–10 ng/L esfenvalerate correlations were significantly positive ($p \leq 0.01$). However, the trend in the treatment exposed to 100 ng/L esfenvalerate was significantly negative ($p < 0.001$), although the correlations substantially dropped only after the second exposure (Figure 5.7d).

5.3.3 Effects of Environmental Conditions

Neither physicochemical parameters (e.g. temperature, oxygen) nor major nutrients varied among the treatments during the post-exposure phase (Table 5.1). While exposure to esfenvalerate significantly disturbed the population development of *D. magna*, the remaining unexplained variance was large (Figure 5.5a). Pre-exposure environmental parameters could not explain this variance (Figure C.3) as there were no significant correlations. Only the pH was mildly positively correlated with the disturbance residuals ($\rho = 0.27$). The concentration of major nutrients was the range of eutrophic lakes (Table C.1), however no significant positive or negative correlations with the final abundance of *D. magna* or *C. pipiens* could be identified. Also, the correlations between other pre-exposure environmental parameters and the final abundance of *D. magna* and *C. pipiens* were insignificant (Tables C.4 and C.5).

5.4 Discussion

In this study we investigated the effect of environmentally realistic esfenvalerate exposures on a 2-species community in a highly competitive environment. The employed detection algorithm for quantifying the population density of *D. magna* based on machine-learning approach was very successful to identify organisms in the water body (Figure 5.2a). Although, the fraction of *D. magna* in the water col-

umn was representative of the system state (Figure 5.2b), future studies should use more homogeneous, dark sediments to facilitate the detection of organisms on the sediment. The detection of slow-moving organisms like *C. pipiens* could be enabled by using permanently installed cameras with longer intervals between images. The improved approach could substantially simplify the employment of experimental nanocosm for routine assessment of population level effects of chemicals. Here, we showed that exposing competing species with similar sensitivities to esfenvalerate results in substantial reduction of *inter*specific competition at low concentrations. These effects were detected far below effect concentrations established in standard tests that were conducted in parallel to the experiment. The exposure to esfenvalerate increased the correlation between *D. magna* and *C. pipiens* with increasing levels of exposure, beginning as low as 3 orders of magnitude below the measured EC_{50} (Figure 5.6). Species correlations of treatments exposed to 0.1, 1 and 10 ng/L significantly increase during the post-exposure period. On the contrary, the concentration closest to the EC_{50} (100 ng/L) decreased the correlation between species and also provoked significant disturbances in the population of *D. magna*.

5.4.1 *Inter*specific Correlation is Associated with *Inter*specific Competition in This Study

Species, experiencing the same environmental conditions are synchronized (Volterra, 1928; Moran, 1953; Ranta et al., 1995; Post and Forchhammer, 2002), i.e. their populations are correlated over time. When species are ecologically similar, co-existing populations will be positively correlated over time, because they react similarly to environmental changes (Hansen et al., 2013; Robertson et al., 2015). However, when competition between species increases, correlations decrease and become negative due to suppression of the less fit species and dominance of the fitter species (Lee et al., 2020). In this study, small systems (3.5 L) were colonized with *D. magna* and *C. pipiens*–species

which occupy different niches but also compete for resources, such as suspended organic particles in the water column (Merritt et al., 1992; Ebert, 2022), which was indeed a scarce resource in this experiment (Tables 5.1 and C.1). Therefore, we assume that the species in this study experienced the same environmental conditions, and were also ecologically similar. Thus, according to theory, high correlations indicate low *inter*specific competition, and low correlations indicate high *inter*specific competition.

Overall, *C. pipiens* were much less abundant than *D. magna* but both species showed a similar decrease in abundance relative to their population density (Figure 5.4). This decrease can be attributed to low levels of primary production, approximated by the density of suspended biomass (Table C.1). We assume that sufficiently large concentrations of N and P could not be converted to biomass in the studied systems. Possible reasons are strong competition of filter feeders, which prevented growth phases of phytoplankton, or insufficient lighting conditions. In the absence of suspended biomass, organisms were observed to graze on periphyton and biofilm, which were not quantified in this study but varied considerably among the experimental replicates.

Resulting from this diversity, dominance and suppression of either species was approximately random, indicated by similar fractions of low density-populations, which led to negative correlations between the species' population densities in the control treatment. This is associated with high *inter*specific competition between *C. pipiens* and *D. magna*, which increased during the post-exposure period (Figure 5.7) after colonization of *C. pipiens* was stopped. These results fit the theory that narrow environments with considerable niche overlap do not favor coexistence of competing species (Pastore et al., 2021).

5.4.2 Exposure to High Doses of Esfenvalerate Disturbs Population and Increases Risk of Single Species Dominance

The exposure to esfenvalerate at 100 ng/L, induced significant, direct short-term disturbances in *Daphnia* populations and decreasing correlations between the species' abundances in the post-exposure phase. Decreasing correlations indicate the suppression of one species, which could be exploited by the dominant species if the composition of the system in terms of suspended biomass, periphyton and biofilm allowed population growth. Since the variation between biomass density and other environmental parameters across experimental replicates could not explain the residual variance of the disturbance of species after exposure nor final population densities of either species, periphyton and biofilm may well have been responsible for the heterogeneity in the systems. However, due to the heterogeneity of the tested systems, the observation of significant population level disturbance of esfenvalerate at 100 ng/L is assumed to be very robust. The direct effect of esfenvalerate at 100 ng/L is also visible in Figure 5.6d, where species abundances increasingly converge to one or the other axes. Similar dynamic behavior has been observed for subpopulations of potato beetle larvae and adults (Costantino et al., 1997). When harvesting rates of adults were experimentally increased, which is comparable to induced direct mortality of 100 ng/L esfenvalerate, beetle populations were pushed out of equilibrium. Although the experimental conditions are only partly comparable, the results show that disturbances competing (sub)populations can lead the way to significant changes in the dynamic of ecological communities.

5.4.3 Exposure to Low Doses of Esfenvalerate Reduces *Inter*specific Competition

From day 70, the control treatment showed a marked *inter*specific competition (Figure 5.7). In contrast, treatments exposed to low doses

of esfenvalerate (0.1–10 ng/L) showed a reduced *inter*specific competition. This already occurred at concentrations 3 orders of magnitude below the EC_{50} and reached its maximum at 10 ng/L (Figure 5.6e–g). The observed results are comparable to a recently conducted simulation study, which found that the covariance of competitors, receiving the same amount of environmental noise, increases when growth rates of species are more similar (Lee et al., 2020). And in marine environments, low pH led to altered competitive interactions between competing algae species and gradually led to a community shift (Kroeker et al., 2013). In a single species population study, exposure to 10 ng/L esfenvalerate reduced the competitiveness of *D. magna* and led to a hormetic increase in population abundance (Schunck and Liess, 2023). Such an effect did not occur in this study. Here, we assume that the presence of a competitor can explain the absence of a stimulatory population effect, suggesting that findings of hormesis are dependent on the environmental context, i.e. only emerge when the environmental conditions do not penalize trade-offs associated with stimulatory effects. With respect to the present study, we hypothesize that ultra-low concentrations of esfenvalerate may have shifted the competitive difference between the species towards an equilibrium. This could be due to a reduction of fitness differences between species (stabilizing mechanism Chesson (2000)). Future work should test this hypothesis in environments with higher population densities and investigate whether competitive differences between species are modified by ultra-low concentrations of pesticides.

Concluding, we showed that concentrations 3 orders of magnitude below the EC_{50} reduced the *inter*specific competition between *D. magna* and *C. pipiens*. Concentrations near the EC_{50} directly impacted *D. magna* populations and led to an increased tendency of single species dominance. This study also highlights, that single species sensitivity tests are insufficient to predict ecological effects on the community level. On the contrary, non-invasive population monitoring is very a promising approach, which can complement the higher tier risk assess-

ment of ecological effects of toxicants, since the absence of sampling removes the most error prone and disturbing part of the method. By monitoring of the correlation between competing species, more subtle effects can be detected and potentially, hazardous long-term effects can be identified before they occur in the field.

Chapter 6

Discussion and Outlook

Pesticides are responsible for ecological effects in the water bodies near agricultural sites and drive sensitive species to extinction far below the half maximal effective concentration (EC_{50}) determined in the effect assessment process (Liess et al., 2021, 2019b; Malaj et al., 2014). Such underestimations can lead to consequences like the decline of bee populations caused by the class of neonicotinoid pesticides (Rundlöf et al., 2015; Cressey, 2017; Stuligross and Williams, 2021); these consequences do not only harm ecosystems but also impact the economy (Vanbergen and the Insect Pollinators Initiative, 2013). However, conflicting results have also been published. It has been shown that overall biodiversity can remain stable, while species colonization and extinction are accelerated (Dornelas et al., 2019). Other studies have observed long-term stability in abundance and biodiversity (van Klink et al., 2020; Crossley et al., 2020). Although studies refuting the loss of biodiversity are viewed with skepticism due to their focus on protected areas (Gonzalez et al., 2016), they do point out that our understanding of the effect of stressors on ecosystems is still limited.

The aim of this work was to assess the effect mechanisms of ultra-low doses of pesticides to understand their influence on observed eco-

logical effects in the environment and to assess the implications for the increasingly discussed hormesis theory. To address these topics, the environmental complexity of the studied systems was stepwise increased. While a variety of factors may modify or mask the effects of pesticides in the environment, in this work we focused on the key factors that modulate the effects of low doses of pesticides. These are *time*, *intraspecific and interspecific competition*, and *environmental conditions*. In the following, the influence of the factors is discussed and findings of this work are synthesized.

6.1 Timing is a Critical Factor for the Interaction between Multiple Stressors

The study described in Chapter 3 assessed the hypothesis, whether interactions between pesticides and environmental stress depend on the timing and order of exposures (see Hypothesis 1). It was shown that, at the individual level, the interval between stress exposures and their order altered the lethality of the stressors. Increased time between stressors shifted interactions from an antagonistic to a synergistic relationship (Figure 3.3). Therefore, Hypothesis 1 can be maintained. An increased effect of stressors applied with an interval between the exposures has also been reported for the mortality of damselflies exposed to heat waves and esfenvalerate (Janssens et al., 2017), and for respiration of marine epifauna exposed to copper and a biocide (Brooks and Crowe, 2019). The novelty of the results reported here lies in the shift in interaction between stressors, when time intervals between exposures were changed. Regrettably, Hypothesis 1 could not be assessed for higher levels of biological organization in this work, because the environmental factors measured in Chapter 5 were not variable enough over time.

The hypothesis that explains these findings is that a in the first step of a two-stage process, stressors may interact antagonistically at the biomolecular level until they are manifested at the physiological level.

It is still unclear whether this outcome resulted from the specific nature of the stressors or is a general phenomenon in multiple stress research. To further develop the theory, more stressor combinations should be tested with the *time-lag and order* approach (Figure 3.1). Also, the usefulness of toxicokinetic-toxicodynamic (TKTD) models in the assessment of dynamic exposure profiles has been demonstrated (Ashauer et al., 2007, 2017; Bart et al., 2021, 2022). For example, azole fungicides have been shown to reduce the biotransformation rate of a pyrethroid insecticide, leading to increased effects (Cedergreen et al., 2017). Approaches like these would be very useful in understanding the variation in effect introduced by temporal differences in the stressor application and should be investigated in future work.

Ultraviolet-B (UV-B) radiation interacted both synergistically and antagonistically with esfenvalerate, depending on the time difference between exposure pulses. The levels of UV-B used in this study were, however, far above environmental realistic exposure levels (Hansson and Hylander, 2009). The findings of Chapter 3 therefore have no direct environmental implication, but they show that environmental factors can distinctly modulate the effects of pesticide exposure. Future work should investigate whether this effect is reproducible at environmentally realistic concentrations, to test if temporal differences in stressor coupling can help explain heterogeneous findings of multiple stressor effects identified in the field (compare e.g. Jackson et al., 2016; Birk et al., 2020).

6.2 The Degree of Competition Modified the Effect of Low Concentrations of Esfenvalerate, but Had No Influence on Acute Concentrations

In this work the sensitivity of *D. magna* to single and repeated pulses of esfenvalerate was evaluated in the context of three levels of biological complexity. The level of the individual (no competition, Chapter 3),

the level of the population (*intra*specific competition, Chapter 4), and the level of the community (*inter*specific competition, Chapter 5). It was hypothesized that the effects of low-dose pesticides on aquatic populations depend on the degree of competition in the system (see Hypothesis 2).

Acute concentrations In individual toxicity tests, 24-hours of exposure to esfenvalerate resulted in an EC_{50} of 0.6 µg/L for *D. magna* (Figure 3.3). Under 48 hours of exposure, the EC_{50} was estimated at 0.18 µg/L (Figure 5.1). These values are very similar to data published in the literature Table 2.1. Similarly, on the population level, the exposure to an esfenvalerate pulse at 0.1 µg/L resulted in the collapse of 2 out of 4 populations after 4–6 weeks (Figure 4.2). When *D. magna* populations were exposed to esfenvalerate in the presence of a competing species, 0.1 µg/L significantly disturbed the populations. Therefore, it is concluded that concentrations, which elicit an acute effect at the individual level will also produce acute effects at the population and community levels. For acute concentrations, thus, the level of competition was not an influential factor in this work. However, it must be noted that the competitors tested in Chapter 5 had similar sensitivities to esfenvalerate. When species with highly different sensitivities are exposed to acute concentrations, this is likely to change (Liess et al., 2013).

Low concentrations Esfenvalerate concentrations between 0.01–0.04 µg/L had a significant antagonistic interaction with UV-B radiation when esfenvalerate was applied immediately before UV-B radiation. The same concentration range of esfenvalerate (0.01 and 0.032 µg/L) induced a stimulated population growth in the study described in Chapter 4. However, it was assumed that the observed population growth only emerged because of the associated reduction in individual competitiveness. This assumption was reinforced by the results reported in Chapter 5; in the context of strong *inter*specific competition, no biomass increase was observed. Instead an increase in the

correlation between population densities of the competitors emerged after exposure to low doses of esfenvalerate (Figures 5.6 and 5.7). This increase was associated with a reduction of competition between the coexisting species, leading to an increased similarity in the population development. The reduction in *inter*specific competition was most pronounced after exposure to 0.01 µg/L esfenvalerate, but it was also present at 0.0001 µg/L, that is 3 orders of magnitude below the acute EC_{50}. These findings indicate that esfenvalerate induces effects far below acute levels. While these effects were beneficial at the individual and population levels, they changed at the community level (in the presence of a competitor).

Given these results, Hypothesis 2 is maintained for low concentrations but cannot be maintained for high concentrations in the context of this work. However, the previously mentioned caveat (i.e. similar sensitivities of competitors) precludes the rejection of Hypothesis 2 for high concentrations in general. In the following, it is considered how the level of competition may modify the response to low doses of stressors.

6.2.1 Hormesis May Only Be Observed, when Environmental Conditions Do Not Penalize Trade-offs

Hormesis is a broad theory that refers to the beneficial effects of low doses of stressors on several fitness endpoints of organisms. It assumes that low levels of stress can activate adaptive mechanisms that increase the competitive fitness of individuals (Schulz, 1888; Townsend and Luckey, 1960; Stebbing, 1998; Calabrese, 2010; Costantini et al., 2010). An increasing number of studies published each year (Calabrese and Mattson, 2017; Sial et al., 2018; Costantini, 2019; Calabrese and Agathokleous, 2019; Wolz et al., 2021; Shang et al., 2021; Schirrmacher, 2021; Agathokleous et al., 2022), indicate the actuality of the concept. However, it has been argued that stimulatory effects of toxicants must be accompanied by trade-offs that are unlikely to result in evolutionary advantages (Calow and Sibly, 1990; Forbes, 2000). This

assumption can be associated with the environmental stress response (ESR), which predicts that a change in environmental conditions (e.g. pesticide exposure, temperature, etc.) triggers a program of transcriptional changes that redistributes the resources spent on various cellular processes (Gasch et al., 2000). In the ESR, one group of genes is induced and another group is repressed with strong temporal anti-correlation. Induced genes are enriched for protection and damage repair while the repressed group is enriched for genes regulating growth and biosynthesis (Hackley and Schmid, 2019).

In Chapter 4, it has been shown that the density and biomass of a *D. magna* population can increase after exposure to low doses of a pyrethroid pesticide. This finding can be interpreted as a hormesis induced stimulation (Costantini, 2019), because negative effects of the associated trade-off (loss in individual competitiveness) were not observed in this study. However, the effect disappeared in the presence of a competitor (Chapter 5). Instead, an increase in correlation between species was observed, suggesting that extremely low esfenvalerate changed the competitive balance between *D. magna* and *C. pipiens*, so that the species reacted in higher synchrony to environmental conditions. When environmental conditions are more influential than competition, such increases in correlations have been observed in field studies (Hansen et al., 2013; Robertson et al., 2015) and are predicted in mathematical models (Lee et al., 2020).

The findings of this work therefore indicate that hormesis theory can be reconciled with trade-offs expected by ESR theory, when the conditions for emergence of positive effects are considered to be context specific. This means, low concentrations of a stressor can positively affect fitness of an organism or a population (see Figure 4.1); but, this occurs only when the environmental conditions do not penalize the associated trade-off (see Figure 5.4). Theoretically, this process can occur both in the laboratory and in nature; however, due to highly controlled conditions in the laboratory, the probability for the absence of a regulating factor (e.g. competitor, predator) increases, making the

observation of hormesis more probable in the laboratory than in nature (see Figure 1.1 to compare different levels of complexity from laboratory to field). Therefore it is hypothesized that hormesis is a special case of the ESR, where trade-offs are not penalized by environmental factors. This hypothesis should be further developed and tested in future work to better assess the consequences of the controversial *hormesis* theory for environmental risk assessment.

6.3 Environmental Conditions that Regulate Food Availability are Important Factors in the Assessment of Pesticide Effects

The identification of common environmental conditions that modify the effect of pesticides was the final aim of this work. In Chapter 5, the limited availability of biomass for feeding led to low densities of *D. magna* and *C. pipiens* populations. After reaching carrying capacity, the same pattern was observed in the experiment described in Chapter 4, where biomass was supplied at a constant rate. It was discussed (Section 4.4) that suppression phases, commonly observed in *Daphnia* populations (e.g. McCauley and Murdoch, 1987) due to population overshoots, were partly responsible for the observed significant increase in population density and biomass after exposure to esfenvalerate at low concentrations. This implies that food density is an important factor for population development which always should be studied when investigating effects of insecticides in population or community contexts. In Chapter 5, the measured environmental parameters like suspended biomass, oxygen, nutrient concentrations and temperature were very similar across experimental replicates and could therefore not explain the high variation in population densities of *Daphnia* and *Culex* (Tables C.4 and C.5), or the residual variation in esfenvalerate-induced population disturbance (Figure C.3). Instead, it is assumed that periphyton on the sediment and biofilm on the glass contributed to the observed variation in population densities and pesticide effects.

This assumption is in line with the previously reported impact of habitat characteristics on community composition under toxic stress (Rico et al., 2016). Although the evidence presented in this work is insufficient to make conclusive judgments about the effects of environmental factors on pesticides, the large unexplained variation in the effects of pesticides on population densities observed in Chapter 5 suggests that hidden factors remain that are responsible for increased or decreased effects of pesticides, even in controlled environments. Therefore, future studies should quantify periphyton, biofilm, and other biologically relevant parameters to better understand the influence of habitat characteristics on pesticide effects in biological systems of higher order. Studies like these may finally bring mechanistic understanding under which circumstances the effects of pesticides escalate and under which circumstances they are dampened.

6.4 Future Perspectives: Non-Invasive Nanocosm Systems Are Effective Tools to Investigate Pesticide Effects in Complex Biological Systems

The effects of experimental handling are factors commonly ignored in laboratory experiments (Rousseaux et al., 2010; Sims et al., 1993). Under low stress exposure, experimental handling, especially invasive monitoring, could obscure relevant effects and lead to wrong conclusions about the harm of toxicants. Non-invasive nanocosm test systems do not have this deficiency and have been successfully applied in a series of investigations on acute concentrations (Pieters and Liess, 2006; Liess et al., 2006, 2013). In this work, nanocosm systems were used in the experiments described in Chapters 4 and 5 and were able to reveal effects of concentrations far below the acute EC_{50}. Although, the test systems used in this work can still be improved as outlined in Section 5.4, the findings of this work show that complex laboratory systems coupled with non-invasive monitoring can contribute to the understanding of effect mechanisms of low doses of pesticides (see Fig-

ure 1.1). In the future, more biological processes should be considered in increasingly automated nanocosms to improve the understanding of the mechanics of the stress response even further. Predation as a key ecological mechanism should be studied under controlled conditions (Riedl et al., 2018). Also, the effects of temperature should be studied in greater depth due to its universal influence on all processes of life (Heugens et al., 2001; van der Meer, 2006), its role as a stressor in a changing world climate (Masson-Delmotte et al., 2021), and modulator of toxicant effects (Heugens et al., 2006; Ribeiro et al., 2011). Other mechanisms that should be studied include adaptation to stressors and the roles of invasive species, infections and parasitism.

In light of these challenges, careful and stepwise development of controlled ecosystems and their disturbance under close, non-invasive monitoring can be of tremendous value in understanding the effect mechanisms of pesticides in systems of high biological organization. These efforts can ultimately help to reduce the risks of chemicals in the environment.

6.5 Conclusion

It was shown that the effects of esfenvalerate are highly context dependent. Time changed the interaction between esfenvalerate and environmental stress, and the stimulated population growth after exposure to low doses of esfenvalerate disappeared when a competitor was present. The latter discovery led to the formulation of the *context-dependent stimulatory response* hypothesis, which should be investigated in future work.

This work has also shown that complex laboratory experiments can reveal subtle effects of pesticides that do not become apparent from single-species, single-substance experiments. Therefore, risk assessment should consider to test new chemicals under higher levels of biological organization, for a safer use of pesticides, which will continue to be applied in the forseeable future. Finally, this work aimed to un-

derstand mechanisms of pesticide effects. This goal was achieved, but many open questions remain, and many avenues for future research emerged. Reproducible and non-invasive protocols for single-species and multi-species nanocosm test systems were a cornerstone of this work; and, to continue their improvement and to stepwise increase their complexity are the final recommendations of this work.

Bibliography

Agathokleous, E., I. Iavicoli, D. Barceló, and E. J. Calabrese
2021. Micro/nanoplastics effects on organisms: A review focusing on 'dose'. *Journal of hazardous materials*, 417:126084. 40

Agathokleous, E., Q. Wang, I. Iavicoli, and E. J. Calabrese
2022. The relevance of hormesis at higher levels of biological organization: Hormesis in microorganisms. *Current Opinion in Toxicology*, 29:1–9. 6, 40, 89

Alexander, A. C., J. M. Culp, D. J. Baird, and A. J. Cessna
2016. Nutrient-insecticide interactions decouple density-dependent predation pressure in aquatic insects. *Freshwater Biology*, 61(12):2090–2101. 4, 59

Allen, J., E. M. Gross, C. Courcoul, S. Bouletreau, A. Compin, A. Elger, J. Ferriol, S. Hilt, V. E. J. Jassey, M. Laviale, B. H. Polst, M. Schmitt-Jansen, H. Stibor, V. Vijayaraj, and J. Leflaive
2021. Disentangling the direct and indirect effects of agricultural runoff on freshwater ecosystems subject to global warming: A microcosm study. *Water Research*, 190:116713. 4, 59

Altenburger, R., T. Backhaus, W. Boedeker, M. Faust, and M. Scholze
2013. Simplifying complexity: Mixture toxicity assessment in the last 20 years. *Environmental toxicology and chemistry*, 32(8):1685–1687. 22

Altenburger, R., T. Backhaus, W. Boedeker, M. Faust, M. Scholze, and L. H. Grimme
2000. Predictability of the toxicity of multiple chemical mixtures to vibrio fischeri: Mixtures composed of similarly acting chemicals. *Environmental Toxicology and Chemistry*, 19(9):2341–2347. 5

Altenburger, R., W. Brack, R. M. Burgess, W. Busch, B. I. Escher, A. Focks, L. Mark Hewitt, B. N. Jacobsen, M. L. de Alda, S. Ait-Aissa, T. Backhaus, A. Ginebreda, K. Hilscherová, J. Hollender, H. Hollert, P. A. Neale, T. Schulze,

E. L. Schymanski, I. Teodorovic, A. J. Tindall, G. de Aragão Umbuzeiro, B. Vrana, B. Zonja, and M. Krauss
2019. Future water quality monitoring: improving the balance between exposure and toxicity assessments of real-world pollutant mixtures. *Environmental Sciences Europe*, 31(1). 22

Andersen, T. H., R. Tjørnhøj, L. Wollenberger, T. Slothuus, and A. Baun
2006. Acute and chronic effects of pulse exposure of daphnia magna to dimethoate and pirimicarb. *Environmental Toxicology and Chemistry*, 25(5):1187–1195. 14

Arce-Funck, J., C. Crenier, M. Danger, C. Cossu-Leguille, F. Guérold, and V. Felten
2016. Stoichiometric constraints modulate impacts of silver contamination on stream detritivores: an experimental test with gammarus fossarum. *Freshwater Biology*, 61(12):2075–2089. 59

Ashauer, R., A. B. A. Boxall, and C. D. Brown
2007. Modeling combined effects of pulsed exposure to carbaryl and chlorpyrifos on gammarus pulex. *Environmental science & technology*, 41(15):5535–5541. 7, 22, 87

Ashauer, R., I. O'Connor, and B. I. Escher
2017. Toxic mixtures in time-the sequence makes the poison. *Environmental science & technology*, 51(5):3084–3092. 7, 22, 34, 87

Backhaus, T. and M. Faust
2012. Predictive environmental risk assessment of chemical mixtures: a conceptual framework. *Environmental science & technology*, 46(5):2564–2573. 22

Bart, S., T. Jager, A. Robinson, E. Lahive, D. J. Spurgeon, and R. Ashauer
2021. Predicting mixture effects over time with toxicokinetic-toxicodynamic models (guts): Assumptions, experimental testing, and predictive power. *Environmental science & technology*, 55(4):2430–2439. 87

Bart, S., S. Short, T. Jager, E. J. Eagles, A. Robinson, C. Badder, E. Lahive, D. J. Spurgeon, and R. Ashauer
2022. How to analyse and account for interactions in mixture toxicity with toxicokinetic-toxicodynamic models. *The Science of the total environment*, 843:157048. 87

Beketov, M. and M. Liess
2007. Acute and delayed effects of the neonicotinoid insecticide thiacloprid

on seven freshwater arthropods. *Environmental Toxicology and Chemistry*, preprint(2007):1. 2

Beketov, M. A., B. J. Kefford, R. B. Schäfer, and M. Liess
2013. Pesticides reduce regional biodiversity of stream invertebrates. *Proceedings of the National Academy of Sciences of the United States of America*, 110(27):11039–11043. 2

Beketov, M. A. and M. Liess
2005. Acute contamination with esfenvalerate and food limitation: chronic effects on the mayfly, cloeon dipterum. *Environmental Toxicology and Chemistry*, 24(5):1281–1286. 9, 12, 55, 57

Beketov, M. A. and M. Liess
2006. The influence of predation on the chronic response of artemia sp. populations to a toxicant. *The Journal of applied ecology*, 43(6):1069–1074. 22

Beketov, M. A., A. Speranza, and M. Liess
2011. Ultraviolet radiation increases sensitivity to pesticides: synergistic effects on population growth rate of daphnia magna at low concentrations. *Bulletin of environmental contamination and toxicology*, 87(3):231–237. 15

Beklioğlu, M., T. Bucak, J. Coppens, G. Bezirci, Ü. Tavşanoğlu, A. Çakıroğlu, E. Levi, Ş. Erdoğan, N. Filiz, K. Özkan, and A. Özen
2017. Restoration of eutrophic lakes with fluctuating water levels: A 20-year monitoring study of two inter-connected lakes. *Water*, 9(2):127. 69

Bennett, E. R., M. T. Moore, C. M. Cooper, S. Smith, F. D. Shields, K. G. Drouillard, and R. Schulz
2005. Vegetated agricultural drainage ditches for the mitigation of pyrethroid-associated runoff. *Environmental Toxicology and Chemistry*, 24(9):2121–2127. 13

Betini, G. S., T. Avgar, K. S. McCann, and J. M. Fryxell
2019. Temperature triggers a non–linear response in resource–consumer interaction strength. *Ecosphere*, 10(8). 15

Bible, J. M., B. S. Cheng, A. L. Chang, M. C. Ferner, K. Wasson, C. J. Zabin, M. Latta, E. Sanford, A. Deck, and E. D. Grosholz
2017. Timing of stressors alters interactive effects on a coastal foundation species. *Ecology*, 98(9):2468–2478. 22, 34

Birk, S., D. Chapman, L. Carvalho, B. M. Spears, H. E. Andersen, C. Argillier, S. Auer, A. Baattrup-Pedersen, L. Banin, M. Beklioğlu, E. Bondar-Kunze,

A. Borja, P. Branco, T. Bucak, A. D. Buijse, A. C. Cardoso, R.-M. Couture, F. Cremona, D. de Zwart, C. K. Feld, M. T. Ferreira, H. Feuchtmayr, M. O. Gessner, A. Gieswein, L. Globevnik, D. Graeber, W. Graf, C. Gutiérrez-Cánovas, J. Hanganu, U. Işkın, M. Järvinen, E. Jeppesen, N. Kotamäki, M. Kuijper, J. U. Lemm, S. Lu, A. L. Solheim, U. Mischke, S. J. Moe, P. Nõges, T. Nõges, S. J. Ormerod, Y. Panagopoulos, G. Phillips, L. Posthuma, S. Pouso, C. Prudhomme, K. Rankinen, J. J. Rasmussen, J. Richardson, A. Sagouis, J. M. Santos, R. B. Schäfer, R. Schinegger, S. Schmutz, S. C. Schneider, L. Schülting, P. Segurado, K. Stefanidis, B. Sures, S. J. Thackeray, J. Turunen, M. C. Uyarra, M. Venohr, P. C. von der Ohe, N. Willby, and D. Hering
2020. Impacts of multiple stressors on freshwater biota across spatial scales and ecosystems. *Nature ecology & evolution*. 3, 5, 87

Bjergager, M.-B. A., K. Dalhoff, A. Kretschmann, K. B. Nørgaard, P. Mayer, and N. Cedergreen
2017. Determining lower threshold concentrations for synergistic effects. *Aquatic toxicology (Amsterdam, Netherlands)*, 182:79–90. 23, 36

Bjergager, M.-B. A., M. L. Hanson, K. R. Solomon, and N. Cedergreen
2012. Synergy between prochloraz and esfenvalerate in daphnia magna from acute and subchronic exposures in the laboratory and microcosms. *Aquatic toxicology (Amsterdam, Netherlands)*, 110-111:17–24. 13, 14, 55

Bliss, C. I.
1939. The toxicity of poisons applied jointly. *Annals of Applied Biology*, 26(3):585–615. 5, 27

Brooks, P. R. and T. P. Crowe
2019. Combined effects of multiple stressors: New insights into the influence of timing and sequence. *Frontiers in Ecology and Evolution*, 7. 22, 34, 86

Calabrese, E. J.
2010. Hormesis is central to toxicology, pharmacology and risk assessment. *Human & experimental toxicology*, 29(4):249–261. 5, 23, 54, 89

Calabrese, E. J. and E. Agathokleous
2019. Building biological shields via hormesis. *Trends in pharmacological sciences*, 40(1):8–10. 89

Calabrese, E. J. and L. A. Baldwin
2003. Toxicology rethinks its central belief. *Nature*, 421(6924):691–692. 6, 23, 36, 40

Calabrese, E. J. and M. P. Mattson
2017. How does hormesis impact biology, toxicology, and medicine? *NPJ aging and mechanisms of disease*, 3:8. 5, 89

Calow, P.
1989. Proximate and ultimate responses to stress in biological systems. *Biological Journal of the Linnean Society*, 37(1-2):173–181. 5

Calow, P. and R. M. Sibly
1990. A physiological basis of population processes: Ecotoxicological implications. *Functional Ecology*, 4(3):283. 40, 55, 89

Cardinale, B. J., J. E. Duffy, A. Gonzalez, D. U. Hooper, C. Perrings, P. Venail, A. Narwani, G. M. Mace, D. Tilman, D. A. Wardle, A. P. Kinzig, G. C. Daily, M. Loreau, J. B. Grace, A. Larigauderie, D. S. Srivastava, and S. Naeem
2012. Biodiversity loss and its impact on humanity. *Nature*, 486(7401):59–67. 1

Carvalho, M. E. A., P. R. C. Castro, and R. A. Azevedo
2020. Hormesis in plants under cd exposure: From toxic to beneficial element? *Journal of hazardous materials*, 384:121434. 54

Cedergreen, N.
2014. Quantifying synergy: a systematic review of mixture toxicity studies within environmental toxicology. *PloS one*, 9(5):e96580. 23

Cedergreen, N., K. Dalhoff, D. Li, M. Gottardi, and A. C. Kretschmann
2017. Can toxicokinetic and toxicodynamic modeling be used to understand and predict synergistic interactions between chemicals? *Environmental science & technology*, 51(24):14379–14389. 87

Chapin, F. S. and S. Díaz
2020. Interactions between changing climate and biodiversity: Shaping humanity's future. *Proceedings of the National Academy of Sciences of the United States of America*, 117(12):6295–6296. 21

Cheng, B. S., J. M. Bible, A. L. Chang, M. C. Ferner, K. Wasson, C. J. Zabin, M. Latta, A. Deck, A. E. Todgham, and E. D. Grosholz
2015. Testing local and global stressor impacts on a coastal foundation species using an ecologically realistic framework. *Global change biology*, 21(7):2488–2499. 5

Chesson, P.
2000. Mechanisms of maintenance of species diversity. *Annual Review of Ecology and Systematics*, 31(1):343–366. 82

Chevalier, J., E. Harscoët, M. Keller, P. Pandard, J. Cachot, and M. Grote
2015. Exploration of daphnia behavioral effect profiles induced by a broad range of toxicants with different modes of action. *Environmental toxicology and chemistry*, 34(8):1760–1769. 13, 14

Chow, R., R. Scheidegger, T. Doppler, A. Dietzel, F. Fenicia, and C. Stamm
2020. A review of long-term pesticide monitoring studies to assess surface water quality trends. *Water research X*, 9:100064. 3

Christensen, B. T., T. L. Lauridsen, H. W. Ravn, and M. Bayley
2005. A comparison of feeding efficiency and swimming ability of daphnia magna exposed to cypermethrin. *Aquatic toxicology (Amsterdam, Netherlands)*, 73(2):210–220. 12

Christopher Cutler, G., K. Ramanaidu, T. Astatkie, and M. B. Isman
2009. Green peach aphid, myzus persicae (hemiptera: Aphididae), reproduction during exposure to sublethal concentrations of imidacloprid and azadirachtin. *Pest management science*, 65(2):205–209. 23, 54

Costantini, D.
2019. Hormesis promotes evolutionary change. *Dose-response : a publication of International Hormesis Society*, 17(2):1559325819843376. 6, 55, 89, 90

Costantini, D., N. B. Metcalfe, and P. Monaghan
2010. Ecological processes in a hormetic framework. *Ecology letters*, 13(11):1435–1447. 36, 89

Costantino, Desharnais, Cushing, and Dennis
1997. Chaotic dynamics in an insect population. *Science (New York, N.Y.)*, 275(5298):389–391. 81

Cressey, D.
2017. The bitter battle over the world's most popular insecticides. *Nature*, 551(7679):156–158. 3, 11, 40, 85

Crossley, M. S., A. R. Meier, E. M. Baldwin, L. L. Berry, L. C. Crenshaw, G. L. Hartman, D. Lagos-Kutz, D. H. Nichols, K. Patel, S. Varriano, W. E. Snyder, and M. D. Moran
2020. No net insect abundance and diversity declines across us long term ecological research sites. *Nature ecology & evolution*, 4(10):1368–1376. 85

Cutler, G. C.
2013. Insects, insecticides and hormesis: evidence and considerations for study.

Dose-response : a publication of International Hormesis Society, 11(2):154–177. 23, 54

da Silva, M. L. N., D. J. Nogueira, J. S. Köerich, V. P. Vaz, N. M. Justino, J. R. A. Schmidt, D. S. Vicentini, M. S. Matias, A. B. de Castilhos Junior, C. F. Fuzinatto, and W. G. Matias
2020. Multigenerational toxic effects on daphnia magna induced by silver nanoparticles and glyphosate mixture. *Environmental toxicology and chemistry*. 14

de Roos, A. M., O. Diekmann, and J. A. J. Metz
1992. Studying the dynamics of structured population models: A versatile technique and its application to daphnia. *The American naturalist*, 139(1):123–147. 8

Dinh, K. V., L. Janssens, and R. Stoks
2016. Exposure to a heat wave under food limitation makes an agricultural insecticide lethal: a mechanistic laboratory experiment. *Global change biology*, 22(10):3361–3372. 5

Dornelas, M., N. J. Gotelli, H. Shimadzu, F. Moyes, A. E. Magurran, and B. J. McGill
2019. A balance of winners and losers in the anthropocene. *Ecology letters*, 22(5):847–854. 85

Dumont, H. J., I. van de Velde, and S. Dumont
1975. The dry weight estimate of biomass in a selection of cladocera, copepoda and rotifera from the plankton, periphyton and benthos of continental waters. *Oecologia*, 19(1):75–97. 45

Duncan, R. P. and B. J. Kefford
2021. Interactions in statistical models: Three things to know. *Methods in Ecology and Evolution*, 12(12):2287–2297. 32

Ebert, D.
2022. Daphnia as a versatile model system in ecology and evolution. *EvoDevo*, 13(1):16. 13, 14, 61, 62, 80

EEA
2018. *European waters - assessment of status and pressures*, EEA Report. Luxembourg: European Environment Agency. 3

European Food Safety Authority
2013. Guidance on tiered risk assessment for plant protection products for

aquatic organisms in edge–of–field surface waters: Efsa panel on plant protection products and their residues (ppr). *EFSA Journal*, 11(7). 14, 59

European Parliament
21.10.2009. Establishing a framework for community action to achieve the sustainable use of pesticides: Directive 2009/128/ec. 3

European Parliament
23.10.2000. Establishing a framework for community action in the field of water policy: Directive 2000/60/ec. 3

European Union
9.8.1988. Council resolution on the protection of the north sea and of other waters in the community: Resolution 88/c 209/02. 3

Faerøvig, P. J., T. Andersen, and D. O. Hessen
2002. Image analysis of daphnia populations: non-destructive determination of demography and biomass in cultures. *Freshwater Biology*, 47(10):1956–1962. 53

Fairchild, J. F., T. W. La Point, J. L. Zajicek, M. K. Nelson, F. J. Dwyer, and P. A. Lovely
1992. Population-, community- and ecosystem-level responses of aquatic mesocosms to pulsed doses of a pyrethroid insecticide. *Environmental Toxicology and Chemistry*, 11(1):115–129. 13

Fleeger, J. W., K. R. Carman, and R. M. Nisbet
2003. Indirect effects of contaminants in aquatic ecosystems. *Science of The Total Environment*, 317(1-3):207–233. 4, 6, 59

Foit, K., O. Kaske, D.-S. Wahrendorf, S. Duquesne, and M. Liess
2012. Automated nanocosm test system to assess the effects of stressors on two interacting populations. *Aquatic toxicology (Amsterdam, Netherlands)*, 109:243–249. 15, 41, 44, 45, 62, 67

Forbes, V. E.
2000. Is hormesis an evolutionary expectation? *Functional Ecology*, 14(1):12–24. 40, 55, 89

Fukami, T.
2001. Sequence effects of disturbance on community structure. *Oikos*, 92(2):215–224. 22

Gasch, A. P., P. T. Spellman, C. M. Kao, O. Carmel-Harel, M. B. Eisen, G. Storz, D. Botstein, and P. O. Brown
2000. Genomic expression programs in the response of yeast cells to environmental changes. *Molecular biology of the cell*, 11(12):4241–4257. 55, 90

Gause, G. F.
1936. The struggle for existence. *Soil Science*, 41(2):159. 8, 60

Gelman, A., A. Jakulin, M. G. Pittau, and Y.-S. Su
2008. A weakly informative default prior distribution for logistic and other regression models. *The Annals of Applied Statistics*, 2(4). 28, 72

Gessner, M. O. and A. Tlili
2016. Fostering integration of freshwater ecology with ecotoxicology. *Freshwater Biology*, 61(12):1991–2001. 4, 59

Ghosh, I., F. Marques, and S. Chakraborty
2021. A new bivariate poisson distribution via conditional specification: properties and applications. *Journal of applied statistics*, 48(16):3025–3047. 72

Gieswein, A., D. Hering, and C. K. Feld
2017. Additive effects prevail: The response of biota to multiple stressors in an intensively monitored watershed. *The Science of the total environment*, 593-594:27–35. 3

Gonzalez, A., B. J. Cardinale, G. R. H. Allington, J. Byrnes, K. Arthur Endsley, D. G. Brown, D. U. Hooper, F. Isbell, M. I. O'Connor, and M. Loreau
2016. Estimating local biodiversity change: a critique of papers claiming no net loss of local diversity. *Ecology*, 97(8):1949–1960. 85

Gordóvil-Merino, A., J. Guàrdia-Olmos, and M. Peró-Ceboller
2012. Estimation of logistic regression models in small samples. a simulation study using a weakly informative default prior distribution. *Psicológica*, 33(2):345–361. 28

Gottardi, M., M. R. Birch, K. Dalhoff, and N. Cedergreen
2017. The effects of epoxiconazole and a-cypermethrin on daphnia magna growth, reproduction, and offspring size. *Environmental Toxicology and Chemistry*, 36(8):2155–2166. 12

Goulson, D.
2013. Review: An overview of the environmental risks posed by neonicotinoid insecticides. *Journal of Applied Ecology*, 50(4):977–987. 2

Graeve, A., I. Ioannidou, J. Reinhard, D. M. Görl, A. Faissner, and L. C. Weiss
2021. Brain volume increase and neuronal plasticity underly predator-induced morphological defense expression in daphnia longicephala. *Scientific reports*, 11(1):12612. 14

Grover, J. P., D. McKee, S. Young, H. C. J. Godfray, and P. Turchin
2000. Periodic dynamics in daphnia populations: Biological interactions and external forcing. *Ecology*, 81(10):2781–2798. 54

Gunderson, A. R., E. J. Armstrong, and J. H. Stillman
2016. Multiple stressors in a changing world: The need for an improved perspective on physiological responses to the dynamic marine environment. *Annual review of marine science*, 8:357–378. 7, 22

Hackley, R. K. and A. K. Schmid
2019. Global transcriptional programs in archaea share features with the eukaryotic environmental stress response. *Journal of molecular biology*, 431(20):4147–4166. 55, 90

Halbach, K., M. Möder, S. Schrader, L. Liebmann, R. B. Schäfer, A. Schneeweiss, V. C. Schreiner, P. Vormeier, O. Weisner, M. Liess, and T. Reemtsma
2021. Small streams-large concentrations? pesticide monitoring in small agricultural streams in germany during dry weather and rainfall. *Water Research*, 203:117535. 3, 7, 21

Halbach, U.
1970. Einfluß der temperatur auf die populationsdynamik des planktischen rädertieres brachionus calyciflorus pallas. *Oecologia*, 4(2):176–207. 54, 62

Hallmann, C. A., M. Sorg, E. Jongejans, H. Siepel, N. Hofland, H. Schwan, W. Stenmans, A. Müller, H. Sumser, T. Hörren, D. Goulson, and H. de Kroon
2017. More than 75 percent decline over 27 years in total flying insect biomass in protected areas. *PloS one*, 12(10):e0185809. 1

Hanazato, T. and H. Hirokawa
2004. Changes in vulnerability of daphnia to an insecticide application depending on the population phase. *Freshwater Biology*, 49(4):402–409. 8

Hansen, B. B., V. Grøtan, R. Aanes, B.-E. Sæther, A. Stien, E. Fuglei, R. A. Ims, N. G. Yoccoz, and A. Ø. Pedersen
2013. Climate events synchronize the dynamics of a resident vertebrate community in the high arctic. *Science (New York, N.Y.)*, 339(6117):313–315. 79, 90

Hansson, L.-A. and S. Hylander
2009. Effects of ultraviolet radiation on pigmentation, photoenzymatic repair, behavior, and community ecology of zooplankton. *Photochemical & photobiological sciences : Official journal of the European Photochemistry Association and the European Society for Photobiology*, 8(9):1266–1275. 15, 87

Hansul, S., A. Fettweis, E. Smolders, and K. de Schamphelaere
2021. Interactive metal mixture toxicity to daphnia magna populations as an emergent property in a dynamic energy budget individual-based model. *Environmental toxicology and chemistry*, 40(11):3034–3048. 14

Hardin, G.
1960. The competitive exclusion principle. *Science (New York, N.Y.)*, 131(3409):1292–1297. 8, 60

Hasenbein, S., H. Poynton, and R. E. Connon
2018. Contaminant exposure effects in a changing climate: how multiple stressors can multiply exposure effects in the amphipod hyalella azteca. *Ecotoxicology (London, England)*, 27(7):845–859. 12

Hawlena, H., M. Garrido, C. Cohen, S. Halle, and S. Cohen
2022. Bringing the mechanistic approach back to life: A systematic review of the experimental evidence for coexistence and four of its classical mechanisms. *Frontiers in Ecology and Evolution*, 10. 60

He, F., R. Arora, and I. Mansour
2023. Multispecies assemblages and multiple stressors: Synthesizing the state of experimental research in freshwaters. *WIREs Water*, Pp. 1–19. 60

Heugens, E. H. W., J. A. Hendriks, T. Dekker, N. M. van Straalen, and W. Admiraal
2001. A review of the effects of multiple stressors on aquatic organisms and analysis of uncertainty factors for use in risk assessment. *Critical Reviews in Toxicology*, 31(3):247–284. 5, 9, 93

Heugens, E. H. W., L. T. B. Tokkie, M. H. S. Kraak, J. A. Hendriks, N. M. van Straalen, and W. Admiraal
2006. Population growth of daphnia magna under multiple stress conditions: joint effects of temperature, food, and cadmium. *Environmental Toxicology and Chemistry*, 25(5):1399–1407. 93

Heys, K. A., R. F. Shore, M. G. Pereira, K. C. Jones, and F. L. Martin
2016. Risk assessment of environmental mixture effects. *RSC Advances*, 6(53):47844–47857. 22

Holmstrup, M., A.-M. Bindesbøl, G. J. Oostingh, A. Duschl, V. Scheil, H.-R. Köhler, S. Loureiro, A. M. V. M. Soares, A. L. G. Ferreira, C. Kienle, A. Gerhardt, R. Laskowski, P. E. Kramarz, M. Bayley, C. Svendsen, and D. J. Spurgeon
2010. Interactions between effects of environmental chemicals and natural stressors: a review. *The Science of the total environment*, 408(18):3746–3762. 5

Hooper, D. U., E. C. Adair, B. J. Cardinale, J. E. K. Byrnes, B. A. Hungate, K. L. Matulich, A. Gonzalez, J. E. Duffy, L. Gamfeldt, and M. I. O'Connor
2012. A global synthesis reveals biodiversity loss as a major driver of ecosystem change. *Nature*, 486(7401):105–108. 1

Hoyer, S. and J. Hamman
2017. xarray: N-d labeled arrays and datasets in python. *Journal of Open Research Software*, 5(1):10. 47

Huang, Y., R. Cartlidge, M. Walpitagama, J. Kaslin, O. Campana, and D. Wlodkowic
2018. Unsuitable use of dmso for assessing behavioral endpoints in aquatic model species. *The Science of the total environment*, 615:107–114. 26, 43

Jackson, M. C., C. J. G. Loewen, R. D. Vinebrooke, and C. T. Chimimba
2016. Net effects of multiple stressors in freshwater ecosystems: a meta-analysis. *Global change biology*, 22(1):180–189. 5, 87

Jactel, H., F. Verheggen, D. Thiéry, A. J. Escobar-Gutiérrez, E. Gachet, and N. Desneux
2019. Alternatives to neonicotinoids. *Environment international*, 129:423–429. 3, 12, 40, 57

Jager, T., C. Albert, T. G. Preuss, and R. Ashauer
2011. General unified threshold model of survival–a toxicokinetic-toxicodynamic framework for ecotoxicology. *Environmental science & technology*, 45(7):2529–2540. 35

Janssens, L., N. Tüzün, and R. Stoks
2017. Testing the time-scale dependence of delayed interactions: A heat wave during the egg stage shapes how a pesticide interacts with a successive heat wave in the larval stage. *Environmental pollution (Barking, Essex : 1987)*, 230:351–359. 86

Johnson, R. M., L. Dahlgren, B. D. Siegfried, and M. D. Ellis
2013. Acaricide, fungicide and drug interactions in honey bees (apis mellifera). *PloS one*, 8(1):e54092. 23

Kath, J., J. R. Thomson, R. M. Thompson, B. J. Kefford, F. J. Dyer, and R. Mac Nally
2018. Interactions among stressors may be weak: Implications for management of freshwater macroinvertebrate communities. *Diversity and Distributions*, 24(7):939–950. 5

Kattwinkel, M., J. Römbke, and M. Liess
2012. Ecological recovery of populations of vulnerable species driving the risk assessment of pesticides. *EFSA Supporting Publications*, 9(9). 22

Klüttgen, B., U. Dülmer, M. Engels, and H. T. Ratte
1994. Adam, an artificial freshwater for the culture of zooplankton. *Water Research*, 28(3):743–746. 25, 41, 62

Knillmann, S., N. C. Stampfli, M. A. Beketov, and M. Liess
2012a. Intraspecific competition increases toxicant effects in outdoor pond microcosms. *Ecotoxicology (London, England)*, 21(7):1857–1866. 4, 59, 60

Knillmann, S., N. C. Stampfli, Y. A. Noskov, M. A. Beketov, and M. Liess
2012b. Interspecific competition delays recovery of daphnia spp. populations from pesticide stress. *Ecotoxicology (London, England)*, 21(4):1039–1049. 4, 59, 60

Kreyling, J., A. H. Schweiger, M. Bahn, P. Ineson, M. Migliavacca, T. Morel-Journel, J. R. Christiansen, N. Schtickzelle, and K. S. Larsen
2018. To replicate, or not to replicate - that is the question: how to tackle nonlinear responses in ecological experiments. *Ecology letters*, 21(11):1629–1638. 22

Kroeker, K. J., F. Micheli, and M. C. Gambi
2013. Ocean acidification causes ecosystem shifts via altered competitive interactions. *Nature Climate Change*, 3(2):156–159. 82

Kruschke, J. K.
2013. Bayesian estimation supersedes the t test. *Journal of experimental psychology. General*, 142(2):573–603. 46

Laetz, C. A., D. H. Baldwin, T. K. Collier, V. Hebert, J. D. Stark, and N. L. Scholz
2009. The synergistic toxicity of pesticide mixtures: implications for risk assessment and the conservation of endangered pacific salmon. *Environmental health perspectives*, 117(3):348–353. 5, 23

Leavitt, P. R.
2020. Don't stressor the small stuff. *Nature ecology & evolution*. 22

Lee, A. M., B.-E. Saether, and S. Engen
2020. Spatial covariation of competing species in a fluctuating environment. *Ecology*, 101(1):e02901. 79, 82, 90

Lemm, J. U. and C. K. Feld
2017. Identification and interaction of multiple stressors in central european lowland rivers. *The Science of the total environment*, 603-604:148–154. 5

Lesser, E., F. N. Sheikh, M. Sikder, M.-N. Croteau, N. Franklin, M. Baalousha, and N. S. Ismail
2022. Water chemistry, exposure routes, and metal forms determine the bioaccumulation dynamics of silver (ionic and nanoparticulate) in daphnia magna. *Environmental toxicology and chemistry*, 41(3):726–738. 15

Lhotka, O., J. Kyselý, and A. Farda
2018. Climate change scenarios of heat waves in central europe and their uncertainties. *Theoretical and Applied Climatology*, 131(3-4):1043–1054. 7, 22

Liess, M.
2002. Population response to toxicants is altered by intraspecific interaction. *Environmental Toxicology and Chemistry*, 21(1):138–142. 12, 57

Liess, M. and K. Foit
2010. Intraspecific competition delays recovery of population structure. *Aquatic toxicology (Amsterdam, Netherlands)*, 97(1):15–22. 60

Liess, M., K. Foit, A. Becker, E. Hassold, I. Dolciotti, M. Kattwinkel, and S. Duquesne
2013. Culmination of low-dose pesticide effects. *Environmental science & technology*, 47(15):8862–8868. 9, 22, 59, 60, 88, 92

Liess, M., K. Foit, S. Knillmann, R. B. Schäfer, and H.-D. Liess
2016. Predicting the synergy of multiple stress effects. *Scientific reports*, 6:32965. 5, 21, 28

Liess, M., S. Henz, and S. Knillmann
2019a. Predicting low-concentration effects of pesticides. *Scientific reports*, 9(1):15248. 6, 23, 40, 55, 56

Liess, M., S. Henz, and N. Shahid
2020. Modeling the synergistic effects of toxicant mixtures. *Environmental Sciences Europe*, 32(1). 56

Liess, M., L. Liebmann, P. Vormeier, O. Weisner, R. Altenburger, D. Borchardt, W. Brack, A. Chatzinotas, B. Escher, K. Foit, R. Gunold, S. Henz, K. L. Hitzfeld, M. Schmitt-Jansen, N. Kamjunke, O. Kaske, S. Knillmann, M. Krauss, E. Küster, M. Link, M. Lück, M. Möder, A. Müller, A. Paschke, R. B. Schäfer, A. Schneeweiss, V. C. Schreiner, T. Schulze, G. Schüürmann, W. von Tümpling, M. Weitere, J. Wogram, and T. Reemtsma
2021. Pesticides are the dominant stressors for vulnerable insects in lowland streams. *Water Research*, 201:117262. 3, 21, 39, 57, 60, 85

Liess, M., B. J. Pieters, and S. Duquesne
2006. Long-term signal of population disturbance after pulse exposure to an insecticide: rapid recovery of abundance, persistent alteration of structure. *Environmental Toxicology and Chemistry*, 25(5):1326–1331. 41, 42, 44, 60, 62, 92

Liess, M., T. Ratte, P. Ebke, and H. Hollert
2019b. 20 years setac glb: increasing realism of pesticide risk assessment. *Environmental Sciences Europe*, 31(1). 6, 85

Liess, M. and R. Schulz
1999. Linking insecticide contamination and population response in an agricultural stream. *Environmental Toxicology and Chemistry*, 18(9):1948–1955. 7, 21, 22

Liess, M., R. Schulz, M.-D. Liess, B. Rother, and R. Kreuzig
1999. Determination of insecticide contamination in agricultural headwater streams. *Water Research*, 33(1):239–247. 21

Loewe, S.
1953. The problem of synergism and antagonism of combined drugs. *Arzneimittelforschung*, 3(6):285–290. 29, 33

Loureiro, S., C. Svendsen, A. L. G. Ferreira, C. Pinheiro, F. Ribeiro, and A. M. V. M. Soares
2010. Toxicity of three binary mixtures to daphnia magna: comparing chemical modes of action and deviations from conceptual models. *Environmental toxicology and chemistry*, 29(8):1716–1726. 36

Lu, Z., J. Gan, X. Cui, L. Delgado-Moreno, and K. Lin
2019. Understanding the bioavailability of pyrethroids in the aquatic environment using chemical approaches. *Environment international*, 129:194–207. 40, 57

Ma, Y., L. Chen, X. Lu, H. Chu, C. Xu, and W. Liu
2009. Enantioselectivity in aquatic toxicity of synthetic pyrethroid insecticide fenvalerate. *Ecotoxicology and environmental safety*, 72(7):1913–1918. 13

MacArthur, R. H.
1958. Population ecology of some warblers of northeastern coniferous forests. *Ecology*, 39(4):599–619. 8, 60

Maggio, S. A. and J. J. Jenkins
2021. Multi- and trans-generational effects on daphnia magna of chlorpyrifos exposures. *Environmental toxicology and chemistry*. 14

Makowski, D., M. S. Ben-Shachar, S. H. A. Chen, and D. Lüdecke
2019. Indices of effect existence and significance in the bayesian framework. *Frontiers in psychology*, 10:2767. 27

Malaj, E., P. C. von der Ohe, M. Grote, R. Kühne, C. P. Mondy, P. Usseglio-Polatera, W. Brack, and R. B. Schäfer
2014. Organic chemicals jeopardize the health of freshwater ecosystems on the continental scale. *Proceedings of the National Academy of Sciences of the United States of America*, 111(26):9549–9554. 2, 85

Malthus, T. R.
1798. *An essay on the principle of population, as it affects the future improvement of society. With remarks on the speculations of Mr. Godwin, M. Condorcet and other writers*. London: [publisher unknown]. 8

Mano, H. and Y. Tanaka
2016. Mechanisms of compensatory dynamics in zooplankton and maintenance of food chain efficiency under toxicant stress. *Ecotoxicology (London, England)*, 25(2):399–411. 60

Margus, A., S. Piiroinen, P. Lehmann, S. Tikka, J. Karvanen, and L. Lindström
2019. Sublethal pyrethroid insecticide exposure carries positive fitness effects over generations in a pest insect. *Scientific reports*, 9(1):11320. 12, 40, 55

Martínez-Jerónimo, F., M. Arzate-Cárdenas, and R. Ortiz-Butrón
2013. Linking sub-individual and population level toxicity effects in daphnia schoedleri (cladocera: Anomopoda) exposed to sublethal concentrations of the pesticide a-cypermethrin. *Ecotoxicology (London, England)*, 22(6):985–995. 12, 14

Masson-Delmotte, V., P. Zhai, A. Pirani, S. L. Connors, C. Péan, Y. Chen, L. Goldfarb, M. I. Gomis, R. B. Matthews, S. Berger, M. Huang, O. Yelekçi,

R. Yu, B. Zhou, E. Lonnoy, T. K. Maycock, T. Waterfield, K. Leitzell, and N. Caud, eds.
2021. *Summary for Policymakers: In: Climate Change 2021: The Physical Science Basis. Contribution of Working Group I to the Sixth Assessment Report of the Intergovernmental Panel on Climate Change*. Cambridge University Press: Intergovernmental Panel on Climate Change. 7, 22, 93

May, R. M.
1974. Biological populations with nonoverlapping generations: stable points, stable cycles, and chaos. *Science (New York, N.Y.)*, 186(4164):645–647. 54

May, R. M.
1988. How many species are there on earth? *Science (New York, N.Y.)*, 241(4872):1441–1449. 1

McCarthy, M. A.
2011. Breathing some air into the single-species vacuum: multi-species responses to environmental change. *Journal of Animal Ecology*, 80(1):1–3. 71

McCauley, E. and W. W. Murdoch
1987. Cyclic and stable populations: Plankton as paradigm. *The American naturalist*, 129(1):97–121. 53, 54, 91

McElreath, R.
2015. *Statistical Rethinking: A Bayesian Course with Examples in R and Stan*. 20, 72

Meng, S., V. Delnat, and R. Stoks
2020. The exposure order strongly modifies how a heat spike increases pesticide toxicity. *Environmental science & technology*, 54(18):11476–11484. 22

Merritt, R. W., R. H. Dadd, and E. D. Walker
1992. Feeding behavior, natural food, and nutritional relationships of larval mosquitoes. *Annual review of entomology*, 37:349–376. 62, 80

Moran, P. A.
1953. The statistical analysis of the canadian lynx cycle. *Australian Journal of Zoology*, 1(3):291. 71, 79

Morrissey, C. A., P. Mineau, J. H. Devries, F. Sanchez-Bayo, M. Liess, M. C. Cavallaro, and K. Liber
2015. Neonicotinoid contamination of global surface waters and associated risk to aquatic invertebrates: a review. *Environment international*, 74:291–303. 2

Murdoch, W. W. and E. McCauley
1985. Three distinct types of dynamic behaviour shown by a single planktonic system. *Nature*, 316(6029):628–630. 54

Navis, S., A. Waterkeyn, T. Voet, L. de Meester, and L. Brendonck
2013. Pesticide exposure impacts not only hatching of dormant eggs, but also hatchling survival and performance in the water flea daphnia magna. *Ecotoxicology (London, England)*, 22(5):803–814. 14

Neale, R. E., P. W. Barnes, T. M. Robson, P. J. Neale, C. E. Williamson, R. G. Zepp, S. R. Wilson, S. Madronich, A. L. Andrady, A. M. Heikkilä, G. H. Bernhard, A. F. Bais, P. J. Aucamp, A. T. Banaszak, J. F. Bornman, L. S. Bruckman, S. N. Byrne, B. Foereid, D.-P. Häder, L. M. Hollestein, W.-C. Hou, S. Hylander, M. A. K. Jansen, A. R. Klekociuk, J. B. Liley, J. Longstreth, R. M. Lucas, J. Martinez-Abaigar, K. McNeill, C. M. Olsen, K. K. Pandey, L. E. Rhodes, S. A. Robinson, K. C. Rose, T. Schikowski, K. R. Solomon, B. Sulzberger, J. E. Ukpebor, Q.-W. Wang, S.-Å. Wängberg, C. C. White, S. Yazar, A. R. Young, P. J. Young, L. Zhu, and M. Zhu
2021. Environmental effects of stratospheric ozone depletion, uv radiation, and interactions with climate change: Unep environmental effects assessment panel, update 2020. *Photochemical & photobiological sciences: Official journal of the European Photochemistry Association and the European Society for Photobiology*, 20(1):1–67. 22

OECD
2004. *Test No. 202: Daphnia sp. Acute Immobilisation Test*, number 202 in OECD guideline for the testing of chemicals. Organisation for Economic Co-operation and Development. 13, 66

OECD
2012. *Test No. 211: Daphnia magna Reproduction Test*, number 211 in OECD guideline for the testing of chemicals. Organisation for Economic Co-operation and Development. 13, 25, 43

Orr, J. A., R. D. Vinebrooke, M. C. Jackson, K. J. Kroeker, R. L. Kordas, C. Mantyka-Pringle, P. J. van den Brink, F. de Laender, R. Stoks, M. Holmstrup, C. D. Matthaei, W. A. Monk, M. R. Penk, S. Leuzinger, R. B. Schäfer, and J. J. Piggott
2020. Towards a unified study of multiple stressors: divisions and common goals across research disciplines. *Proceedings. Biological sciences*, 287(1926):20200421. 6

Palamara, G. M., S. R. Dennis, C. Haenggi, N. Schuwirth, and P. Reichert
2022. Investigating the effect of pesticides on daphnia population dynamics by inferring structure and parameters of a stochastic model. *Ecological Modelling*, 472:110076. 15, 54

Palmquist, K., J. Salatas, and A. Fairbrother
2012. *Pyrethroid Insecticides: Use, Environmental Fate, and Ecotoxicology*. 12, 34

Parker, E. D., V. E. Forbes, S. L. Nielsen, C. Ritter, C. Barata, D. J. Baird, W. Admiraal, L. Levin, V. Loeschke, P. Lyytikainen-Saarenmaa, H. Hogh-Jensen, P. Calow, and B. J. Ripley
1999. Stress in ecological systems. *Oikos*, 86(1):179. 5

Pastore, A. I., G. Barabás, M. D. Bimler, M. M. Mayfield, and T. E. Miller
2021. The evolution of niche overlap and competitive differences. *Nature ecology & evolution*, 5(3):330–337. 8, 57, 80

Persson, L., B. M. Carney Almroth, C. D. Collins, S. Cornell, C. A. de Wit, M. L. Diamond, P. Fantke, M. Hassellöv, M. MacLeod, M. W. Ryberg, P. Søgaard Jørgensen, P. Villarrubia-Gómez, Z. Wang, and M. Z. Hauschild
2022. Outside the safe operating space of the planetary boundary for novel entities. *Environmental science & technology*, 56(3):1510–1521. 1

Pieters, B. J. and M. Liess
2006. Population developmental stage determines the recovery potential of daphnia magna populations after fenvalerate application. *Environmental science & technology*, 40(19):6157–6162. 8, 15, 60, 92

Pieters, B. J., A. Paschke, S. Reynaldi, M. H. S. Kraak, W. Admiraal, and M. Liess
2005. Influence of food limitation on the effects of fenvalerate pulse exposure on the life history and population growth rate of daphnia magna. *Environmental Toxicology and Chemistry*, 24(9):2254–2259. 9

Pimm, S. L., C. N. Jenkins, R. Abell, T. M. Brooks, J. L. Gittleman, L. N. Joppa, P. H. Raven, C. M. Roberts, and J. O. Sexton
2014. The biodiversity of species and their rates of extinction, distribution, and protection. *Science (New York, N.Y.)*, 344(6187):1246752. 1

Post, E. and M. C. Forchhammer
2002. Synchronization of animal population dynamics by large-scale climate. *Nature*, 420(6912):168–171. 79

Preuss, T. G., M. Hammers-Wirtz, U. Hommen, M. N. Rubach, and H. T. Ratte
2009. Development and validation of an individual based daphnia magna population model: The influence of crowding on population dynamics. *Ecological Modelling*, 220(3):310–329. 54

R Core Team
2018. R: A language and environment for statistical computing. 28

Ranta, E., J. Lindstrom, and H. Linden
1995. Synchrony in tetraonid population dynamics. *Journal of Animal Ecology*, 64(6):767. 71, 79

Relyea, R. A. and N. Diecks
2008. An unforeseen chain of events: lethal effects of pesticides on frogs at sublethal concentrations. *Ecological Applications*, 18(7):1728–1742. 14

Reynaldi, S., S. Duquesne, K. Jung, and M. Liess
2006. Linking feeding activity and maturation of daphnia magna following short-term exposure to fenvalerate. *Environmental Toxicology and Chemistry*, 25(7):1826–1830. 12

Ribeiro, F., N. C. G. Ferreira, A. Ferreira, A. M. V. M. Soares, and S. Loureiro
2011. Is ultraviolet radiation a synergistic stressor in combined exposures? the case study of daphnia magna exposure to uv and carbendazim. *Aquatic toxicology (Amsterdam, Netherlands)*, 102(1-2):114–122. 93

Rico, A., P. J. van den Brink, P. Leitner, W. Graf, and A. Focks
2016. Relative influence of chemical and non-chemical stressors on invertebrate communities: a case study in the danube river. *The Science of the total environment*, 571:1370–1382. 6, 92

Riedl, V., A. Agatz, R. Benstead, and R. Ashauer
2018. A standardized tritrophic small-scale system (tricosm) for the assessment of stressor-induced effects on aquatic community dynamics. *Environmental Toxicology and Chemistry*, 37(4):1051–1060. 93

Ritz, C., F. Baty, J. C. Streibig, and D. Gerhard
2015. Dose-response analysis using r. *PloS one*, 10(12):e0146021. 28, 128, 132

Robert, C. and G. Casella
2011. A short history of markov chain monte carlo: Subjective recollections from incomplete data. *Statistical Science*, 26(1). 17

Robertson, G. S., M. Bolton, P. Morrison, and P. Monaghan
2015. Variation in population synchrony in a multi-species seabird community: Response to changes in predator abundance. *PloS one*, 10(6):e0131543. 79, 90

Rösch, A., B. Beck, J. Hollender, and H. Singer
2019a. Picogram per liter quantification of pyrethroid and organophosphate insecticides in surface waters: a result of large enrichment with liquid-liquid extraction and gas chromatography coupled to mass spectrometry using atmospheric pressure chemical ionization. *Analytical and bioanalytical chemistry*, 411(14):3151–3164. 13, 57

Rösch, A., B. Beck, J. Hollender, C. Stamm, and H. Singer
2019b. Geringe konzentration mit großer wirkung: Nachweis von pyrethroid- und organophosphat- insektiziden in schweizer bächen im pg l-1 bereich. *Aqua & Gas*, 11:54–66. 13, 40

Rousseaux, S., J. Vanoverbeke, J. Aerts, and S. A. J. Declerck
2010. Effects of medium renewal and handling stress on life history traits in daphnia. *Hydrobiologia*, 643(1):63–69. 15, 92

Rozman, K. K. and J. Doull
2000. Dose and time as variables of toxicity. *Toxicology*, 144(1-3):169–178. 22

Rundlöf, M., G. K. S. Andersson, R. Bommarco, I. Fries, V. Hederström, L. Herbertsson, O. Jonsson, B. K. Klatt, T. R. Pedersen, J. Yourstone, and H. G. Smith
2015. Seed coating with a neonicotinoid insecticide negatively affects wild bees. *Nature*, 521(7550):77–80. 1, 3, 11, 40, 85

Rutter, E. M., H. T. Banks, G. A. LeBlanc, and K. B. Flores
2017. Continuous structured population models for daphnia magna. *Bulletin of mathematical biology*, 79(11):2627–2648. 53

Ryo, M., C. A. Aguilar-Trigueros, L. Pinek, L. A. H. Muller, and M. C. Rillig
2019. Basic principles of temporal dynamics. *Trends in ecology & evolution*, 34(8):723–733. 7, 21

Salvatier, J., T. V. Wiecki, and C. Fonnesbeck
2016. Probabilistic programming in python using pymc3. *PeerJ Computer Science*, 2:e55. 20, 27, 47, 72, 123

Schäfer, R. B., T. Caquet, K. Siimes, R. Mueller, L. Lagadic, and M. Liess
2007. Effects of pesticides on community structure and ecosystem functions in

agricultural streams of three biogeographical regions in europe. *The Science of the total environment*, 382(2-3):272–285. 2

Schirrmacher, V.
2021. Less can be more: The hormesis theory of stress adaptation in the global biosphere and its implications. *Biomedicines*, 9(3). 89

Schoetter, R., J. Cattiaux, and H. Douville
2015. Changes of western european heat wave characteristics projected by the cmip5 ensemble. *Climate Dynamics*, 45(5-6):1601–1616. 22

Schramm, H., M. L. Jaramillo, T. de Quadros, E. C. Zeni, Y. M. R. Müller, D. Ammar, and E. M. Nazari
2017. Effect of uvb radiation exposure in the expression of genes and proteins related to apoptosis in freshwater prawn embryos. *Aquatic toxicology (Amsterdam, Netherlands)*, 191:25–33. 34

Schulz, H.
1888. Ueber hefegifte. *Pflüger, Archiv für die Gesammte Physiologie des Menschen und der Thiere*, 42(1):517–541. 5, 23, 54, 89

Schunck, F. and M. Liess
2023. Ultra-low esfenvalerate concentrations increase biomass and may reduce competitiveness of daphnia magna populations. *The Science of the total environment*, P. 163916. 61, 82

Seabold, S. and J. Perktold
2010. Statsmodels: Econometric and statistical modeling with python. In *Proceedings of the 9th Python in Science Conference*, S. van der Walt and J. Millman, eds. Austin, Texas: [publisher unknown]. 47

Serra, T., M. F. Müller, A. Barcelona, V. Salvadó, N. Pous, and J. Colomer
2019. Optimal light conditions for daphnia filtration. *The Science of the total environment*, 686:151–157. 15, 69

Shahid, N., M. Liess, and S. Knillmann
2019. Environmental stress increases synergistic effects of pesticide mixtures on daphnia magna. *Environmental science & technology*, 53(21):12586–12593. 5, 9, 23, 25, 36, 135

Shang, J., Y.-S. Yao, L.-L. Chen, X.-Z. Zhu, L. Niu, X.-K. Gao, J.-Y. Luo, J.-C. Ji, and J.-J. Cui
2021. Sublethal exposure to deltamethrin stimulates reproduction and alters

symbiotic bacteria in aphis gossypii. *Journal of agricultural and food chemistry*, 69(50):15097–15107. 5, 12, 40, 55, 89

Sial, M. U., Z. Zhao, L. Zhang, Y. Zhang, L. Mao, and H. Jiang
2018. Evaluation of insecticides induced hormesis on the demographic parameters of myzus persicae and expression changes of metabolic resistance detoxification genes. *Scientific reports*, 8(1):16601. 89

Simmons, B. I., P. S. A. Blyth, J. L. Blanchard, T. Clegg, E. Delmas, A. Garnier, C. A. Griffiths, U. Jacob, F. Pennekamp, O. L. Petchey, T. Poisot, T. J. Webb, and A. P. Beckerman
2021. Refocusing multiple stressor research around the targets and scales of ecological impacts. *Nature ecology & evolution*, 5(11):1478–1489. 6, 21

Sims, I. R., S. Watson, and D. Holmes
1993. Toward a standard daphnia juvenile production test. *Environmental Toxicology and Chemistry*, 12(11):2053. 15, 92

Singh, S., R. K. Mall, and N. Singh
2021. Changing spatio–temporal trends of heat wave and severe heat wave events over india: An emerging health hazard. *International Journal of Climatology*, 41(S1). 22

Soderlund, D. M.
2005. Sodium channels. In *Comprehensive Molecular Insect Science*, L. I. Gilbert, ed., Pp. 1–24. Elsevier. 12, 28

Soetaert, A., K. van der Ven, L. N. Moens, T. Vandenbrouck, P. van Remortel, and W. M. de Coen
2007. Daphnia magna and ecotoxicogenomics: gene expression profiles of the anti-ecdysteroidal fungicide fenarimol using energy-, molting- and life stage-related cdna libraries. *Chemosphere*, 67(1):60–71. 14

Sokolova, I. M.
2013. Energy-limited tolerance to stress as a conceptual framework to integrate the effects of multiple stressors. *Integrative and comparative biology*, 53(4):597–608. 5

Sokolova, I. M., M. Frederich, R. Bagwe, G. Lannig, and A. A. Sukhotin
2012. Energy homeostasis as an integrative tool for assessing limits of environmental stress tolerance in aquatic invertebrates. *Marine environmental research*, 79:1–15. 5

Song, Y., L. Xie, Y. Lee, and K. E. Tollefsen
2020. De novo development of a quantitative adverse outcome pathway (qaop) network for ultraviolet b (uvb) radiation using targeted laboratory tests and automated data mining. *Environmental science & technology*, 54(20):13147–13156. 15, 28, 34

Šorf, M., T. A. Davidson, S. Brucet, R. F. Menezes, M. Søndergaard, T. L. Lauridsen, F. Landkildehus, L. Liboriussen, and E. Jeppesen
2015. Zooplankton response to climate warming: a mesocosm experiment at contrasting temperatures and nutrient levels. *Hydrobiologia*, 742(1):185–203. 69

Stark, J. D. and J. A. Banken
1999. Importance of population structure at the time of toxicant exposure. *Ecotoxicology and environmental safety*, 42(3):282–287. 8

Stebbing, A.
1982. Hormesis — the stimulation of growth by low levels of inhibitors. *Science of The Total Environment*, 22(3):213–234. 40

Stebbing, A.
1998. A theory for growth hormesis. *Mutation Research/Fundamental and Molecular Mechanisms of Mutagenesis*, 403(1-2):249–258. 5, 23, 54, 89

Stehle, S. and R. Schulz
2015. Agricultural insecticides threaten surface waters at the global scale. *Proceedings of the National Academy of Sciences of the United States of America*, 112(18):5750–5755. 2, 3

Stevenson, L. M., K. E. Krattenmaker, E. Johnson, A. J. Bowers, A. S. Adeleye, E. McCauley, and R. M. Nisbet
2017. Standardized toxicity testing may underestimate ecotoxicity: Environmentally relevant food rations increase the toxicity of silver nanoparticles to daphnia. *Environmental toxicology and chemistry*, 36(11):3008–3018. 9

Stokstad, E.
2018. European union expands ban of three neonicotinoid pesticides. *Science (New York, N.Y.)*. 3

Stuligross, C. and N. M. Williams
2021. Past insecticide exposure reduces bee reproduction and population growth rate. *Proceedings of the National Academy of Sciences of the United States of America*, 118(48). 1, 3, 22, 85

Suter, G. W. and S. M. Cormier
2015. Why care about aquatic insects: uses, benefits, and services. *Integrated environmental assessment and management*, 11(2):188–194. 2

Townsend, J. F. and T. D. Luckey
1960. Hormoligosis in pharmacology. *Journal of the American Medical Association*, 173:44–48. 40, 89

UNEP
2019. *Global Chemicals Outlook II: From Legacies to Innovative Solutions: Synthesis Report (2019)*. United Nations Environment Programme. 1

van den Brink, P. J., A. B. A. Boxall, L. Maltby, B. W. Brooks, M. A. Rudd, T. Backhaus, D. Spurgeon, V. Verougstraete, C. Ajao, G. T. Ankley, S. E. Apitz, K. Arnold, T. Brodin, M. Cañedo-Argüelles, J. Chapman, J. Corrales, M.-A. Coutellec, T. F. Fernandes, J. Fick, A. T. Ford, G. Giménez Papiol, K. J. Groh, T. H. Hutchinson, H. Kruger, J. V. K. Kukkonen, S. Loutseti, S. Marshall, D. Muir, M. E. Ortiz-Santaliestra, K. B. Paul, A. Rico, I. Rodea-Palomares, J. Römbke, T. Rydberg, H. Segner, M. Smit, C. A. M. van Gestel, M. Vighi, I. Werner, E. I. Zimmer, and J. van Wensem
2018. Toward sustainable environmental quality: Priority research questions for europe. *Environmental toxicology and chemistry*, 37(9):2281–2295. 6, 60

van der Meer, J.
2006. Metabolic theories in ecology. *Trends in ecology & evolution*, 21(3):136–140. 93

van Doorslaer, W., R. Stoks, C. Duvivier, A. Bednarska, and L. de Meester
2009. Population dynamics determine genetic adaptation to temperature in daphnia. *Evolution; international journal of organic evolution*, 63(7):1867–1878. 15

van Klink, R., D. E. Bowler, K. B. Gongalsky, A. B. Swengel, A. Gentile, and J. M. Chase
2020. Meta-analysis reveals declines in terrestrial but increases in freshwater insect abundances. *Science (New York, N.Y.)*, 368(6489):417–420. 85

Vanbergen, A. J. and the Insect Pollinators Initiative
2013. Threats to an ecosystem service: pressures on pollinators. *Frontiers in Ecology and the Environment*, 11(5):251–295. 1, 85

Vaugeois, M., P. A. Venturelli, S. L. Hummel, C. Accolla, and V. E. Forbes
2020. Population context matters: Predicting the effects of metabolic stress

mediated by food availability and predation with an agent- and energy budget-based model. *Ecological Modelling*, 416:108903. 4, 59

Vinebrooke, R. D., K. L. Cottingham, M. S. J. Norberg, S. I. Dodson, S. C. Maberly, and U. Sommer
2004. Impacts of multiple stressors on biodiversity and ecosystem functioning: the role of species co-tolerance. *Oikos*, 104(3):451–457. 21

Vlaeminck, K., K. P. J. Viaene, P. van Sprang, and K. A. C. de Schamphelaere
2020. Development and validation of a mixture toxicity implementation in dedibm: Effects of copper and zinc on daphnia magna populations. *Environmental toxicology and chemistry*. 15

Vlaeminck, K., K. P. J. Viaene, P. van Sprang, and K. A. C. de Schamphelaere
2022. Predicting combined effects of chemical stressors: Population-level effects of organic chemical mixtures with a dynamic energy budget individual-based model. *Environmental toxicology and chemistry*, 41(9):2240–2258. 54

Volterra, V.
1928. Variations and fluctuations of the number of individuals in animal species living together. *ICES Journal of Marine Science*, 3(1):3–51. 8, 79

Wagner, D. L.
2020. Insect declines in the anthropocene. *Annual review of entomology*, 65:457–480. 1

Wang, S., B. Huang, D. Fan, E. Agathokleous, Y. Guo, Y. Zhu, and J. Han
2021. Hormetic responses of soil microbiota to exogenous cd: A step toward linking community-level hormesis to ecological risk assessment. *Journal of hazardous materials*, 416:125760. 54

Werner, I. and K. Moran
2008. Effects of pyrethroid insecticides on aquatic organisms. In *Synthetic Pyrethroids*, J. Gan, F. Spurlock, P. Hendley, and D. P. Weston, eds., volume 991 of *ACS Symposium Series*, Pp. 310–334. Washington, DC: American Chemical Society. 12, 14

Wittmer, I. K., H.-P. Bader, R. Scheidegger, H. Singer, A. Lück, I. Hanke, C. Carlsson, and C. Stamm
2010. Significance of urban and agricultural land use for biocide and pesticide dynamics in surface waters. *Water Research*, 44(9):2850–2862. 7, 21

Wojtal-Frankiewicz, A.
2012. The effects of global warming on daphnia spp. population dynamics: a review. *Aquatic Ecology*, 46(1):37–53. 15

Wolz, M., A. Schrader, and C. Müller
2021. Direct and delayed effects of exposure to a sublethal concentration of the insecticide l-cyhalothrin on food consumption and reproduction of a leaf beetle. *The Science of the total environment*, 760:143381. 5, 12, 40, 55, 89

Wonkwon, K., E. Ayna, Am Shahabuddin, T. Araki, and T. Yoshimatsu
2019. Negative effects of full spectrum light exposure along with uv radiation on survival and reproduction of cladocera daphnia magna. *International Journal of Fisheries and Aquatic Studies*, Pp. 40–44. 15

Wood, T. J. and D. Goulson
2017. The environmental risks of neonicotinoid pesticides: a review of the evidence post 2013. *Environmental science and pollution research international*, 24(21):17285–17325. 2

Yang, W., F. Spurlock, W. Liu, and J. Gan
2006. Inhibition of aquatic toxicity of pyrethroid insecticides by suspended sediment. *Environmental toxicology and chemistry*, 25(7):1913–1919. 57

Zhu, H., X. G. Liu, and S. P. Cheng
2021. Phytoplankton community structure and water quality assessment in an ecological restoration area of baiyangdian lake, china. *International Journal of Environmental Science and Technology*, 18(6):1529–1536. 69

Appendix A

Supporting Information for Chapter 3

Method A.1. Bayesian parameter estimation

We used the modelling framework Python Markov Chain Monte Carlo (MCMC) library (PyMC) (Salvatier et al., 2016) for fitting dose response curves with bayesian parameter estimation. The description of the statistical model is as follows Survival y follows a binomial distribution according to mortality probability p and the number of *trials* in each treatment.

$$y \sim Binomial(p,\ trials) \tag{A.1}$$

$$p = c + \frac{1-c}{1 + exp(-dlog(\frac{x}{e}))} \tag{A.2}$$

Mortality probability p is deterministically modelled as a log logistic function dependent on the parameters c, d, and e and the stressor dose x. For the individual model parameters, priors were chosen as follows

$$c_{control} \sim Beta(alpha = 1,\ beta = 10) \tag{A.3}$$

$$c \sim Uniform(a = 0,\ b = 1) \tag{A.4}$$

$$e_{esfenvalerate} \sim PositiveNormal(loc = 1.5,\ scale = 3) \tag{A.5}$$

$$e_{uvb} \sim PositiveNormal(loc = 500,\ scale = 2000) \tag{A.6}$$

$$b_{esfenvalerate} \sim LogNormal(loc = 3,\ scale = 1) \tag{A.7}$$

$$b_{uvb} \sim LogNormal(loc = 2.6,\ scale = 0.7) \tag{A.8}$$

$$\tag{A.9}$$

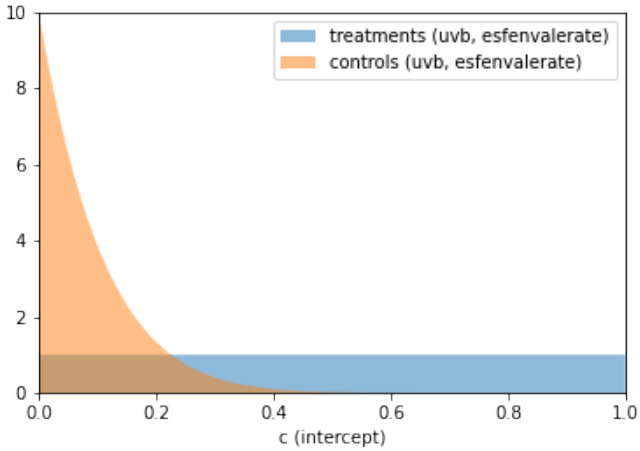

Figure A.1: Prior distribution for the y-intercept (parameter c) of the log-logistic model. Note that we used different priors the y intercept (parameter c) for control treatments to incorporate prior knowledge that control effects (no stress) should be near null. For the contaminated treatments we chose a uniform prior, in order not to impose any knowledge on the fitting of the intercept.

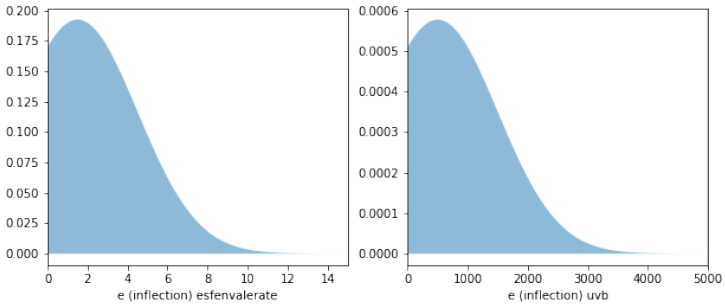

Figure A.2: Priors for inflection point (parameter e) of the log-logistic model for esfenvalerate (a) and UV-B radiation (b). Since UV-B radiation and esfenvalerate act on vastly different scales, different priors were required for the parameters e (inflection point).

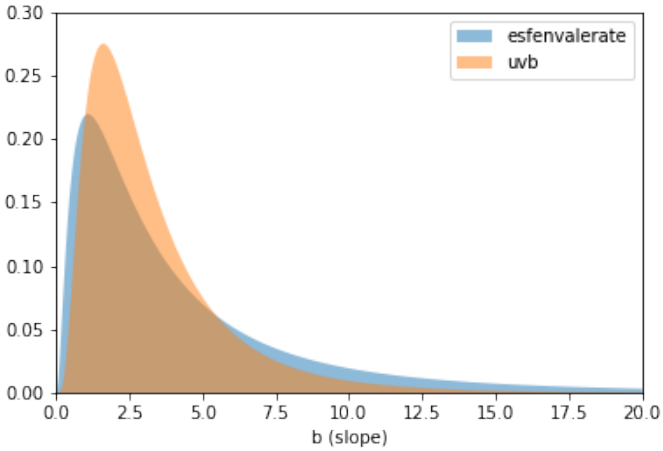

Figure A.3: Priors for the slope of the log-logistic regression (parameter b) of esfenvalerate and UV-B radiation. To address the issue of separation, we used an informative Log-Normal prior for the slope in order to assign low probability to flat and nearly vertical intercepts. Note that slope parameter priors are slightly different because the sampler had some problems with very high values of b in the case of UV-B.

Table A.1: Nominal and measured esfenvalerate concentrations (µg/L) applied in the experiment described in Chapter 3.

Contaminant	Nominal concentration (µg/L)	Measured Concentration (µg/L)	Deviation (%)
Esfenvalerate	0.01	0.014	40
	0.02	0.027	35
	0.04	0.039	2.5
	0.08	0.1	-20
	0.16	0.18	12.5
	0.32	0.15	-53[1]
	0.64	0.61	-4.7
	1.28	1.1	-14
	2.56	2.5	-2.3

[1] The Large deviation in this sample most likely results from a sampling error. It can be clearly observed by comparison of Figure A.5 k, l (0.16 µg/L) and Figure A.5 m, n (0.32 µg/L) that nominal concentration of 0.32 µg/L had a much stronger effect than the nominal concentration of 0.16 µg/L

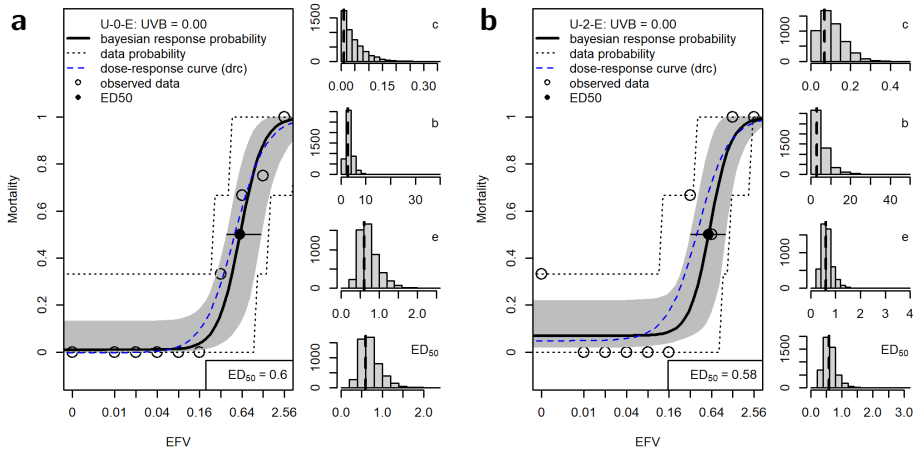

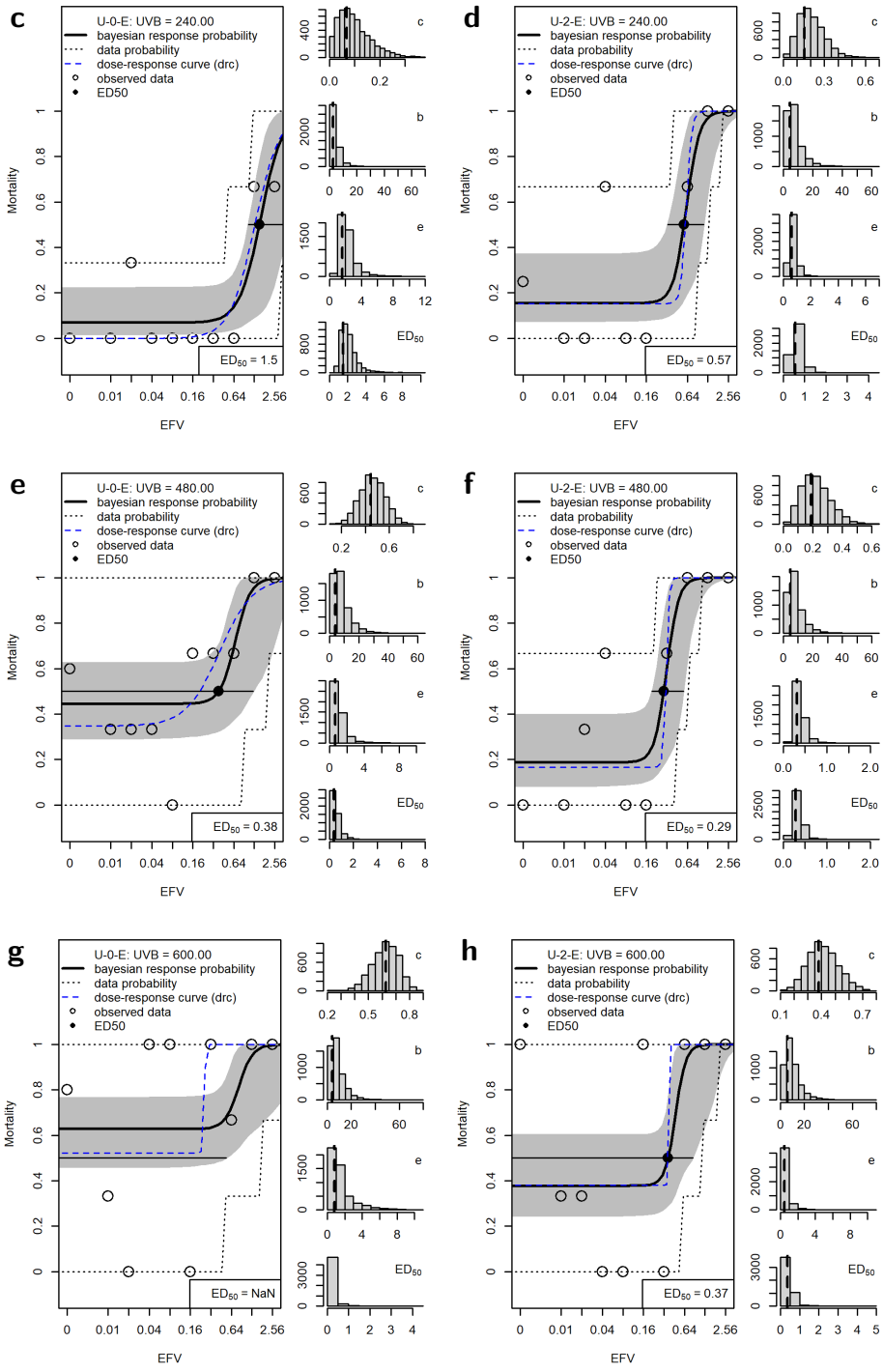
c
U-0-E: UVB = 240.00
bayesian response probability
data probability
dose-response curve (drc)
observed data
ED50
Mortality
EFV
ED50 = 1.5
d
U-2-E: UVB = 240.00
ED50 = 0.57
e
U-0-E: UVB = 480.00
ED50 = 0.38
f
U-2-E: UVB = 480.00
ED50 = 0.29
g
U-0-E: UVB = 600.00
ED50 = NaN
h
U-2-E: UVB = 600.00
ED50 = 0.37
b
e
ED50

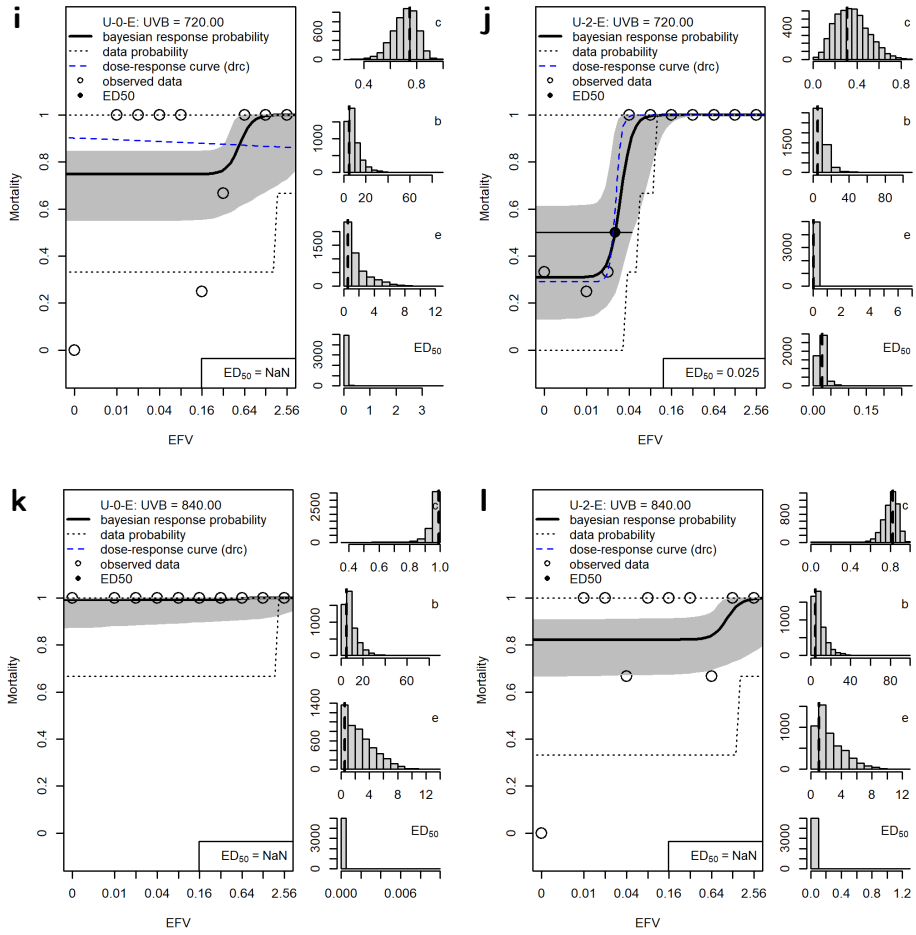

Figure A.4: Dose response curves of esfenvalerate after Exposure to UV-B radiation. **(a, c, e, g, i, k)** Dose response curves for zero-day time-gap between stress exposure. **(b, d, f, h, j, l)** Dose response curves for exposure scenarios with a two-day time gap between exposures. The histograms beside the curves indicate posterior estimates of the parameters of the log-logistic dose response curves. To visualize the issue of division, the dashed blue line indicates maximum likelihood fits obtained with the R language (R) package *drc* (Ritz et al., 2015). Absence, of the dashed blue line indicates that a maximum likelihood fit was not possible. The shaded area indicates the 95% credible interval (CI) of the true dose response curve. The solid black line indicates the dose response curve with the highest probability (maximum a posteriori (MAP) estimate) and dotted black lines enclose the 95% CI interval of plausible data under the fitted parameter distributions of the model.

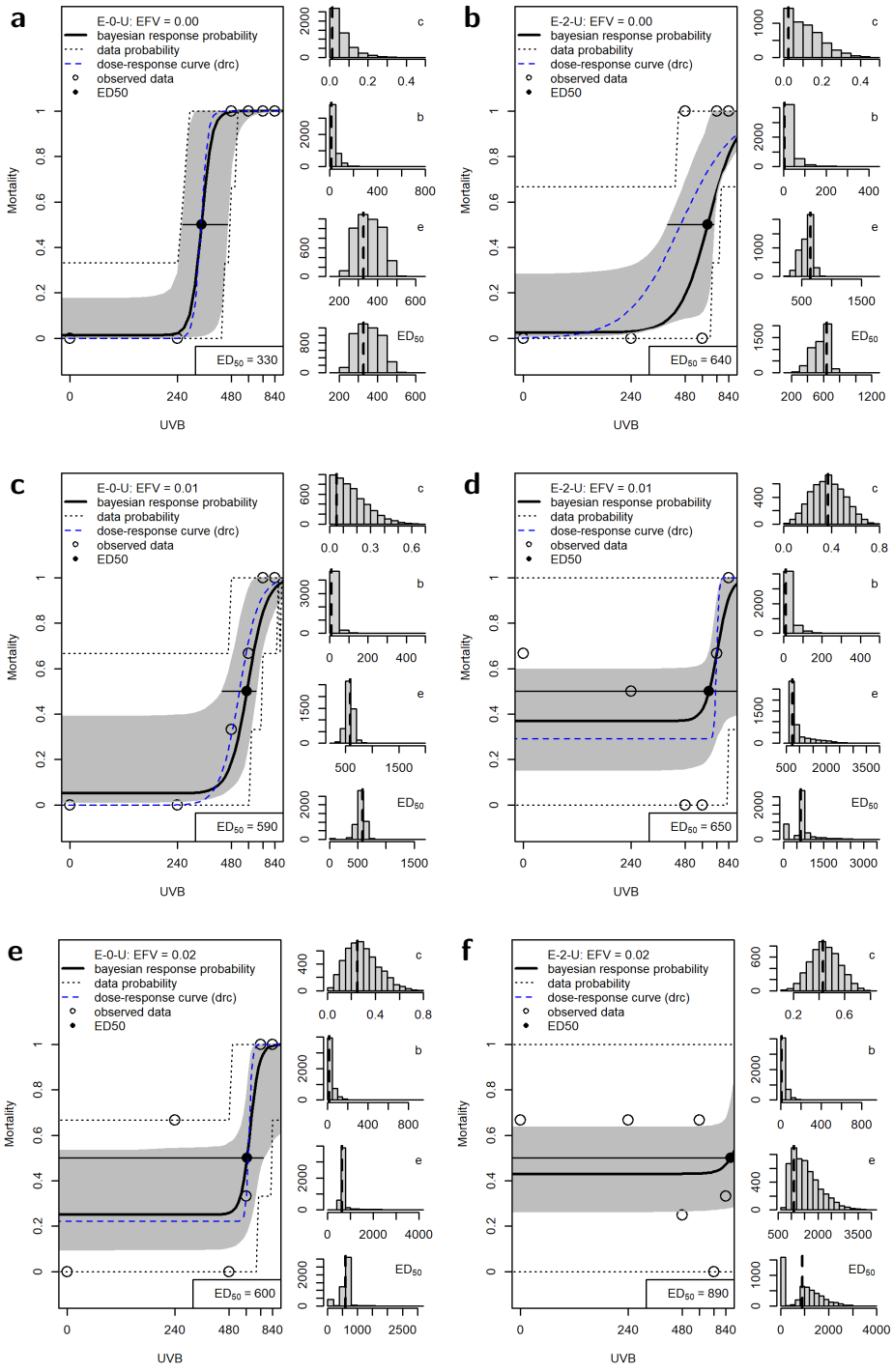
a
E-0-U: EFV = 0.00
bayesian response probability
data probability
dose-response curve (drc)
observed data
ED50
Mortality
UVB
ED50 = 330
b
E-2-U: EFV = 0.00
ED50 = 640
c
E-0-U: EFV = 0.01
ED50 = 590
d
E-2-U: EFV = 0.01
ED50 = 650
e
E-0-U: EFV = 0.02
ED50 = 600
f
E-2-U: EFV = 0.02
ED50 = 890
ED50

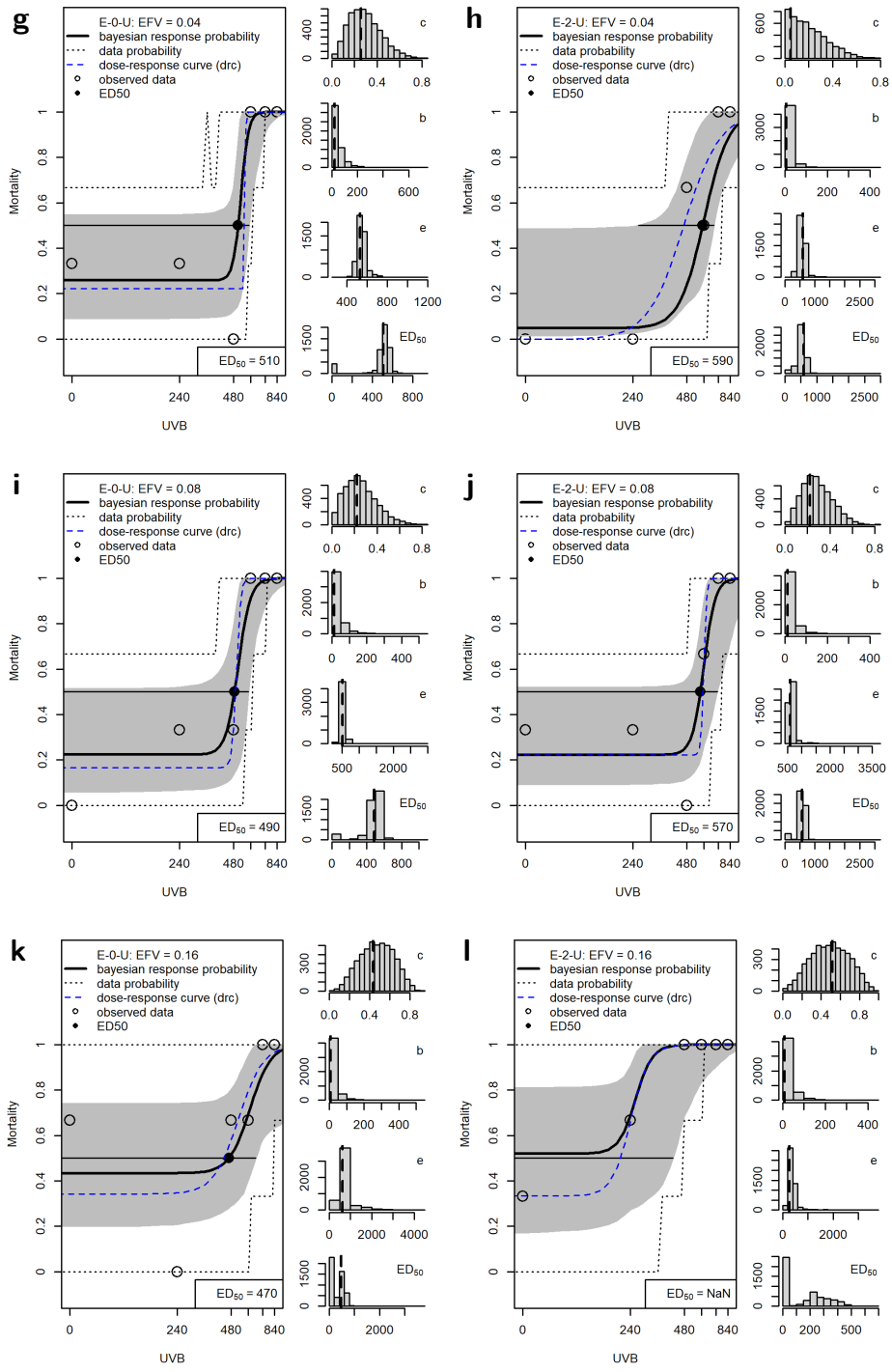
g
E-0-U: EFV = 0.04
bayesian response probability
data probability
dose-response curve (drc)
observed data
ED50
ED50 = 510
h
E-2-U: EFV = 0.04
ED50 = 590
i
E-0-U: EFV = 0.08
ED50 = 490
j
E-2-U: EFV = 0.08
ED50 = 570
k
E-0-U: EFV = 0.16
ED50 = 470
l
E-2-U: EFV = 0.16
ED50 = NaN
Mortality
UVB
ED50
c
b
e

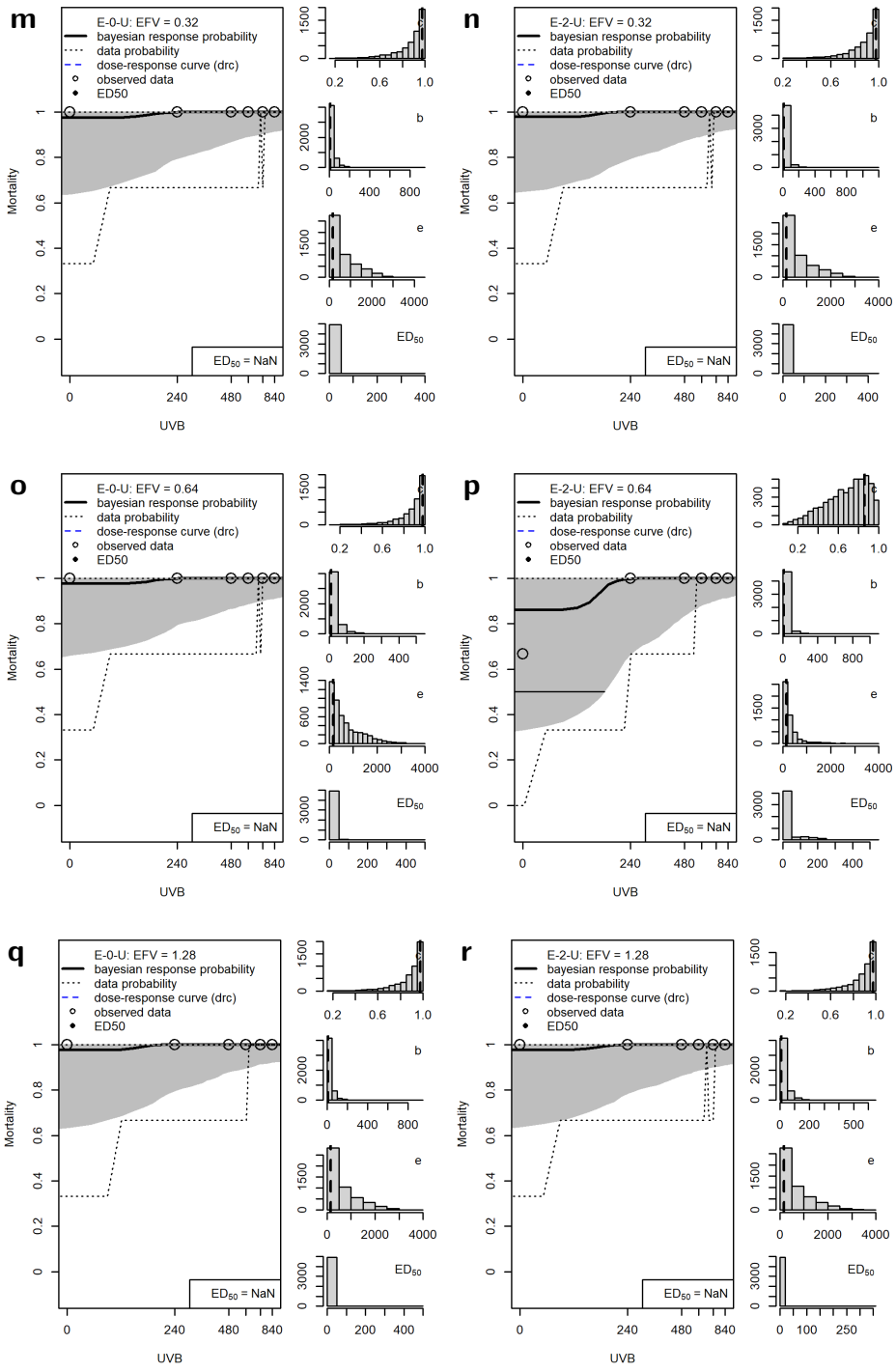
m
E-0-U: EFV = 0.32
bayesian response probability
data probability
dose-response curve (drc)
observed data
ED50
Mortality
UVB
ED50 = NaN
b
e
ED50
n
E-2-U: EFV = 0.32
o
E-0-U: EFV = 0.64
p
E-2-U: EFV = 0.64
q
E-0-U: EFV = 1.28
r
E-2-U: EFV = 1.28

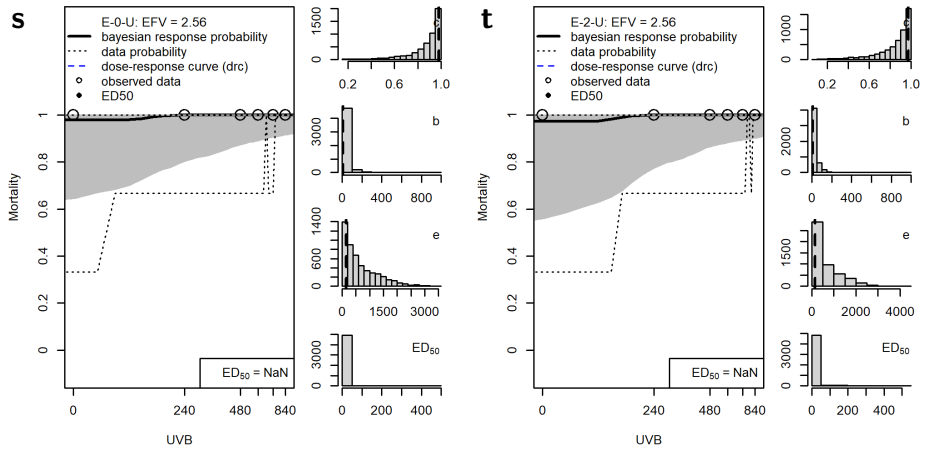

Figure A.5: Dose response curves of UV-Bradiation after exposure to esfenvalerate. **(a, c, e, g, i, k, m, o, q, s)** Dose response curves for zero-day time-gap between stress exposure. **(b, d, f, h, j, l, n, p, r, t)** Dose response curves for exposure scenarios with a two-day time gap between exposures. The histograms beside the curves indicate posterior estimates of the parameters of the log-logistic dose response curves. To visualize the issue of division, the dashed blue line indicates maximum likelihood fits obtained with the R package *drc* (Ritz et al., 2015). Absence, of the dashed blue line indicates that a maximum likelihood fit was not possible. The shaded area indicates the 95% CI of the true dose response curve. The solid black line indicates the dose response curve with the highest probability (MAP estimate) and dotted black lines enclose the 95% CI interval of plausible data under the fitted parameter distributions of the model.

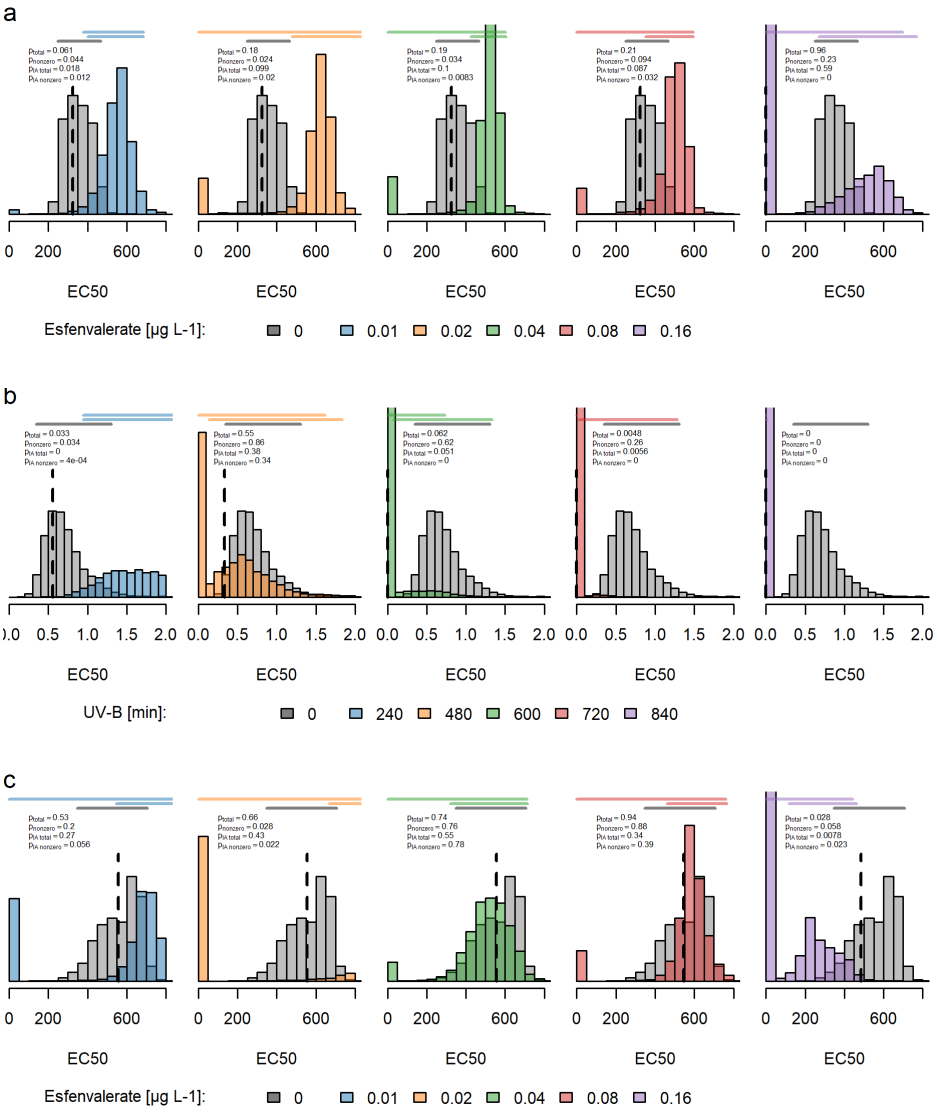
a
Ptotal = 0.061
Pnonzero = 0.044
PIA total = 0.018
PIA nonzero = 0.012
Ptotal = 0.18
Pnonzero = 0.024
PIA total = 0.099
PIA nonzero = 0.02
Ptotal = 0.19
Pnonzero = 0.034
PIA total = 0.1
PIA nonzero = 0.0083
Ptotal = 0.21
Pnonzero = 0.094
PIA total = 0.087
PIA nonzero = 0.032
Ptotal = 0.96
Pnonzero = 0.23
PIA total = 0.59
PIA nonzero = 0
0 200 600
EC50
Esfenvalerate [µg L-1]: 0 0.01 0.02 0.04 0.08 0.16
b
Ptotal = 0.033
Pnonzero = 0.034
PIA total = 0
PIA nonzero = 4e-04
Ptotal = 0.55
Pnonzero = 0.86
PIA total = 0.38
PIA nonzero = 0.34
Ptotal = 0.062
Pnonzero = 0.62
PIA total = 0.051
PIA nonzero = 0
Ptotal = 0.0048
Pnonzero = 0.26
PIA total = 0.0056
PIA nonzero = 0
Ptotal = 0
Pnonzero = 0
PIA total = 0
PIA nonzero = 0
0.0 0.5 1.0 1.5 2.0
EC50
UV-B [min]: 0 240 480 600 720 840
c
Ptotal = 0.53
Pnonzero = 0.2
PIA total = 0.27
PIA nonzero = 0.056
Ptotal = 0.66
Pnonzero = 0.028
PIA total = 0.43
PIA nonzero = 0.022
Ptotal = 0.74
Pnonzero = 0.76
PIA total = 0.55
PIA nonzero = 0.78
Ptotal = 0.94
Pnonzero = 0.88
PIA total = 0.34
PIA nonzero = 0.39
Ptotal = 0.028
Pnonzero = 0.058
PIA total = 0.0078
PIA nonzero = 0.023
0 200 600
EC50
Esfenvalerate [µg L-1]: 0 0.01 0.02 0.04 0.08 0.16

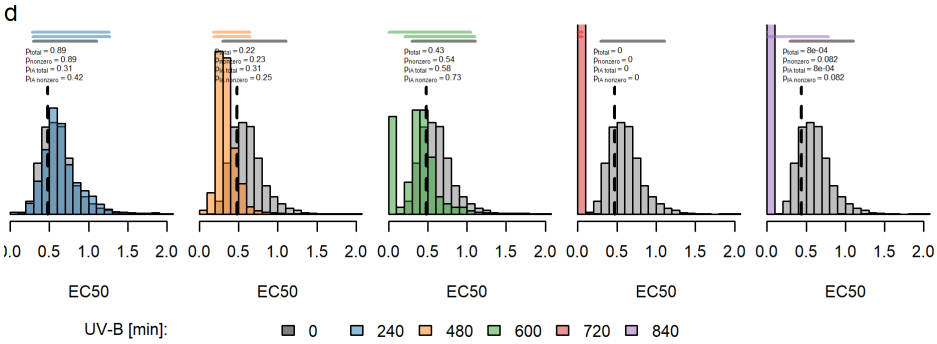

Figure A.6: Histograms of posterior distributions of EC_{50} values. The panels **(a-d)** correspond to panels a-d in Figure 3.3 of the manuscript. **(a)** E-0-U, **(b)** U-0-E, **(c)** E-2-U, **(d)** U-2-E. These histograms are the actual data where vertical posterior density intervals of Figure 3.3 are derived from. In the above figure complete EC_{50} distributions of respective concentrations of the second stressor are compared to the EC_{50}-distribution of the control, which only received the first stressor. The dashed line indicates the independent action EC_{50} prediction. Bars on top indicate the 95% quantile in the distribution (= 95% posterior density interval (PDI)), including the *NaN* values that were converted to zeros (top) and with removed NANs (bottom), which were selected for the analysis.

Appendix B

Supporting Information for Chapter 4

Method B.1. Preparation and supply of feeding suspensions used in the experiment

Two suspensions were prepared for feeding:

(a) 0.3 g ground dog food and 0.3g ground stinging nettle were mixed with 100 mL doubly distilled water. The mixture was stirred for 15 minutes and 1.45 ml of the suspension was given to each system. On the first 5 feeding dates (first 10 days of the experiment), the volume of supplied feeding suspension was doubled (2.9 ml).

(a) green algae (*Desmodesmus subspicata*) was batch cultured in the Helmholtz Centre for Environmental Research—UFZ. The procedure is detailed described in (Shahid et al., 2019). The fed volume of the algae suspension was calculated based on the counted cell density and cell volume in the suspension with a *Casy* cell counter (OLS OMNI Life Science GmbH & Co KG, Bremen, Germany). The systems were fed with a target volume 0.75 µl algae per feeding. Again, the volume was doubled during the first 10 days of the experiment.

Table B.1: Nominal and measured esfenvalerate concentrations (µg/L) used in the experiment described in Chapter 4.

Contaminant	Nominal concentration (µg/L)	Measured Concentration (µg/L)	DMSO (v/v)	Deviation (%)
Control	0.0		0.0	
Esfenvalerate	0.01	0.011	0.0002	+10.0
	0.0316	0.038	0.0001	+20.2
	0.1	0.089	0.0002	-11.0
	0.316	0.32	0.0001	+1.3
	1.0	1.1	0.0002	+10.0
	3.16	3.0	0.0001	-5.0
	10.0	10.0	0.0002	0.0

Table B.2: Ordinary least squares regression results of the model: post-exposure biomass growth rate ∼ pre-exposure biomass growth rate + esfenvalerate concentration, where the applied concentration is treated as a categorical variable. Adjusted-$R^2 = 0.84$.

	coefficient	[0.025	0.975]	t	p-values
Intercept	0.005	-0.13	0.14	0.07	0.944
0.01	0.117	-0.072	0.307	1.287	0.212
0.031	0.082	-0.108	0.271	0.892	0.382
0.1	-0.043	-0.232	0.146	-0.47	0.643
0.316	**-0.338**	-0.527	-0.149	-3.702	**0.001**
1.0	**-0.246**	-0.446	-0.047	-2.559	**0.018**
3.16	**-0.25**	-0.439	-0.06	-2.728	**0.012**
10.0	**-0.326**	-0.53	-0.121	-3.297	**0.003**
***pre*-exposure**	**-1.106**	-1.381	-0.832	-8.367	$<$ **0.001**

Table B.3: Ordinary least squares regression results of the model: post-exposure biomass growth rate ∼ pre-exposure biomass growth rate. Adjusted-$R^2 = 0.60$.

	coefficient	[0.025	0.975]	t	p-values
Intercept	**-0.092**	-0.18	-0.005	-2.162	**0.039**
***pre*-exposure**	**-1.305**	-1.699	-0.91	-6.768	$<$ **0.001**

Table B.4: Camera Settings of Canon PowerShot G12 used in the experiment described in Chapter 4.

Exposure	1/30
Manual exposure compensation	+1
Aperture	F/2.8
Iso	400
Resolution	2816 x 2112 pixels

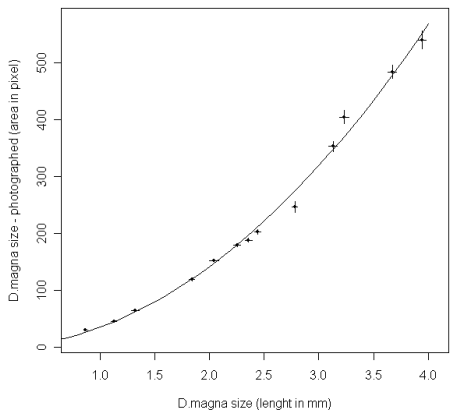

Figure B.1: Calibration of *D. magna* size from the counted number of pixels $A = 35.5L^2$. Created by Oliver Kaske.

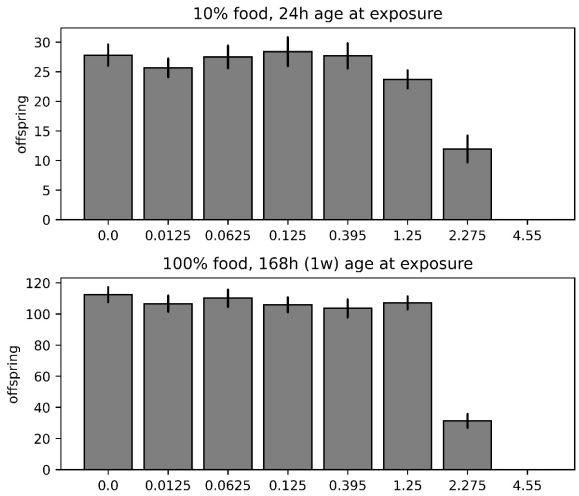

Figure B.2: Effects of DMSO on reproduction of *D. magna* until 21 days after contamination. Effects of low food availability and different size/age classes are tested. No effects evident below 1% volumetric concentration.

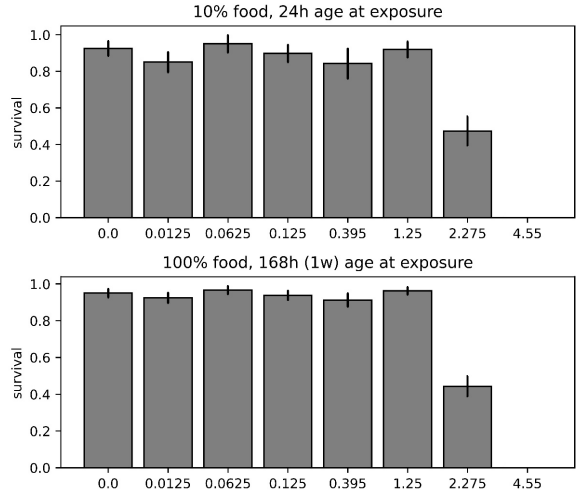

Figure B.3: Effects of DMSO on survival of *D. magna* until 21 days after contamination. Effects of low food availability and different size/age classes are tested. No effects evident below 1% volumetric concentration.

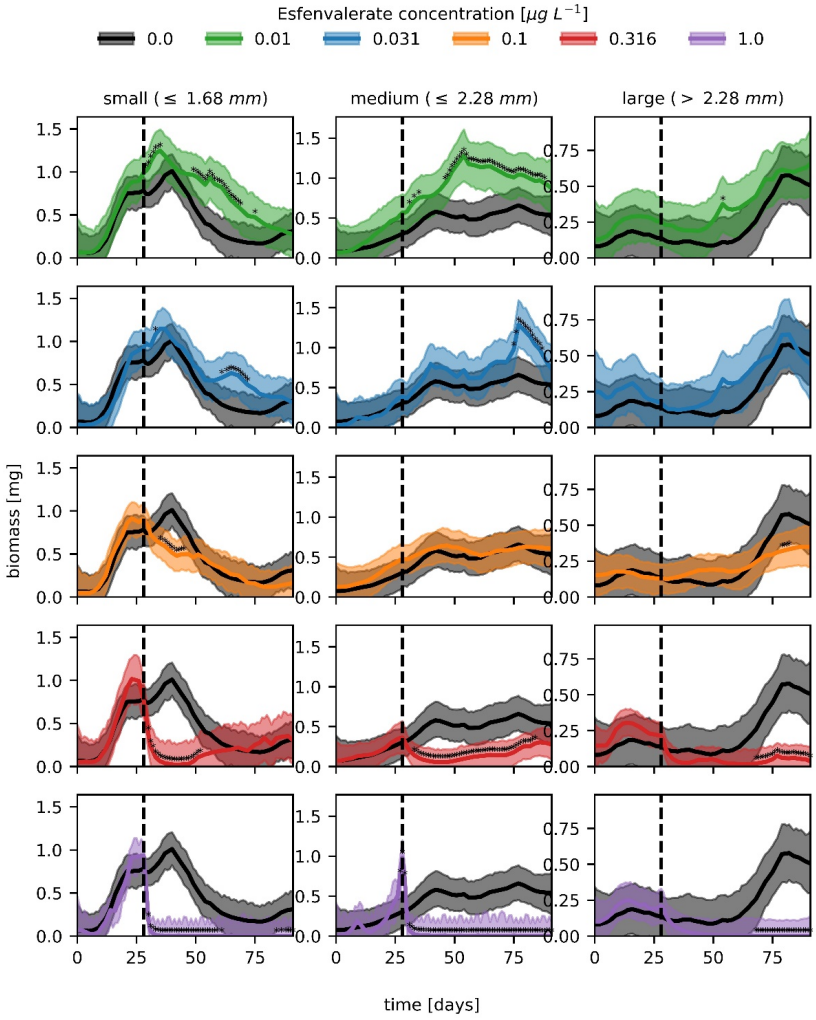

Figure B.4: Time-series analysis of population biomass, separated into three size classes.

Appendix C

Supporting Information for Chapter 5

Method C.1. Systems removed from analysis with the associated reasons for removal

In 4 systems (4, 15, 22, 64) an accidental spill of glucose feeding solution entered the water body. In these systems massive bacteria growth developed in the following weeks followed by a population explosion of *C. pipiens* followed by oxygen depletion and consequent extinction of *D. magna* population. While this cascade is highly interesting, it has nothing to do with the effect of pesticides in the experiment and was therefore excluded. 8 systems were additionally colonized with *D. magna* throughout the 2-month pre-exposure period. For some of these systems this had lasting effects until after the first exposure. Therefore, the 8 affected systems (8, 33, 37, 43, 45, 46, 56, 77) were removed from the analysis. 3 systems (63, 68, 80) was removed because the *D. magna* population got extinct just before the first exposure. 1 System (34) was removed because it was kept in a different location and 1 system (57) was removed because there an exceptionally large fraction of organism was dwelling near the sediment and could not be represented well with the image analysis technique.

Table C.1: Environmental parameters during the pre-exposure period of the experiment described in Chapter 5.

variable	mean	std-dev	median	5%-Q	95%-Q	n
Temperature (°C)	20.2	0.3	20.2	19.6	20.7	499
Conductivity (µS/cm)	987	84	977	903	1095	504
Oxygen saturation (mg/L)	10.1	0.53	10.0	9.23	11.01	562
pH	7.27	0.35	7.14	6.98	8.090	351
PO_4^{3-} (mg/L)	0.18	0.13	0.16	0.00	0.398	188
NO_3^- (mg/L)	0.72	0.40	0.65	0.11	1.467	252
NO_2^- (mg/L)	0.02	0.01	0.01	0.01	0.028	314
NH_4^+ (mg/L)	0.03	0.04	0.01	0.00	0.116	308
suspended biomass (mg/L)	1.61	14.6	0.21	0.01	2.97	309

Table C.2: Nominal and measured esfenvalerate stock concentrations (ng/L) used in the experiment described in Chapter 5.

Contaminant	Nominal (ng/L)	Measured Concentrations (ng/L)		Avg. Deviation
		03.06.2021	30.06.2021	
Control	0.0			
Esfenvalerate	0.1	< LOQ	< LOQ	
Esfenvalerate	1.0	0.5	0.8	35%
Esfenvalerate	10.0	6.0	8.0	30%
Esfenvalerate	100.0	80	50	35%

Table C.3: Measured esfenvalerate concentrations in random replicates of the 100 ng/L treatment described in Chapter 5.

Replicate id	Nominal (ng/L)	Measured Concentrations (ng/L)			
		03.06.2021		30.06.2021	
		1h	48h	1h	48h
5	100.0	40	< 20	40	< 20
17	100.0	60	< 20	< 20	< 20
38	100.0	40	< 20	40	< 20
67	100.0	30	< 20	40	< 20
average		42.5	NaN	40	NaN

Table C.4: Correlation (Spearman-ρ) between *Culex* larvae at end of experiment and pre-exposure environmental parameters. Significant correlations ($\alpha = 0.05$, $k = 45$ Bonferroni corrected) are marked with an asterisk (*).

	Culex	Temp.	Cond.	Oxy.	pH	PO_4^{3-}	NO_3^-	NO_2^-	NH_4^+	W susp.[1]
Culex	1	-0.28	-0.07	-0.05	0.17	0.13	0.13	0.3	-0.07	0.13
Temp.	-0.28	1	-0.14	-0.03	0.1	-0.34	-0.08	0.08	-0.07	-0.13
Cond.	-0.07	-0.14	1.0	-0.1	-0.41*	0.18	-0.19	-0.3	0.13	0.18
Oxy.	-0.05	-0.03	-0.1	1	0.13	0.08	-0.01	-0.17	-0	0.23
pH	0.17	0.1	-0.41*	0.13	1.0	-0.14	0.08	0.27	-0.09	-0.03
PO_4^{3-}	0.13	-0.34	0.18	0.08	-0.14	1	0.17	-0.28	0.05	0.25
NO_3^-	0.13	-0.08	-0.19	-0.01	0.08	0.17	1	0.15	0.01	-0.03
NO_2^-	0.3	0.08	-0.3	-0.17	0.27	-0.28	0.15	1	0	-0.22
NH_4^+	-0.07	-0.07	0.13	-0	-0.09	0.05	0.01	0	1	-0.03
W susp.	0.13	-0.13	0.18	0.23	-0.03	0.25	-0.03	-0.22	-0.03	1

[1] Suspended biomass

Table C.5: Correlation (Spearman-ρ) between *Daphnia* at end of experiment and pre-exposure environmental parameters. Significant correlations ($\alpha = 0.05$, $k = 45$ Bonferroni corrected) are marked with an asterisk (*).

	Culex	Temp.	Cond.	Oxy.	pH	PO_4^{3-}	NO_3^-	NO_2^-	NH_4^+	W susp.[1]
Culex	1	-0.03	-0.18	-0.06	0.12	0.06	0.02	0.29	-0.07	0.16
Temp.	-0.03	1	-0.14	-0.03	0.1	-0.34	-0.08	0.08	-0.07	-0.13
Cond.	-0.18	-0.14	1.0	-0.1	-0.41*	0.18	-0.19	-0.3	0.13	0.18
Oxy.	-0.06	-0.03	-0.1	1	0.13	0.08	-0.01	-0.17	-0	0.23
pH	0.12	0.1	-0.41*	0.13	1.0	-0.14	0.08	0.27	-0.09	-0.03
PO_4^{3-}	0.06	-0.34	0.18	0.08	-0.14	1	0.17	-0.28	0.05	0.25
NO_3^-	0.02	-0.08	-0.19	-0.01	0.08	0.17	1	0.15	0.01	-0.03
NO_2^-	0.29	0.08	-0.3	-0.17	0.27	-0.28	0.15	1	0	-0.22
NH_4^+	-0.07	-0.07	0.13	-0	-0.09	0.05	0.01	0	1	-0.03
W susp.	0.16	-0.13	0.18	0.23	-0.03	0.25	-0.03	-0.22	-0.03	1

[1] Suspended biomass

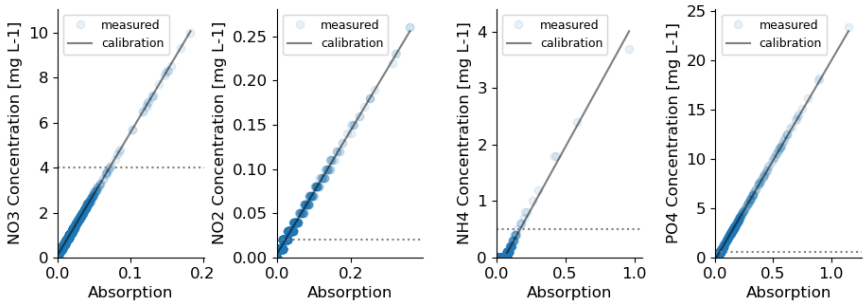

Figure C.1: Relationship between spectral absorbance and nutrient measurement of the photometer *PF-12Plus*. Due to low precision of the returned concentration values of NO_2^-, values were re-calculated by using the fitted regression line. The dotted line indicates the limit of quantification. However, due to high similarity between medium samples in terms of color, turbidity and physicochemical parameters we included also values below the detection limit.

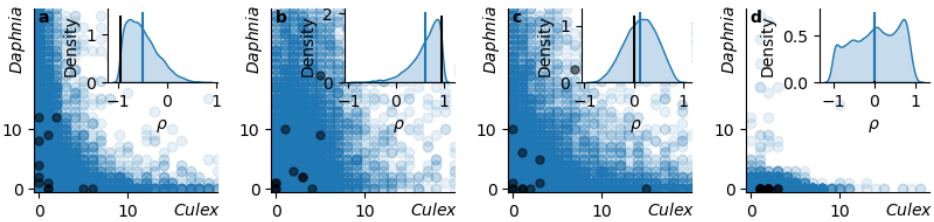

Figure C.2: Estimated correlation coefficients (ρ) from bayesian model (equations 2.3–2.8) from simulated correlated data (black dots). The black vertical line indicates the true correlation coefficient. Blue dots indicate the region in the phase space where observations are expected and the blue curve represents the posterior probability density function (pdf) and its mean (blue vertical line). Due to the low amount of data the pdfs are very wide, but the mean estimate is an accurate, conservative representation of the true value. **(a)** highly negative correlated data. **(b)** highly positively correlated data. **(c)** uncorrelated data. It should be noted that this scenario is sensitive to few data points, which can shift the estimate to positive or negative correlations by chance, however, those will be indicated by large confidence intervals between –1 and 1 **(d)** special case where one species is suppressed and the other is dominant, here the posterior becomes flat, which means that a correlation coefficient is meaningless when one species is not present, but averages to zero, which is also intuitive. Note that values below –1 or above 1 in the inset axes are only because the true posterior density function was visualized with a Gaussian kernel density estimate (KDE); the true, reported, values will always follow the constraints of the posterior to be in the interval [–1, 1].

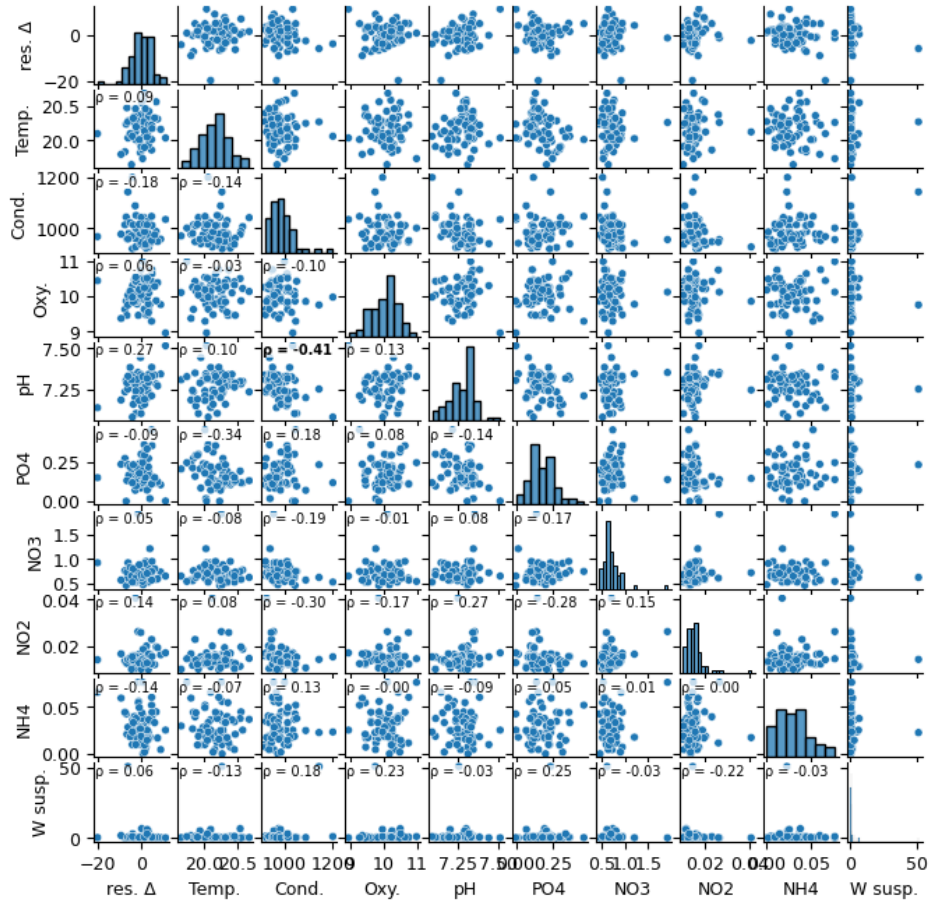

Figure C.3: Correlation (Spearman-ρ) between residual disturbance (Δ) of *D. magna* and pre-exposure environmental parameters. Significant correlations ($\alpha = 0.05$, $k = 45$ Bonferroni corrected) are printed in bold letters.

Eidesstattliche Erklärung

Ich, Florian Schunck erklärt hiermit, dass diese Dissertation und die darin dargelegten Inhalte die eigenen sind und selbstständig, als Ergebnis der eigenen originären Forschung, generiert wurden.

Hiermit erkläre ich an Eides statt

1. Diese Arbeit wurde vollständig oder größtenteils in der Phase als Doktorand dieser Fakultät und Universität angefertigt;
2. Sofern irgendein Bestandteil dieser Dissertation zuvor für einen akademischen Abschluss oder eine andere Qualifikation an dieser oder einer anderen Institution verwendet wurde, wurde dies klar angezeigt;
3. Wenn immer andere eigene- oder Veröffentlichungen Dritter herangezogen wurden, wurden diese klar benannt;
4. Wenn aus anderen eigenen- oder Veröffentlichungen Dritter zitiert wurde, wurde stets die Quelle hierfür angegeben. Diese Dissertation ist vollständig meine eigene Arbeit, mit der Ausnahme solcher Zitate;
5. Alle wesentlichen Quellen von Unterstützung wurden benannt;
6. Wenn immer ein Teil dieser Dissertation auf der Zusammenarbeit mit anderen basiert, wurde von mir klar gekennzeichnet, was von anderen und was von mir selbst erarbeitet wurde;
7. Ein Teil oder Teile dieser Arbeit wurden zuvor veröffentlicht und zwar in: *Environmental Science & Technology (ES&T)* und *Science of the Total Environment*.

Leipzig, 19. Februar 2024
Florian Schunck

Contributions to the Published Articles and Chapters

Chapter 1	This chapter was written by **Florian Schunck**.
Chapter 2	This chapter was written by **Florian Schunck**.
Chapter 3	This chapter is based on the publication *Time Between Stressors Turns Antagonism into Synergism*, published in Environmental Science & Technology (ES&T). **Florian Schunck** (70%) designed the study, conducted lab toxicity experiments, analyzed the data and drafted the original manuscript. Matthias Liess (30%) conceived the research idea, guided the analytical cognition process in the interpretation of results, supervised the study, and revised the manuscript.

Chapter 4 — This chapter is based on the publication *Ultra-low Esfenvalerate Concentrations Increase Biomass and May Reduce Competitiveness of* Daphnia magna *Populations*, published in Science of the total Environment. **Florian Schunck** (75%) designed and planned the study, led the investigation, monitored population abundance, developed the statistical approach, analyzed the data and drafted the original manuscript. Matthias Liess (25%) conceived the research idea, supervised the study, guided the analytical cognition process, and revised the manuscript.

Chapter 5 — This chapter is based on the publication *Persistent Disruption of* Inter*specific Competition after Ultra-low Esfenvalerate Exposure*, published in Science of the total Environment. **Florian Schunck** (80%) developed the research idea, conducted all lab experiments, developed the statistical approach, analyzed the data, and drafted the original manuscript. Matthias Liess (20%) developed the research idea, supervised the study, contributed to the interpretation of results, and revised the manuscript.

Chapter 6 — This chapter was written by **Florian Schunck**.

Curriculum Vitae

Florian Schunck

Birthplace and -date: Göttingen | March 18, 1990

Education

2019–today	**Dr. rer. nat.** Department System Eco-toxicology, Helmholtz Centre for Environmental Research—UFZ, Leipzig, Germany, and Institute for Environmental Research (Biology V), RWTH Aachen University, Germany.
2017–2019	***College of Natural Sciences*** Studienstiftung des deutschen Volkes
2016–2019	**M.Sc. Management of Natural Resources** Martin-Luther-Universität (MLU), Halle-Wittenberg

2012–2016	**B.Sc. Environmental and Resource Management** Brandenburg Technical University (BTU), Cottbus-Senftenberg
2000–2009	**University entrance diploma (Abitur)** Ruhrtal Gymnasium, Schwerte

Experience

2016–2017	**Scientific Assistant** Fraunhofer-Centre for International Management and Knowledge Economy (IMW), Leipzig Organisation of the knowledge management of the group innovation funding. Support of the research project "Knowledge and Technology Transfer from Research Institutions to the Public Domain".
2013–2014	**Student assistant** International Office of the BTU Cottbus-Senftenberg Coordination of outgoing Erasmus exchange students. Organizational support with bilateral agreements between universities.
2009–2012	**Apprenticeship in banking and finances** Sparkasse Unna-Kamen

Supervision

2019	Bachelor Thesis, Patrick Wallner, Die Wirkung von Pestiziden auf aquatische Ökosysteme im Kontext multipler Umweltstressoren
2020	Master Thesis, Kasthuri Gudaniya, Effect of low dose pulse exposure of Esfenvalerate on population dynamics of *Daphnia magna*—A Nanocosm Study
2020	Bachelor Thesis, Lisa Hertges, Der Einfluss von UV-Strahlung in Kombination mit dem Pestizid Esfenvalerat auf den Organismus *Daphnia magna*

Scholarships and Funding

2016–2019	Scholar of the *Studienstiftung des deutschen Volkes*

Publications

1. Klotzbücher A, **Schunck F**, Klotzbücher T, Kaiser K, Glaser B, Spohn M, Widdig M, Mikutta R. 2020. Goethite-Bound Phosphorus in an Acidic Subsoil Is Not Available to Beech (*Fagus sylvatica L.*). *Front. For. Glob. Change.* 3(94). doi:10.3389/ffgc.2020.00094.
2. **Schunck F**, Wiedermann M, Heitzig J, Donges JF. 2021. A dynamic network model of societal complexity and resilience inspired by Tainter's theory of collapse. arxiv:2102.06698v2.
3. **Schunck F**, Liess M. 2022. Time between Sequential Exposures to Multiple Stress Turns Antagonism into Synergism. *Environ. Sci. Technol.* 56(20):14660–14667. doi:10.1021/acs.est.2c04345.

4. **Schunck F**, Liess M. 2023. Ultra-low Esfenvalerate concentrations increase biomass and may reduce competitiveness of Daphnia magna populations. *Sci Total Environ.* 163916. doi:10.1016/j.scitotenv.2023.163916.

5. **Schunck F**, Liess M. 2024. Ultra-low esfenvalerate exposure may disrupt interspecific competition. *Sci Total Environ.* 167455. doi:10.1016/j.scitotenv.2023.167455.

Conference Contributions

1. **Schunck F**, Liess M. 2022. Temporally Coupled Stress Provokes Antagonistic Response at Low Concentrations. SETAC Europe 32nd annual meeting. Copenhagen, Denmark.

2. **Schunck F**, Liess M. 2023. Including Experimental Conditions in Parameter Uncertainty Estimation. SETAC Europe 33nd annual meeting. Dublin, Ireland.